

# FINAL REPORT

Subsurface Thermal Energy Storage for Improved  
Heating and Air Conditioning Efficiency

ESTCP Project EW-201013

NOVEMBER 2016

Ronald W. Falta  
Fred Molz  
**Clemson University**

Charles J. Newell  
**GSI Environmental, Inc.**

***Distribution Statement A***  
*This document has been cleared for public release*



*Page Intentionally Left Blank*

This report was prepared under contract to the Department of Defense Environmental Security Technology Certification Program (ESTCP). The publication of this report does not indicate endorsement by the Department of Defense, nor should the contents be construed as reflecting the official policy or position of the Department of Defense. Reference herein to any specific commercial product, process, or service by trade name, trademark, manufacturer, or otherwise, does not necessarily constitute or imply its endorsement, recommendation, or favoring by the Department of Defense.

*Page Intentionally Left Blank*

| REPORT DOCUMENTATION PAGE   |             |  | Form Approved<br>OMB No. 0704-0188 |  |
|---|-------------|--|------------------------------------|--|
| Public reporting burden for this collection of information is estimated to average 1 hour per response, including the time for reviewing instructions, searching existing data sources, gathering and maintaining the data needed, and completing and reviewing this collection of information. Send comments regarding this burden estimate or any other aspect of this collection of information, including suggestions for reducing this burden to Department of Defense, Washington Headquarters Services, Directorate for Information Operations and Reports (0704-0188), 1215 Jefferson Davis Highway, Suite 1204, Arlington, VA 22202-4302. Respondents should be aware that notwithstanding any other provision of law, no person shall be subject to any penalty for failing to comply with a collection of information if it does not display a currently valid OMB control number. <b>PLEASE DO NOT RETURN YOUR FORM TO THE ABOVE ADDRESS.</b>   |             |  |                                    |  |
| 1. REPORT DATE (DD-MM-YYYY)<br>21-11-2016   |             | 2. REPORT TYPE<br>Final Report   |                                    | 3. DATES COVERED (From - To)<br>May 2010 - December 2016   |
| 4. TITLE AND SUBTITLE<br>Final Report. Subsurface Thermal Energy Storage for Improved<br><br>Air Conditioning Efficiency  |             | 5a. CONTRACT NUMBER<br>10-C-0027-A   |                                    |  |
|   |             | 5b. GRANT NUMBER   |                                    |  |
|   |             | 5c. PROGRAM ELEMENT NUMBER   |                                    |  |
| 6. AUTHOR(S)<br>Falta, R.W., Molz, F., and Newell, C.J.   |             | 5d. PROJECT NUMBER   |                                    |  |
|   |             | 5e. TASK NUMBER  |                                    |  |
|   |             | 5f. WORK UNIT NUMBER   |                                    |  |
| 7. PERFORMING ORGANIZATION NAME(S) AND ADDRESS(ES)<br><br>Clemson University<br>340C Brackett Hall<br>Clemson, SC 29634   |             | 8. PERFORMING ORGANIZATION REPORT<br>NUMBER<br><br>GSI Environmental, Inc.<br>2211 Norfolk Suite 1000<br>Houston, TX 77098 |                                    |  |
| 9. SPONSORING / MONITORING AGENCY NAME(S) AND ADDRESS(ES)<br>Environmental Security<br>Technology Certification<br>Program<br>4800 Mark Center Drive<br>Suite 17D08<br>Alexandria, VA 22350-3605  |             | 10. SPONSOR/MONITOR'S ACRONYM(S)<br>ESTCP  |                                    |  |
|   |             | 11. SPONSOR/MONITOR'S REPORT<br>NUMBER(S)  |                                    |  |
| 12. DISTRIBUTION / AVAILABILITY STATEMENT<br><br>Approved for public release; distribution is unlimited   |             |  |                                    |  |
| 13. SUPPLEMENTARY NOTES   |             |  |                                    |  |
| 14. ABSTRACT<br>This project involved a field demonstration of subsurface thermal energy storage for improving the geothermal heat pump air conditioning efficiency. Many buildings in the U.S. are cooling dominated with relatively low heating demands. When these buildings are cooled using conventional geothermal heat pump systems, undesirable heating of the ground may occur. This demonstration was performed at the MCAS, Beaufort, SC, where several buildings with geothermal heat pump systems were exhibiting excessively high ground loop temperatures. These buildings were retrofitted with dry fluid coolers that were operated to remove excess heat from the loops when outside air temperatures were favorable, especially in the winter. Operation of the coolers substantially reduced the ground loop temperatures. An analysis of the system performance shows that using dry fluid coolers for wintertime cooling of the geothermal ground loops can eliminate loop temperature increases over time, and improve the system efficiency over conventional geothermal systems. |             |  |                                    |  |
| 15. SUBJECT TERMS<br>geothermal heat pumps, dry fluid coolers   |             |  |                                    |  |
| 16. SECURITY CLASSIFICATION OF:   |             |  | 17. LIMITATION<br>OF ABSTRACT      | 18. NUMBER<br>OF PAGES<br><br>78   |
| a. REPORT   | b. ABSTRACT | c. THIS PAGE   |                                    |  |
|   |             |  |                                    | 19a. NAME OF RESPONSIBLE PERSON<br>Ronald W. Falta<br><br>19b. TELEPHONE NUMBER (include area<br>code)<br>864-656-0125 |

*Page Intentionally Left Blank*

## Table of Contents

|   |           |
|---|-----------|
| Acknowledgements  | ix        |
| Executive Summary   | x         |
| <b>1.0 INTRODUCTION</b>   | <b>1</b>  |
| 1.1 BACKGROUND  | 1         |
| 1.2 OBJECTIVE OF THE DEMONSTRATION  | 2         |
| <b>2.0 TECHNOLOGY DESCRIPTION</b>   | <b>3</b>  |
| 2.1 TECHNOLOGY OVERVIEW   | 3         |
| 2.2 TECHNOLOGY DEVELOPMENT  | 9         |
| 2.3 ADVANTAGES AND LIMITATIONS OF THE TECHNOLOGY                              | 12        |
| <b>3.0 PERFORMANCE OBJECTIOVES</b>  | <b>14</b> |
| 3.1 INCREASE ENERGY EFFICIENCY  | 15        |
| 3.2 NO INCREASE IN WATER USAGE  | 15        |
| 3.3 REDUCE CARBON FOOTPRINT   | 15        |
| 3.4 SYSTEM ECONOMICS  | 15        |
| 3.5 EFFICIENCY OF ENERGY STORAGE  | 16        |
| 3.6 AVAILABILITY  | 16        |
| 3.7 RELIABILITY   | 16        |
| 3.8 EASE OF IMPLEMENTATION  | 16        |
| <b>4.0 FACILITY/SITE DESCRIPTION</b>  | <b>17</b> |
| 4.1 FACILITY/SITE LOCATION AND OPERATIONS                                     | 17        |
| 4.2 FACILITY/SITE CONDITIONS  | 18        |
| <b>5.0 TEST DESIGN</b>  | <b>19</b> |
| 5.1 CONCEPTUAL TEST DESIGN  | 19        |
| 5.2 BASELINE CHARACTERIZATION   | 19        |
| 5.2.1 Building 584  | 19        |
| 5.2.2 Building 601  | 24        |
| 5.2.3 Building 2085   | 27        |
| 5.3 DESIGN AND LAYOUT OF TECHNOLOGY COMPONENTS                                | 29        |
| 5.3.1 Building 584 Dry Fluid Cooler   | 29        |
| 5.3.2 Building 601 Dry Fluid Cooler Addition                                  | 30        |
| 5.3.3 Building 2085 Dry fluid Cooler  | 33        |
| 5.4 OPERATIONAL TESTING   | 34        |
| <b>6.0 PERFORMANCE ASSESSMENT</b>   | <b>36</b> |
| 6.1 BUILDING 584  | 36        |
| 6.1.1 Ground Loop Temperature Data  | 36        |
| 6.1.2 Numerical Simulations   | 41        |
| 6.1.3 Calculation of Ground Loop Size Necessary to Stabilize Loop Temperature | 44        |

|  |           |
|--|-----------|
| 6.1.4 Optimal Sizing and Operation of Dry Fluid Cooler with Existing Ground Loop | 45        |
| 6.2 BUILDING 601   | 49        |
| 6.2.1 Ground Loop Temperature Data   | 49        |
| 6.2.2 Freeze Damage  | 50        |
| 6.2.3 Temperature Monitoring Well Data   | 51        |
| 6.3 BUILDING 2085  | 55        |
| 6.3.1 Freeze Damage  | 55        |
| 6.4 ANALYSES FOR OTHER LOCATIONS IN THE UNITED STATES                            | 56        |
| 6.4.1 Methodology  | 56        |
| 6.4.2 Balanced Heating/Cooling Load Base Case                                    | 57        |
| 6.4.3 Cooling Dominated Examples   | 59        |
| <b>7.0 COST ASSESSMENT</b>   | <b>68</b> |
| 7.1 COST MODEL   | 68        |
| 7.2 COST DRIVERS   | 69        |
| 7.3 COST ANALYSIS AND COMPARISON   | 70        |
| <b>8.0 IMPLEMENTATION ISSUES</b>   | <b>76</b> |
| <b>9.0 REFERENCES</b>  | <b>77</b> |
| APPENDIX A: Points of Contact  | 78        |



## List of Acronyms

|        |       |  |
|--------|-------|--|
| ASHRAE | ----- | American Society for Heating, Refrigeration and Air-conditioning Engineers |
| BTU    | ----- | British Thermal Unit   |
| EER    | ----- | energy efficiency ratio  |
| GSI    | ----- | GSI Environmental, Inc.  |
| HDPE   | ----- | high density polyethylene  |
| HVAC   | ----- | heating, ventilation and air conditioning                                  |
| IGHSPA | ----- | International Ground Source Heat Pump Association                          |
| kBTU   | ----- | thousand BTU   |
| kW     | ----- | kilo-Watt  |
| kWhr   | ----- | kilo-Watt hour   |
| MCAS   | ----- | Marine Corps Air Station   |
| VFD    | ----- | variable frequency drive   |

## List of Figures

|   |    |
|---|----|
| <i>Figure 2.1. Schematic diagram of a heat pump during cooling operation.</i>   | 3  |
| <i>Figure 2.2. A closed loop geothermal heat pump system with borehole heat exchangers operating in air conditioning mode. Heat is rejected from the building into the ground.</i>  | 4  |
| <i>Figure 2.3. A closed loop geothermal heat pump system with borehole heat exchangers operating in heating mode. Heat extracted from the ground and delivered to the building.</i> | 5  |
| <i>Figure 2.4. Simulated annual heating (red) and cooling (blue) loads in million BTUs for a 25,000 sq. ft. two-story office building in different U.S. Cities.</i>                 | 7  |
| <i>Figure 2.5. 96 ton dry fluid cooler.</i>   | 10 |
| <i>Figure 2.6. Heat rejection and energy efficiency ratio for a 48 ton dry fluid cooler with fan speed controlled by the temperature difference.</i>                                | 12 |
| <i>Figure 4.1. MCAS Beaufort Location (Google Maps, 2016)</i>   | 17 |
| <i>Figure 4.2. Building locations at the MCAS Beaufort (Google Maps, 2016).</i>   | 18 |
| <i>Figure 5.1. Building 584, MCAS, Beaufort, SC.</i>  | 20 |
| <i>Figure 5.2. Borehole heat exchanger locations for the Building 584 geothermal heat pump ground loop.</i>   | 21 |
| <i>Figure 5.3. Ground loop and outside air temperatures at Building 584 in August, 2012.</i>  | 23 |
| <i>Figure 5.4. Ground loop and outside air temperatures at Building 584 in January, 2013.</i>   | 23 |
| <i>Figure 5.5. Building 601, MCAS Beaufort.</i>   | 24 |
| <i>Figure 5.6. Borehole heat exchanger locations for the Building 601 geothermal heat pump ground loop.</i>   | 25 |
| <i>Figure 5.7. Ground loop and outside air temperatures at Building 601 in August, 2012.</i>  | 26 |
| <i>Figure 5.8. Ground loop and outside air temperatures at Building 601 in January, 2013.</i>   | 26 |
| <i>Figure 5.9. Building 2085, MCAS Beaufort.</i>  | 27 |
| <i>Figure 5.10. Ground loop and outside air temperatures at Building 2085 in August, 2012.</i>  | 28 |

|   |    |
|---|----|
| <i>Figure 5.11. Ground loop and outside air temperatures at Building 2085 in January, 2013.</i>   | 28 |
| <i>Figure 5.12. Dry fluid cooler installed at Building 584.</i>   | 29 |
| <i>Figure 5.13. Layout of the Building 584 dry fluid cooler and ground loop piping.</i>   | 30 |
| <i>Figure 5.14. Dry fluid cooler installed in series with an existing cooler at Building 601.</i>   | 31 |
| <i>Figure 5.15. Layout of the Building 601 dry fluid coolers and ground loop piping.</i>  | 31 |
| <i>Figure 5.16. Location of four 300 foot deep temperature monitoring wells installed in and around the Building 601 borehole heat exchangers.</i>  | 32 |
| <i>Figure 5.17. Design of the temperature monitoring wells.</i>   | 33 |
| <i>Figure 5.18. Dry fluid cooler installed at Building 2085.</i>  | 34 |
| <i>Figure 5.19. Typical wintertime operation of the dry fluid cooler and geothermal heat pump system at Building 584.</i>   | 35 |
| <i>Figure 6.1. Ground loop temperatures at Building 584 in January 2014.</i>  | 37 |
| <i>Figure 6.2. Ground loop temperatures in Building 584 in August, 2014.</i>  | 37 |
| <i>Figure 6.3. Ground loop temperatures in Building 584 in August, 2015.</i>  | 38 |
| <i>Figure 6.4. Observed dry fluid cooler normalized heat rejection (kBTU/hr/<math>\Delta T</math>) as a function of the ground loop flowrate with cooler fans operating at 100%.</i>                | 40 |
| <i>Figure 6.5. Results of GLHEPro simulation of Building 584 ground loop prior to the installation of the dry fluid cooler.</i>   | 43 |
| <i>Figure 6.6. GLHEPro simulation showing predicted temperatures for 30 years of operation.</i>   | 43 |
| <i>Figure 6.7. Simulated and observed ground loop temperatures. The dry fluid cooler began operation in November, 2013.</i>   | 44 |
| <i>Figure 6.8. GLHEPro simulation of Building 584 using 75 three-hundred foot deep borehole heat exchangers.</i>  | 45 |
| <i>Figure 6.9. Simulated Building 584 ground loop temperatures with optimized dry fluid cooler heat rejection. The dry fluid cooler begins operation immediately after the system is installed.</i> | 48 |
| <i>Figure 6.10. Ground loop temperatures at Building 601 in January, 2014.</i>  | 49 |
| <i>Figure 6.11. Ground loop temperatures in Building 601 in August, 2014.</i>   | 50 |
| <i>Figure 6.12. Freeze damage to coils in the Building 601 dry fluid cooler.</i>  | 51 |
| <i>Figure 6.13. Subsurface temperature measured at a depth of 190 feet in a temperature monitoring well located in the Building 601 borehole heat exchanger field.</i>                              | 52 |
| <i>Figure 6.14. Vertical temperature profiles measured in the eastern temperature monitoring well at Building 601.</i>  | 53 |

|   |    |
|---|----|
| <i>Figure 6.15. Vertical temperature profiles measured in the western temperature monitoring well at Building 601.</i>  | 53 |
| <i>Figure 6.16. Vertical temperature profiles measured in the northern temperature monitoring well at Building 601.</i>   | 54 |
| <i>Figure 6.17. Vertical temperature profiles measured in the southern temperature monitoring well at Building 601.</i>   | 54 |
| <i>Figure 6.18. Freeze damage to the Building 2085 dry fluid cooler that occurred on January 6-7, 2014.</i>   | 55 |
| <i>Figure 6.19. Simulated ground loop temperatures for a two-story office building in Minneapolis, MN.</i>  | 59 |
| <i>Figure 6.20. Simulated ground loop temperatures for a two-story office building in Chicago, IL.</i>  | 60 |
| <i>Figure 6.21. Simulated ground loop temperatures for a two-story office building in Philadelphia, PA.</i>   | 62 |
| <i>Figure 6.22. Simulated ground loop temperatures for a two-story office building in Oklahoma City, OK.</i>  | 63 |
| <i>Figure 6.23. Simulated ground loop temperatures for a two-story office building in Jacksonville, FL.</i>   | 65 |
| <i>Figure 6.24. Simulated ground loop temperatures for a two-story office building in Phoenix, AZ.</i>  | 66 |
| <i>Figure 7.1. Simulated monthly energy use for Building 584 in year 30. The red bars represent the base case and the blue bars include the dry fluid cooler.</i> | 71 |
| <i>Figure 7.2. Cumulative electrical energy costs for the base case and the case with a dry fluid cooler.</i>   | 73 |
| <i>Figure 7.3. Cumulative electrical energy cost savings with energy inflation rates of 2%, 5%, and 8% with a general inflation rate of 2%.</i>                   | 74 |

## List of Tables

|  |           |
|--|-----------|
| <i>Table 2.1. Simulated monthly heating and cooling loads (kBTU) for a hypothetical 25,000 sq. ft. two-story office building in Beaufort, SC</i>           | <i>7</i>  |
| <i>Table 2.2. Heat pump cooling efficiency as a function of loop temperature. Data are from the GLHEPro (IGSHPA, 2016) standard library of heat pumps.</i> | <i>8</i>  |
| <i>Table 2.3. Calculated heat rejection energy efficiency ratio (kBTU/hr/kW) for a 48 ton dry fluid cooler at various fan speeds.</i>                      | <i>11</i> |
| <i>Table 3.1. Performance Objectives</i>   | <i>14</i> |
| <i>Table 5.1. Average observed heating and cooling loads (kBTU) for Building 584 at the MCAS, Beaufort, SC.</i>  | <i>22</i> |
| <i>Table 6.1. Average monthly heat rejection by the Building 584 dry fluid cooler, kBTU.</i>   | <i>39</i> |
| <i>Table 6.2. Monthly average dry fluid cooler data from Building 584.</i>   | <i>41</i> |
| <i>Table 6.3. Sorted hourly temperatures from 2010-2011 at the MCAS Beaufort, SC.</i>  | <i>46</i> |
| <i>Table 6.4. Simulated dry fluid cooler performance for optimized design.</i>   | <i>47</i> |
| <i>Table 6.5. Monthly distribution of dry fluid cooler heat rejection assumed in the GLHEPro simulations.</i>  | <i>57</i> |
| <i>Table 6.6. Simulated building heating and cooling loads for Minneapolis, MN example.</i>  | <i>58</i> |
| <i>Table 6.7. Simulated building heating and cooling loads for Chicago, IL example.</i>  | <i>60</i> |
| <i>Table 6.8. Simulated building heating and cooling loads for Philadelphia, PA example.</i>   | <i>61</i> |
| <i>Table 6.9. Simulated building heating and cooling loads for Oklahoma City, OK example.</i>  | <i>63</i> |
| <i>Table 6.10. Simulated building heating and cooling loads for Jacksonville, FL example.</i>  | <i>64</i> |
| <i>Table 6.11. Simulated building heating and cooling loads for Phoenix, AZ example.</i>   | <i>66</i> |
| <i>Table 7.1. Cost Model for Including a Dry Fluid Cooler in a Geothermal Heat Pump System</i>   | <i>68</i> |
| <i>Table 7.2. Simulated Building 584 electrical energy use (kW-hr) for the geothermal heat pump system with and without a dry fluid cooler.</i>            | <i>70</i> |
| <i>Table 7.3. Comparison of monthly electricity costs (in current dollars) after 10 and 30 years of system operation.</i>                                  | <i>72</i> |

## **Acknowledgements**

The authors would like to thank the Environmental Security Technology Certification Program (ESTCP) for funding this project.

The authors also would like to thank Neil Tisdale and Bill Rogers at the MCAS Beaufort and Poonam Kulkarni and Elizabeth Piña at GSI Environmental for all of their support and help on this project. Their participation is greatly appreciated.

## Executive Summary

Geothermal heat pump systems are one of the most efficient ways to heat and cool buildings. During air conditioning, heat pumps move a liquid refrigerant to an evaporator coil connected to the building heating, ventilation, and air conditioning (HVAC) system. The refrigerant evaporates in the coil, removing heat from the building. The refrigerant vapor is then compressed into a hot, high pressure vapor using a compressor powered by electricity. The hot vapor is directed to a condensing coil, where the refrigerant vapor condenses back into a liquid, releasing its heat of vaporization. During building heating, this cycle is reversed, and the refrigerant condenses inside the building, releasing heat.

A geothermal heat pump system uses the ground as the heat sink (for air conditioning) or heat source (for heating). The coil that is used to reject (during air conditioning) or absorb (during heating) heat is connected to a heat exchanger with a water ground loop. This ground loop typically consists of a series of vertical borehole heat exchangers containing grouted in place U-tubes. The ground loop water passes through the borehole heat exchangers, transferring heat between the loop and the ground. For buildings that have similar heating and cooling loads, the ground serves as a highly efficient heat source/sink. Under these balanced load conditions, the ground loop temperature is cooler than the outside air temperature in the summer, and it is warmer than the outside air temperature in the winter.

Many buildings in the United States, particularly in the south and southwest have building loads that are strongly cooling dominated, with small heating loads. When a conventional geothermal heat pump system is used in these buildings, the excessive amount of heat rejection by the heat pumps can lead to long term heating of the borehole heat exchangers and surrounding ground. As the ground loop temperature increases, the heat pump air conditioning efficiency drops, and in some cases, the ground loop temperature may exceed the safe working limits of the heat pumps. The ground heating caused by the geothermal system is difficult to reverse, and limits future application of geothermal heat pumps at the location.

One possible way to avoid excessive ground loop temperatures is to remove heat from the system in the wintertime using a supplemental cooling device such as a dry fluid cooler. This is a form of subsurface thermal energy storage (STES), where cooling that takes place in the winter benefits the geothermal heat pump system the following summer. This project demonstrated the technology of using dry fluid coolers to perform wintertime cooling of geothermal ground loops.

Dry fluid coolers were retrofitted to three buildings at the Marine Corps Air Station, Beaufort, SC. These buildings ranged in size from 12,500 to 24,000 sq. ft. and they had conventional geothermal heat pump systems installed with between 24 and 39 three-hundred foot deep borehole heat exchangers at each building. These geothermal systems were installed in 2004, and by 2012, the ground loop temperatures at each of these buildings had increased to undesirable levels.

The dry fluid coolers take the loop water leaving the buildings and cool it by blowing outside air across copper coils. By operating these coolers mainly in the winter, it is possible to take advantage of cold air temperatures to efficiently remove heat from the ground loop, and the ground itself. Two of the dry fluid coolers suffered freeze damage during unusually cold

periods, limiting the data from those buildings (propylene glycol antifreeze has since been added to the systems to prevent this in the future). The third cooler has been in continuous operation for almost 3 years, and has resulted in a ground loop temperature decrease of about 10 degrees F.

An analysis of the data collected at this building shows if a dry fluid cooler was installed at the same time as the geothermal system, and operated efficiently, that it would eliminate the problem of ground loop temperature increase over time. The resulting savings in costs are large compared to the alternative of increasing the number of borehole heat exchangers to reduce the ground loop temperature.

A primary Performance Objective for this demonstration was to show an increase in electrical efficiency of more than 15% compared to a conventional geothermal heat pump system without a dry fluid cooler. Using the same building and geothermal ground loop characteristics, a comparison was made between a system with and without a dry fluid cooler. During the first year of operation, the energy costs with and without the dry fluid are similar, because the system without a dry fluid cooler has not heated up much. After 10 years of operation, the annual energy costs are calculated to be about 12% lower for the system with the dry fluid cooler. This difference increases over time to about 19% by 30 years.

Considering the capital cost for the dry fluid cooler, the payback period is calculated to be about 23 years (assuming an energy inflation rate of 5% and a general inflation rate of 2%). With a lower energy inflation rate of 2%, the payback period is 30 years or more.

A key assumption in these calculations was that the system without the dry fluid cooler would be able to operate for decades with very high ground loop water temperatures. There is a high likelihood that an external cooler would be required at some point in the near future simply to continue operation of the system. If this is the case, then it would be far better to install the cooler initially when the system is constructed and avoid the high ground loop temperatures from the start. The capital costs would be nearly the same, and the energy and energy cost savings would be substantial.



## 1.0 INTRODUCTION

### 1.1 BACKGROUND

The DoD spends about \$3.5 billion per year on facility energy consumption. Much of this energy goes to heat and cool buildings. Beyond this large current cost liability is the potential for several significant structural changes at DoD facilities around the world. These challenges include:

- Expected long-term increases in the underlying cost of fossil fuels used for heating and cooling or to generate electricity for these purposes;
- High likelihood for governmental mandates for DoD facilities to significantly reduce their carbon footprint;
- Acceleration of the on-going market trend where electricity cost is variable both diurnally and seasonally, particularly for large users (i.e., smart meters that result in very high cost for power during periods when demand is high and very low costs during low-demand periods, either diurnally or seasonally).
- Requirements that renewable energy be incorporated into the DoD facilities energy mix.
- Energy sources may be more unreliable in the future, due to shortages, disruption of the grid, etc.

Geothermal heat pump systems use a ground loop consisting of a series of borehole heat exchangers to serve as a heat sink and source for the heat pumps. For locations where building heating and cooling loads are balanced, the ground temperature stays relatively constant over time, as the system rejects heat to the ground loop in the summer, and it removes heat in the winter. Under these conditions, geothermal heat pump systems are among the most efficient of all heating and air conditioning systems.

This demonstration was performed at the Marine Corps Air Station in Beaufort, South Carolina (MCAS Beaufort). The original intent of this project was to improve both heating and cooling efficiency of a building geothermal system by using two ground loop systems, with off-season (summer) heating of one loop, and off-season (winter) cooling of the other loop. For a load balanced system, this type of operation could improve both the heating and cooling efficiency.

As the project progressed, it became apparent that few large buildings have balanced heating and cooling loads. Instead, there are many locations where building loads are strongly cooling dominated, and the heating and cooling loads are unbalanced. This is particularly true at the MCAS Beaufort, where almost all of the building loads are from cooling, with only a small amount of heating load. With a conventional ground source heat pump system, this load imbalance leads to excessive ground heating with resulting losses of heat pump efficiency over time. Based on this observation, this project focused on using dry fluid coolers in the winter to efficiently remove most of the excess heat from the ground loop in strongly cooling dominated systems. Three buildings at the MCAS Beaufort were retrofitted with dry fluid coolers to evaluate efficient heat removal from the ground loop.

## **1.2 OBJECTIVE OF THE DEMONSTRATION**

The objective of this demonstration was to show that geothermal heat pump efficiency during summer air conditioning could be improved by removing heat from the ground loop in the wintertime using dry fluid coolers. A secondary objective was to develop an Application Manual for this technology to help DoD facility managers determine if this technology could be applied to their facility, and to help them design the systems.

## 2.0 TECHNOLOGY DESCRIPTION

### 2.1 TECHNOLOGY OVERVIEW

Geothermal heat pump systems use the ground as a heat source and heat sink to heat and cool buildings. These systems, also known as ground source heat pump systems, use reversible heat pumps (Figure 2.1) to either extract or reject heat into a water loop (the ground loop) that runs through the building, and interacts with the subsurface through trenches, wells, or boreholes.

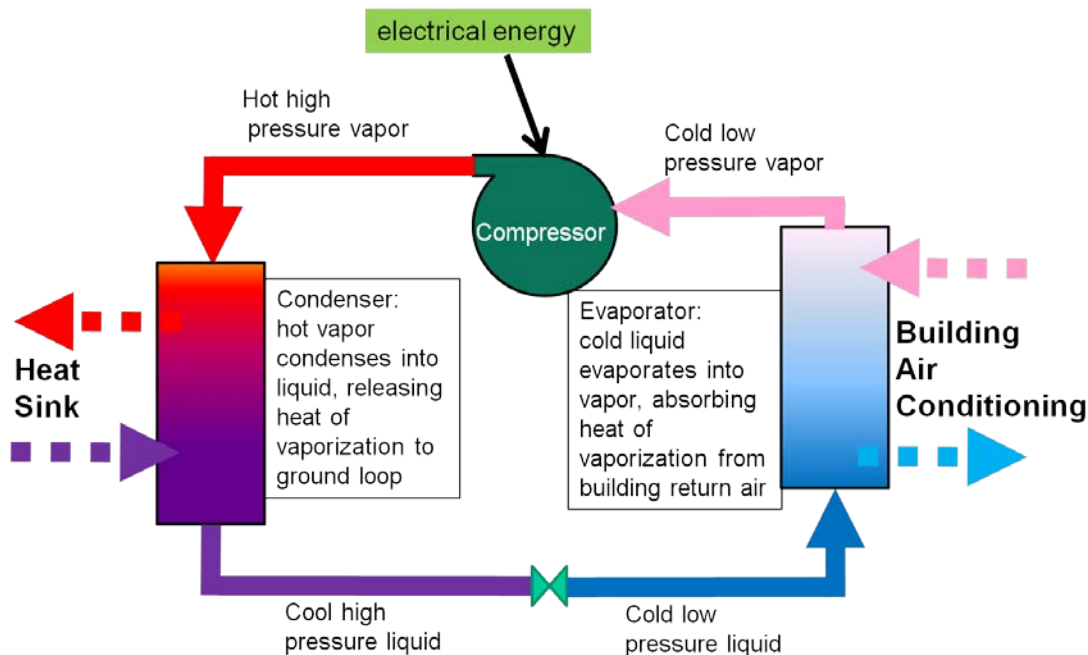


**Figure 2.1. Schematic diagram of a heat pump during cooling operation.**

When the building is being cooled, heat from the building is absorbed by a liquid refrigerant in the evaporator, converting the liquid into a vapor. The cool low pressure vapor is compressed in an electrically driven compressor to convert it into a hot, high pressure vapor. A heat sink (the ground loop) is used to remove heat from the hot vapor causing it to condense back into a liquid. The liquid is then routed back to the evaporator to complete the cycle. The basic principle of operation is that the building heat is transferred using the latent heat of vaporization of the refrigerant from the heat source to the heat sink. This is an extremely efficient method of heat transfer, because several units of heat energy can be transferred per unit of electricity consumed by the compressor.

When the building is being heated, the refrigeration cycle is reversed, and heat is extracted from the heat source (the ground loop) to evaporate the liquid refrigerant. The refrigerant vapor condenses in a coil inside the building, releasing heat to heat the building.

There are three main types of ground loops: open loops using wells, closed loops using trenches, and closed loops that use boreholes. With an open loop, groundwater is pumped from a well

through the heat pump system, and back into the ground through another well. This type of system can be very effective, but it requires access to a productive aquifer with associated permitting and water chemistry considerations.

Closed loop systems use sealed piping to move a mixture of water and antifreeze through the ground. Small household geothermal systems often use shallow trenches for these closed loops, but trenches become impractical for larger buildings, where the necessary length of the ground loop may be thousands of feet. The most common ground loop configuration for larger buildings consists of an array of vertical boreholes extending up to several hundred feet deep into the ground with a horizontal spacing of 20 feet or more (Figure 2.2). These vertical boreholes are typically constructed by drilling a 6 inch diameter borehole. A high density polyethylene (HDPE) U-tube is installed in the borehole, and is grouted into place using a thermally conductive grout. This design isolates the ground loop fluid from the groundwater system, and heat transfer between the ground loop and the subsurface occurs by thermal conduction.

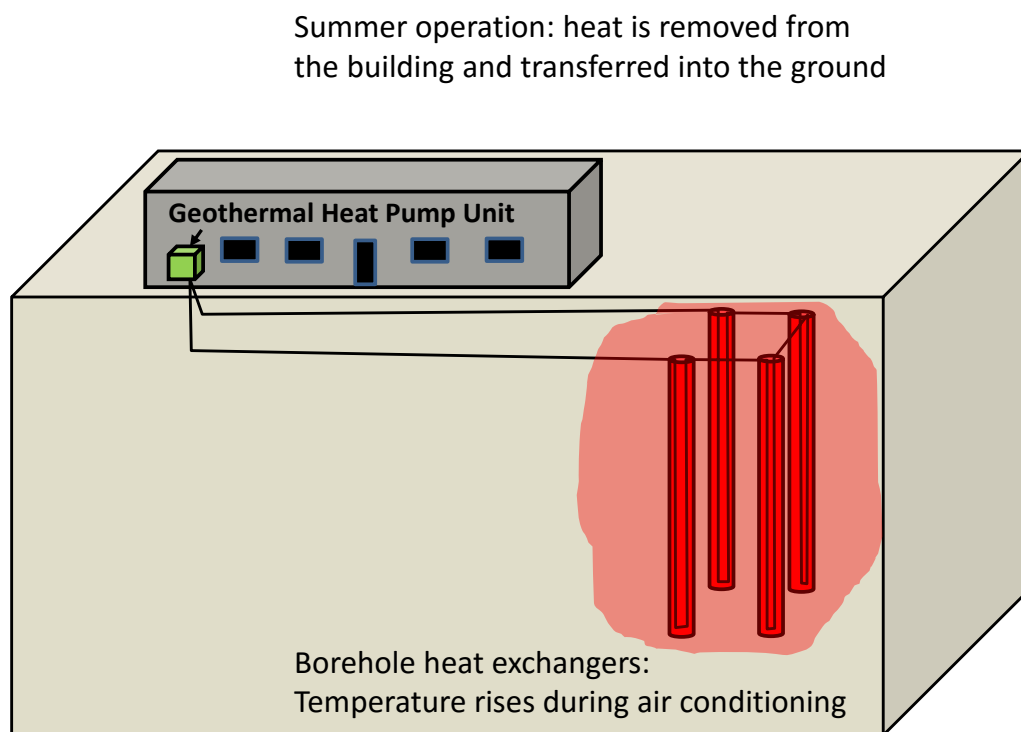


**Figure 2.2.** A closed loop geothermal heat pump system with borehole heat exchangers operating in air conditioning mode. Heat is rejected from the building into the ground.

When the heat pump system is in air conditioning mode, the ground loop rejects the building heat into the ground loop, resulting in an increase in temperature in the subsurface (Figure 2.2). When the heat pump is in heating mode, heat is extracted from the ground loop, and delivered to the building, causing the ground to cool (Figure 2.3).

Winter operation: heat is removed from the ground and transferred into the building

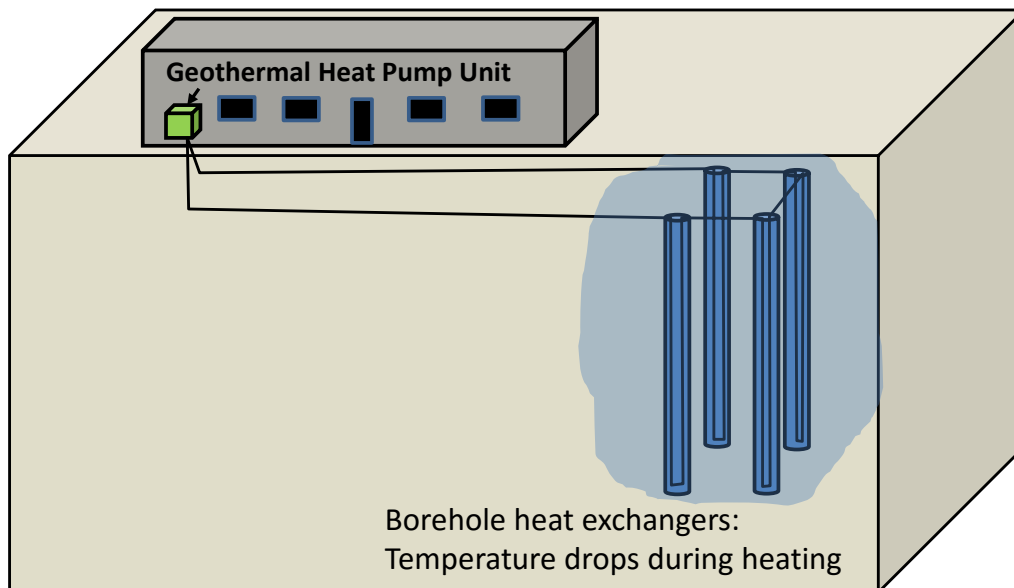


**Figure 2.3.** A closed loop geothermal heat pump system with borehole heat exchangers operating in heating mode. Heat is extracted from the ground and delivered to the building.

When the building heating and cooling loads (including the waste heat from the heat pumps) are exactly balanced, then the heating of the subsurface during the summer air conditioning period is offset by the cooling of the subsurface during the winter heating period. The case of balanced heating and cooling loads is an ideal condition for use of geothermal heat pumps. Although the ground temperature rises some in the summer, the average ground loop temperature remains well below the outside air temperature, making it an efficient heat sink for the heat pump. Similarly, in the winter, the ground temperature drops some, but it remains higher than the outside air temperature, making it an efficient heat source for the heat pumps.

It appears, however, that many medium to large buildings in the United States do not have balanced heating and cooling loads, and they tend to be strongly cooling dominated. This imbalance may lead to substantial heating of geothermal ground loops which causes the heat pump performance and energy efficiency to degrade over time.

The load imbalance arises from waste heat caused by lighting and other appliances, industrial machinery, communications and computing equipment, and people. Medium to large buildings have interior rooms that may never require heating, and the ratio of building surface area to volume decreases as the building size increases. Geothermal heat pumps themselves generate substantial waste heat, equal to about 20-25% of the building cooling load. This heat must also be removed from a building in order to cool it.

The occurrence of unbalanced, cooling dominated buildings is not unique to the MCAS Beaufort site. It is a widespread characteristic of medium to large commercial and institutional buildings

across most of the country. To illustrate this point, building heating and cooling loads were calculated for a variety of locations using the eQUEST (Hirsch & Associates, 2016) building energy simulation tool (<http://www.doe2.com/equest/>). The eQUEST tool uses the DOE-2 energy modeling program that was developed by the U.S. Department of Energy Lawrence Berkeley National Laboratory. The eQUEST program uses a detailed description of the building layout, construction, equipment, usage, and local weather conditions to perform hourly simulations of heating and cooling loads and energy consumption over the course of a year.

The building simulation program contains templates for dozens of typical buildings (office buildings, schools, multi-family apartments, restaurants, retail buildings, motels, hospitals, etc.). Each of these building templates is populated with realistic default values for the important building layout, construction, and usage details. These default values can be entered manually in the 43 pages of building characteristics that are used in each simulation. The program also allows the user to select the location, and it uses long-term average weather files for each location (with about 300 locations available in North America).

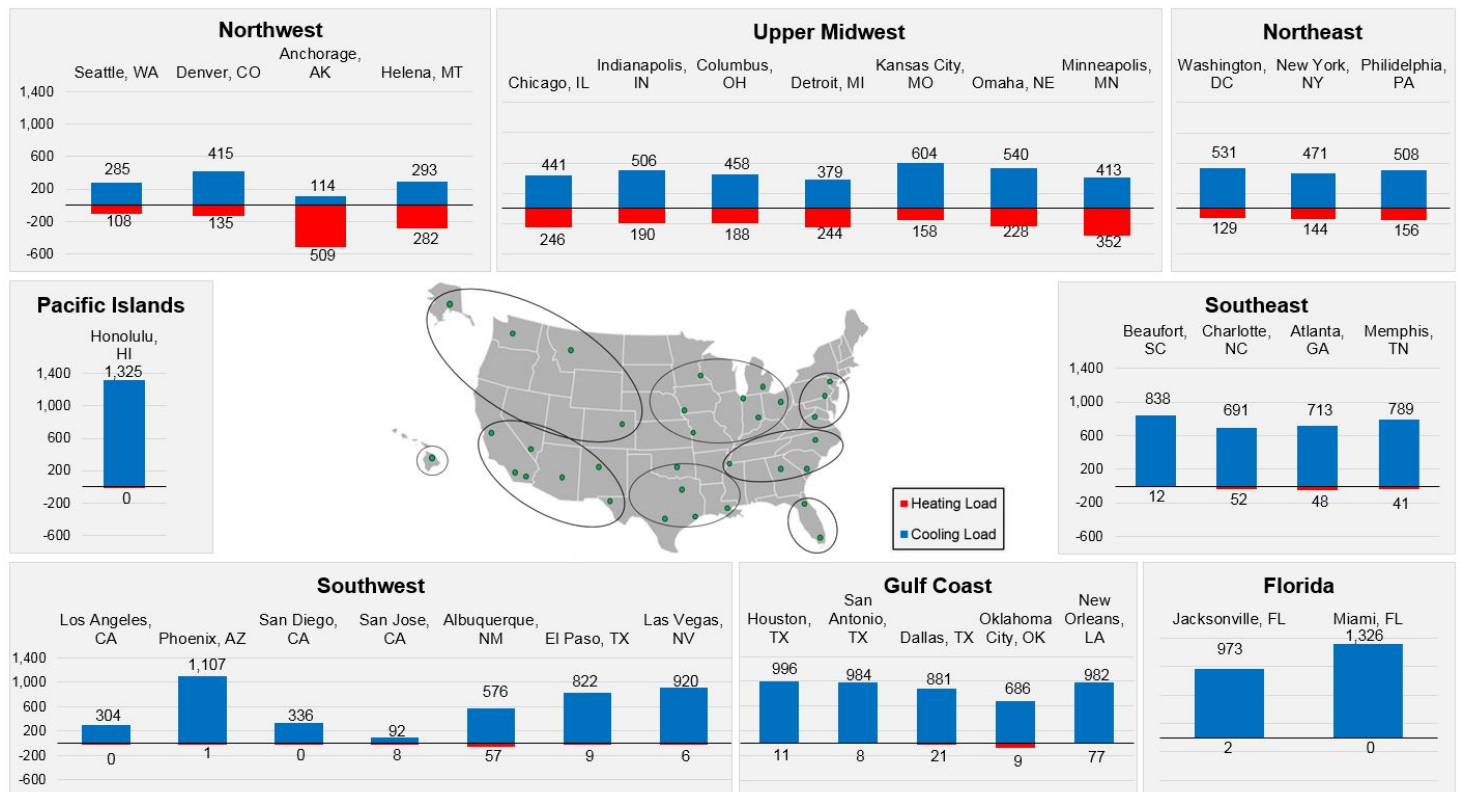
Building load simulations were performed for a hypothetical 25,000 sq. ft. two-story office building that is primarily occupied during normal weekday working hours. This building has a square footprint, with metal frame construction, and insulated exterior walls and roof surfaces. The building details used in these simulations are the default values for the building type “Office Bldg, Two Story” in eQUEST. The eQUEST program computes the building loads every hour for one year. Those results can be processed in a separate program called the Peak Load Analysis Tool that is provided with the GLHEPro geothermal heat pump simulation model (IGSHPA, 2016). The Peak Load Analysis Tool is used to convert the hourly eQUEST results into monthly building heating and cooling loads (which is the input format for the GLHEPro program).

Table 2.1 shows the computed building loads for a 25,000 sq. ft. two-story office building in Beaufort, SC. These simulated monthly loads are similar to what we observed at the Military Police Building 584 at the MCAS, Beaufort. The simulated heating and cooling loads show an extreme imbalance, with 98.6% of the total load going to cool the building. This simulated building cooling/heating load imbalance is very close to the observed value of 99.5% for Building 584.

Using the same methodology, the eQUEST program was used to compute the building heating and cooling loads for a two-story office building located in 33 cities across the United States (Figure 2.4). The bar graphs associated with each city show the annual heating loads (in red) and the cooling loads (in blue) in units of million BTUs. Out of the 33 cities, only one, Anchorage, AK is heating dominated, and only two, Helena, MT, and Minneapolis, MN have balanced heating and cooling loads. The remaining 30 cities are moderately to very strongly cooling dominated.

**Table 2.1. Simulated monthly heating and cooling loads (kBtu) for a hypothetical 25,000 sq. ft. two-story office building in Beaufort, SC**

|           | Heating | Cooling |
|-----------|---------|---------|
| January   | 6653    | 7027    |
| February  | 2942    | 11875   |
| March     | 611     | 37932   |
| April     | 2       | 67894   |
| May       | 0       | 90897   |
| June      | 0       | 120145  |
| July      | 0       | 129384  |
| August    | 0       | 133305  |
| September | 0       | 114993  |
| October   | 0       | 72249   |
| November  | 45      | 37997   |
| December  | 2126    | 14217   |



**Figure 2.4. Simulated annual heating (red) and cooling (blue) loads in million BTUs for a 25,000 sq. ft. two-story office building in different U.S. Cities.**

Locations in the Southeast, Florida, Gulf Coast, the Southwest, and Hawaii were extremely cooling dominated, with very low heating loads (<5% of the total). In the Northeast, the buildings were still strongly cooling dominated, but with larger heating loads (~25% of the total). In the Upper Midwest and Northwest, the buildings also tended to be cooling dominated except for Anchorage, AK, Minneapolis, MN, and Helena, MT. The other locations in those regions had cooling loads that were 2 to 4 times larger than the heating loads.

Our experience at MCAS Beaufort shows that unbalanced cooling dominated loads can lead to ground loop temperatures that exceed 100 °F in the summer months. These high ground loop temperatures degrade the performance of the geothermal heat pumps during air conditioning. Table 2.2 shows heat pump cooling efficiency for a water source heat pump (the use of brand names does not constitute an endorsement, and is used only for illustrative purposes).

**Table 2.2. Heat pump cooling efficiency as a function of loop temperature. Data are from the GLHEPro (IGSHPA, 2016) standard library of heat pumps.**

| <b>Trane WPHF021 heat pump performance ratings</b> |  |
|--|--|
| <b>Ground loop temperature</b>                     | <b>Cooling energy efficiency ratio (EER), kBTUh/kW</b> |
| 45 °F  | 28.0 (+133%)   |
| 60 °F  | 21.5 (+79%)  |
| 70 °F  | 18.5 (+54%)  |
| 80 °F  | 16.0 (+33%)  |
| 90 °F  | 13.8 (+15%)  |
| 100 °F   | 12.0   |

The cooling efficiency is expressed in units of kBTU/hr of cooling per kW of electrical power. The cooling efficiency drops by about 1-2% per degree F increase. Once the loop temperature exceeds about 110 °F, it may be necessary to shut down the heat pumps. During heating, the increased loop temperature improves the heat pump efficiency, but this is only a significant benefit in locations where the heating loads are large.



The heating of the subsurface by the borehole heat exchangers represents a fairly long-term damage to the natural system. Once a large volume of the subsurface associated with a building geothermal heat pump system has been excessively heated, it is no longer as suitable for use as a heat sink. This means that performance of the geothermal heat pump system is permanently degraded unless some of the excess heat is removed from the subsurface. It also limits the applicability of future applications of geothermal heat pump systems at the location.

## **2.2 TECHNOLOGY DEVELOPMENT**

There are two primary methods for reducing the build-up of heat in borehole heat exchangers subject to cooling dominated loads. The most common method is to increase the size of the ground loop by installing more boreholes, or by making them deeper. Geothermal heat exchanger simulation programs such as GLHEPro (IGSHPA, 2016) are used predict future ground loop temperatures given the building loads, location, heat pump characteristics, subsurface thermal properties, and the geometry and properties of the borehole heat exchangers. With this design process, the size of the ground loop is increased in size until the predicted future temperature rise falls within an acceptable range.

The major disadvantage of increasing the ground loop size is that it may greatly increase the system capital cost. The cost of drilling and installing the borehole heat exchangers is a major part of the overall system expense, with drilling costs ranging from about \$10 per foot to \$20 per foot or more. Moreover, space may not be available for increasing the size of the ground loop beyond a certain point. Finally, while increasing the size of the ground loop decreases the rate of subsurface temperature increase, it does not eliminate the problem.

A more cost effective option for reducing ground loop heat build-up involves the use of a supplemental cooling device such as a cooling tower or dry fluid cooler (IGSHPA, 2016). These systems are known as hybrid geothermal heat pump systems. With a hybrid system, the cooling device is used mainly during the peak cooling months to reduce the excess heat rejection into the ground loop. If the cooling device capacity is high enough, it is possible to remove enough heat to balance the heating and cooling load delivered to the ground loop, thus eliminating long-term ground loop heating without increasing the size of the ground loop. This heat removal comes at the cost of added electricity use, water use (for cooling towers), and maintenance.

Several simulation-based optimization methods have been proposed for hybrid geothermal heat pump system design (Cullin and Spitler, 2010; Cullin, 2008; IGSHPA, 2016; Kavanaugh, 1998; Xu, 2007; Hackel et al., 2009; Chaisson and Yavuzturk, 2009). Given permissible ground loop temperature limits, capital costs for the ground loop and cooling device, and the cooling device operating costs, these methods optimize the size of the ground loop and cooling device to minimize the system costs.

Hybrid systems most commonly use cooling towers, with operation mainly in the peak cooling months of summer. Cooling towers remove heat primarily through water evaporation, although some cooling also occurs due to sensible heat transfer. Cooling towers are very effective heat transfer devices, but they consume significant amounts of water, and they have relatively high maintenance requirements associated with the process water. Summertime operation of cooling towers also adds to electrical demand during peak electricity use periods.

Dry fluid coolers are an alternative to cooling towers that have the advantage of not requiring any process water or associated maintenance. Dry fluid coolers remove heat through sensible heat transfer, and the rate of heat rejection depends on the temperature difference between the water entering the cooler, and the outside air temperature. Dry fluid coolers are less efficient than cooling towers during summertime operation, but they can be operated in the wintertime with very high efficiency, and during periods of low electricity demand.

An alternative approach to managing ground loop temperatures involves the use of dry fluid coolers operated mainly in the wintertime. Dry fluid coolers are similar in operation to automobile radiators. The ground loop fluid (a mixture of water and antifreeze) is pumped through copper coils that are attached to aluminum fins. Outside air is pulled across the coils using fans (Figure 2.5) to extract heat from the loop water.

Dry fluid coolers have a nominal heat rejection rating that corresponds to a specific set of operating conditions. Commercial dry fluid coolers range in rated capacity from about 24 kBTU/hr (a 2 ton cooler) up to about 1200 kBTU/hr (a 100 ton cooler), and have anywhere from 1 to 8 fans (typically 1 horsepower each). Each fluid cooler is designed to operate within a certain water flow rate range, and flow rates that are below the design range tend to result in a linear decrease in performance.



***Figure 2.5. 96 ton dry fluid cooler.***

Dry fluid cooler manufacturers publish tables and graphs that show the cooler performance under different conditions (water flow rate, outside air temperature, and entering water temperature). For a particular dry fluid cooler with a specified flow rate, the heat rejection is a nearly linear function of the temperature difference between the incoming fluid and the air temperature. For example, a Technical Systems FC Series model FC-48-597A operating at a fluid flow rate of 80 gpm with a 40% glycol solution has a heat rejection rating of 20.2 kBTU/hr/ΔT (Technical Systems, 2016). If the incoming fluid temperature is 90 °F, and the air temperature is 70 °F, the heat rejection by the cooler is 404 kBTU/hr or about 34 tons (in the cooling industry, a ton is a unit of power based on the amount of heat adsorbed when a ton of ice is melted over a 24 hour period. One ton of cooling is approximately equivalent to 12,000 BTU per hour or 3,500 watts).

Dry fluid coolers can be ordered with variable frequency drive (VFD) motors that allow for lower fan speed operation when 100% capacity is not needed. Use of VFD fans can result in major improvements in electrical efficiency due to the nature of fan power. Heat rejection from a dry fluid cooler is approximately a linear function of fan speed. Fan power however varies with the cube of the fan speed. Therefore, if a fan is operated at 50% of maximum speed, the cooler can reject about half the heat that it would at 100% fan speed, while using only 1/8 of the power. In other words, the cooler has a heat rejection efficiency (kBTU/hr/kW) that is about 4 times larger with a fan speed of 50% compared to a fan speed of 100% (actual efficiency may be lower depending of fluid pumping costs).

Table 2.3 shows the calculated energy efficiency ratio (EER, kBTU/hr/kW) of a Technical Systems FC Series model FC-48-597A operating at a fluid flow rate of 80 gpm over a range of fan speeds and temperature differences. The efficiency includes pumping costs associated with the fluid pressure drop (10 ft of head) through the cooler. The fluid pumping power becomes a significant part of the cooler power consumption at fan speeds below 30% in this case.

**Table 2.3. Calculated heat rejection energy efficiency ratio (kBTU/hr/kW) for a 48 ton dry fluid cooler at various fan speeds.**

|                 | Fan speed |     |     |     |     |     |     |      |     |
|-----------------|-----------|-----|-----|-----|-----|-----|-----|------|-----|
| delta T (deg F) | 100       | 90  | 80  | 70  | 60  | 50  | 40  | 30   | 20  |
| 5               | 32        | 39  | 48  | 60  | 75  | 95  | 116 | 128  | 112 |
| 10              | 64        | 78  | 96  | 119 | 151 | 190 | 232 | 256  | 225 |
| 15              | 96        | 116 | 143 | 179 | 226 | 285 | 348 | 384  | 337 |
| 20              | 128       | 155 | 191 | 239 | 302 | 380 | 464 | 512  | 449 |
| 25              | 160       | 194 | 239 | 298 | 377 | 476 | 581 | 639  | 561 |
| 30              | 192       | 233 | 287 | 358 | 452 | 571 | 697 | 767  | 674 |
| 35              | 224       | 272 | 334 | 418 | 528 | 666 | 813 | 895  | 786 |
| 40              | 256       | 310 | 382 | 477 | 603 | 761 | 929 | 1023 | 898 |

The dry fluid cooler control system can be designed to maximize the efficiency by using a fan speed ramp that is proportional to the temperature drop. For example, using the cooler described above, the fan speed could be set to vary linearly from a minimum of 30% with a temperature difference of 5 degrees up to a maximum of 80% with a temperature difference of

40 degrees. That control scheme would result in an energy efficiency ratio greater than 200 for temperature differences larger than 10 degrees (Figure 2.6)

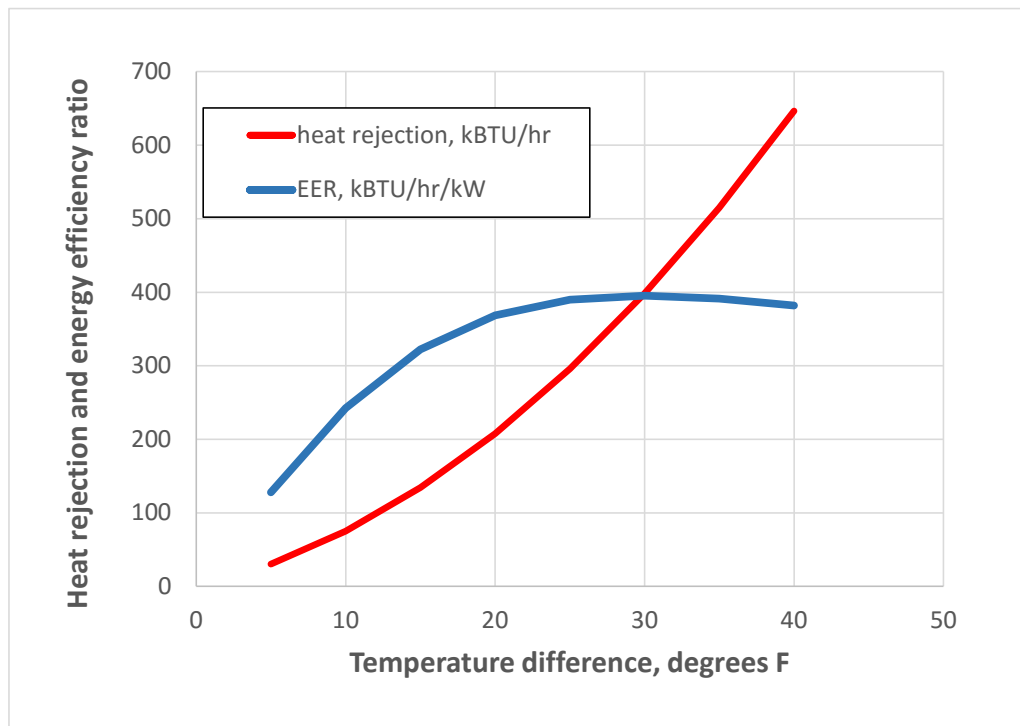


**Figure 2.6.** Heat rejection and energy efficiency ratio for a 48 ton dry fluid cooler with fan speed controlled by the temperature difference.

## 2.3 ADVANTAGES AND LIMITATIONS OF THE TECHNOLOGY

The advantage of this technology is that it makes it possible preserve the high efficiency of geothermal heat pump air conditioning systems at sites where the building loads are strongly cooling dominated. By adding wintertime cooling using dry fluid coolers, the system remains closed, with no additional water use, and minimal system maintenance. It allows for the use of a smaller borehole heat exchanger ground loop to be used, with only a small electrical energy requirement for operating the dry fluid cooler. The fluid cooler energy consumption mainly occurs in the wintertime, when most of the excess heat is removed from the ground loop system.

A limitation of the technology is that it requires an additional capital expenditure during construction of the system. However, without the addition of a heat rejection device such as a dry fluid cooler, the ground loop in a cooling dominated system would heat up, reducing the air conditioning efficiency over time. There is a tradeoff between this additional upfront capital cost and the benefit of maintaining the heat pump system efficiency over time.

The addition of a dry fluid cooler may also make the system more prone to freeze damage during wintertime cooling. This damage can be avoided by use of an appropriate propylene glycol antifreeze mixture in the ground loop. Note that the closed loop nature of the ground loop provides some protection against potential releases of anti-freeze to groundwater as the u-tubes

are typically grouted or cemented in the borehole. The USEPA recommends that children be exposed to no more than 20 mg/L (20 ppm) ethylene glycol in drinking water for 1 day, or 6 mg/L (6 ppm) per day over 10 days. They also recommend that adults be exposed to no more than a daily total of 7 mg/L (7 ppm) for a lifetime (ASTDR, 2007) . In the unlikely event of a release, both ethylene and propylene glycol anti-freeze compounds were found to *“be readily biodegradable under both oxic and anoxic conditions, without formation of toxic or persistent intermediates. Long-term groundwater contamination by the glycols is therefore not expected”* (Klozbucher et al., 2007). However, the use of corrosion inhibitors or biocides can inhibit antifreeze biodegradation and therefore the benefits of using these additives must be balanced against the risk of a release of the working fluid in the ground loop.

### 3.0 PERFORMANCE OBJECTIVES

The performance objectives for this project are listed in Table 3.1, and are discussed in more detail below.

**Table 3.1. Performance Objectives**

| Performance Objective                      | Metric   | Data Requirements  | Success Criteria   | Results   |
|--|--|--|--|---|
| <b>Quantitative Performance Objectives</b> |  |  |  |   |
| Increase energy efficiency                 | Electrical energy use, kWhr per year   | Electrical energy consumption for heat pumps, water pumps, fluid coolers, and air handlers before and after startup                                | > 15% improvement in energy efficiency compared with conventional ground coupled heat pump system  | Can be achieved after 10-20 years of operation. Does not occur in early years for a new system  |
| No increase in water usage                 | Water usage (gallons per year)   | Additional water consumption for system  | No additional water consumption  | Achieved.   |
| Reduce carbon footprint                    | Carbon emissions (lbs per year)  | Inventory of carbon emissions and sequestrations related building heating and cooling  | > 15% reduction in building heating and cooling carbon footprint compared with conventional ground coupled heat pump system  | Similar to increase in energy efficiency.   |
| System Economics                           | Comparison with conventional GSHP; Savings to investment ratio; net present value (\$); payback period (years); lifecycle savings (\$) | Capital cost for installing additional equipment; operating cost to heat and cool building before and after installation                           | Lower lifetime cost compared to conventional GSHP;<br>> 1.2 savings to investment ratio over the 30-year life<br>< 10-year payback period<br>> 20% return on investment<br>> net present value of savings of \$50,000<br>> life-cycle savings of \$100,000 | Depends on whether conventional geothermal system could run without a dry fluid cooler. If no cooler would be required economics are less favorable |
| Efficiency of energy storage               | Ratio of heat/chill recovered to heat/chill delivered to subsurface (kBtu/kBtu)  | Metering data for thermal inputs and withdrawals from subsurface in the form of water flow rates and temperatures; subsurface temperature profiles | > 60% thermal energy (hot or cold) storage efficiency after system reaches operating temperatures  | Achieved. If the excess cooling load from building is removed from ground, temperature stabilizes   |
| Availability                               | Percentage of time system is operational or ready to operated (days/days)  | System monitoring  | > 95%  | Achieved. Note that antifreeze is required in ground loop.  |
| Reliability                                | Percentage of time system performs as designed (days/days)   | System monitoring  | > 95%  | Likely achieved. Note that antifreeze is required in ground loop, some sensor malfunctions noted  |
| <b>Qualitative Performance Objectives</b>  |  |  |  |   |
| Ease of implementation                     | Ability of an engineer experienced with ground source heat pump systems to use the technology  | Feedback from the project engineer and base engineers on usability of the technology and time required to design system                            | An experienced ground source heat pump system engineer is able to design, install, and operate system with minimal additional training   | Achieved.   |

### **3.1. INCREASE ENERGY EFFICIENCY**

The objective was to demonstrate an increase in electrical energy efficiency of more than 15% compared to a conventional geothermal heat pump system without a dry fluid cooler. The primary building that was evaluated in this study had an existing geothermal heat pump system that was about 9 years old when the dry fluid cooler was added. At this time, the ground loop temperature was far above the desirable range for heat pump air conditioning. Over the course of two years of cooling using the dry fluid cooler, the ground loop temperature was reduced by about 10 degrees. Based on heat pump efficiency curves (Table 2.2), this reduction in temperature would lead to an energy efficiency increase of about 15 %. However, this increase in efficiency was more than offset by the electrical energy consumed by the dry fluid cooler as it was removing the excess heat from the system. In other words, the dry fluid cooler was working to remediate the thermal damage done to the ground loop system over the previous 9 years.

A better comparison is to consider new geothermal heat pumps systems that are installed with and without dry fluid coolers (Sections 6 and 7). In this case, using a system that was optimized for the building during the first year of operation, both systems are efficient, and the ground loop temperature has not increased excessively. However, by 10 years of operation, the system with a dry fluid cooler is 11% more energy efficient than the system without a cooler. After 30 years of operation, the system with a dry fluid cooler is 18% more efficient.

This analysis assumed that the system without a dry fluid cooler could continue to operate with the very high ground loop temperatures. In reality, it would probably be necessary to add a cooling device just to keep the system operating.

### **3.2. NO INCREASE IN WATER USAGE**

Unlike a cooling tower, which evaporates water to perform cooling, a dry fluid cooler operates on a closed water loop and does not consume any water.

### **3.3. REDUCE CARBON FOOTPRINT**

The lifetime carbon footprint of these HVAC systems is related to their large consumption of electricity. The reduction in the carbon footprint is therefore proportional to the increase in electrical efficiency described in the first Performance Objective.

### **3.4. SYSTEM ECONOMICS**

The system economics depend on whether or not the conventional geothermal heat pump system could continue to operate without a supplemental cooling device such as a dry fluid cooler. If that is the case, then the economic benefits accrue rather slowly as described in Section 3.1. It is shown in Section 7 that for an optimized system using the characteristics of the building studied, that it would take between 20 and 25 years to recover the cost of the dry fluid cooler from energy

savings (assuming an energy inflation rate of 5% and a general inflation rate of 2%). On that basis, the system economics success criteria listed in Table 3.1 would not be met.

On the other hand, it is likely that a supplemental cooling device would eventually be required in order to keep the geothermal heat pump system running. If that is the case, it is much better to install the cooling device from the start and avoid the high ground loop temperatures that occur after several years of operation. Since the cost of the cooler would be included in both systems (although at different times), the system that used the cooler from the start as proposed here would achieve significant energy cost savings at almost no capital cost.

### **3.5. EFFICIENCY OF ENERGY STORAGE**

The analyses shown in Section 6 show that the key to maintaining favorable ground loop temperatures is to approximately balance the heat load to the ground on a yearly basis. For the building studied, most of the heat (74%) enters the ground loop in the months of April through September. The analysis shows that if a similar amount of the heat is removed in the cooler months of October through March, that the system temperature can be stabilized. This indicates an annual thermal storage efficiency that is much higher than 60%.

### **3.6. AVAILABILITY**

The systems were available more than 95% of the time except that two of the dry fluid coolers suffered severe freeze damage. This could be avoided by using a propylene glycol antifreeze solution in the ground loop.

### **3.7. RELIABILITY**

The system reliability was probably more than 95% not considering the freeze damage. There were occasional problems with the data collection and storage system, but these did not appear to affect the cooler operation. It is important, however, to periodically verify that the system controls have not been altered from the desired settings by local maintenance personnel.

### **3.8. EASE OF IMPLEMENTATION**

An experienced geothermal heat pump system engineer would be able to design, install, and operate this system with minimal additional training.



## 4.0 FACILITY/SITE DESCRIPTION

### 4.1 FACILITY/SITE LOCATION AND OPERATIONS

This project was performed at the Marine Corps Air Station, Beaufort, SC (MCAS Beaufort). MCAS Beaufort is located near the coast of South Carolina near the town of Beaufort (Figure 4.1). The air station supports establishment operations for the 2<sup>nd</sup> Marine Aircraft Wing, attached II MEF units, and Marine Corps Recruit Depot Parris Island/Eastern Recruiting Region. The site is located approximately 25 feet above sea level, and is adjacent to tidal salt water marshes and estuaries. This location is in the Atlantic Coastal Plain geologic province, and the subsurface is composed of unconsolidated sand, silt, and clay zones to a depth of more than 300 feet.

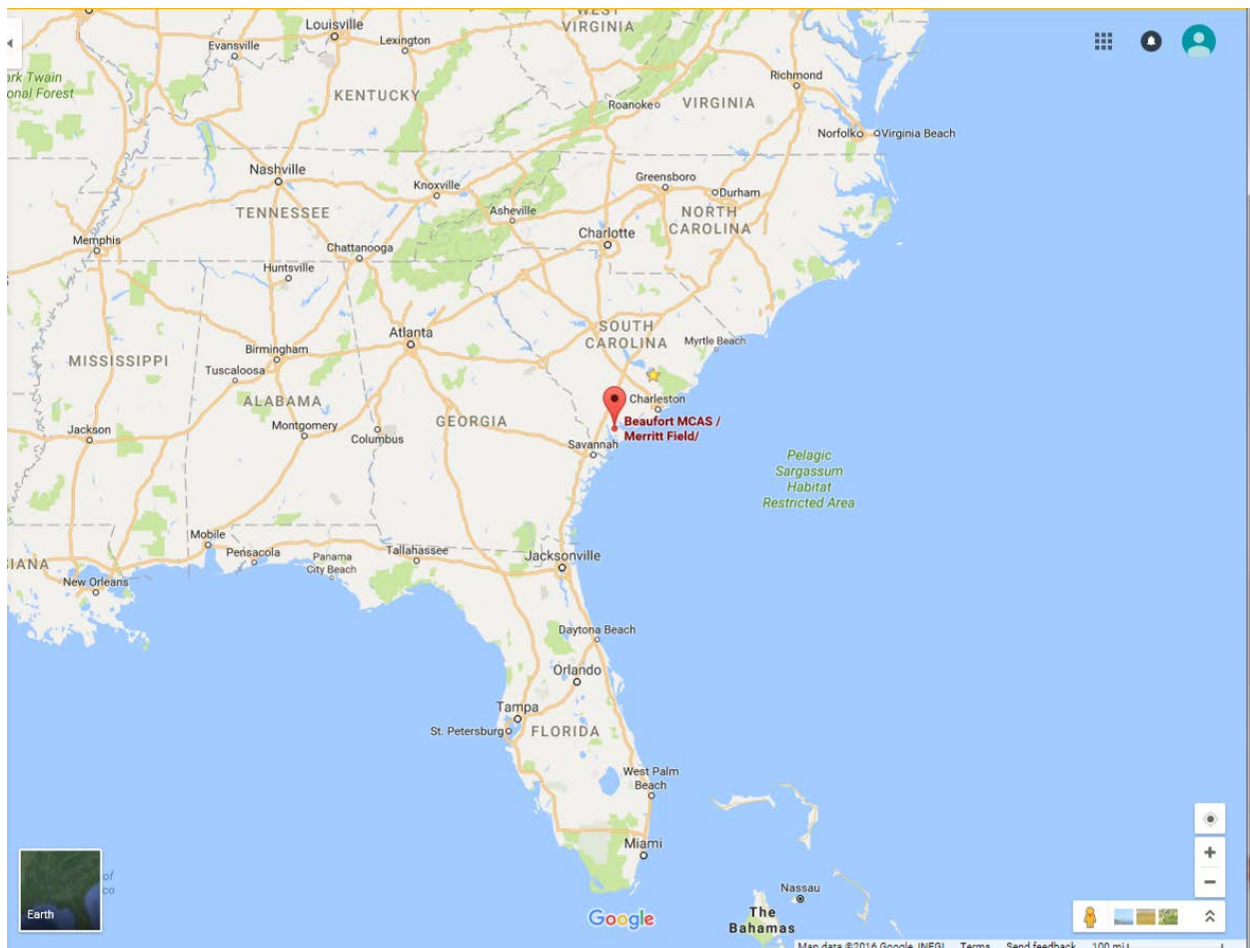


**Figure 4.1. MCAS Beaufort Location (Google Maps, 2016)**

The MCAS Beaufort has a large collection of buildings (approximately 30) and numerous single family houses that are cooled and heated using geothermal heat pumps. These heat pump systems use closed ground loops that consist of vertical boreholes that extend about 300 feet

deep. The borehole heat exchangers contain high density polyethylene (HDPE) U-tubes that are grouted in place.

Beaufort, SC has a humid subtropical climate, with an average high temperature of 90 degrees in July, and an average low temperature of 39 in January. The annual average temperature is 65.6 degrees, with an average rainfall of 49.76 inches.

## 4.2 FACILITY/SITE CONDITIONS

Three buildings that are heated and cooled with geothermal heat pumps were used in this demonstration. Building 601 is the Base Headquarters, Building 584 is the Military Police station, and Building 2085 is the Structural Fire Station (Figure 4.2). These buildings range in size from 12,500 to 24,000 sq. ft., and they have geothermal ground loops with between 24 and 39 borehole heat exchangers. At the start of this project, each of these buildings were suffering from high summertime ground loop temperatures due to the large cooling loads in the buildings compared to the heating loads.

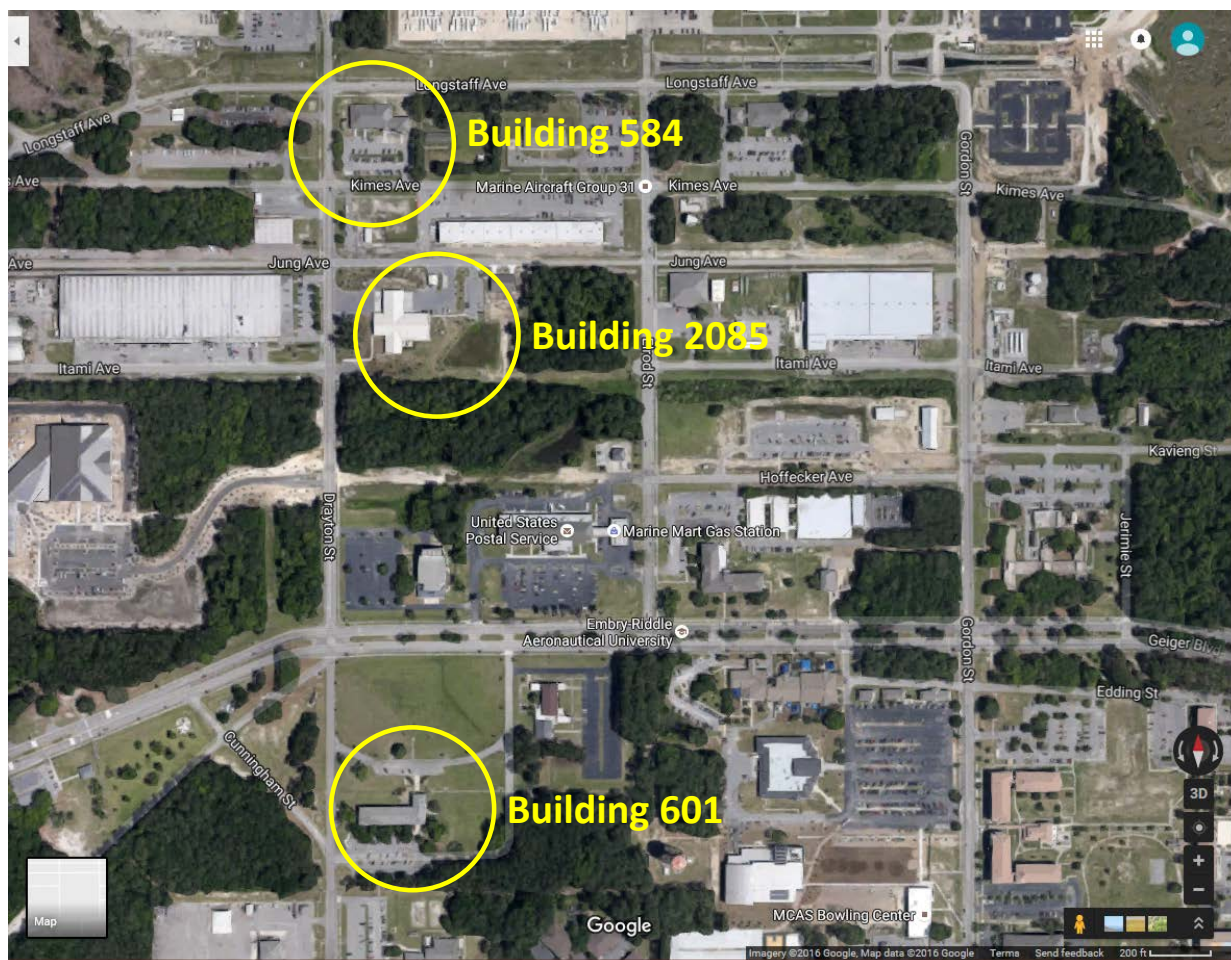


**Figure 4.2.** Building locations at the MCAS Beaufort (Google Maps, 2016).

## **5.0 TEST DESIGN**

### **5.1 CONCEPTUAL TEST DESIGN**

This test involved retrofitting the geothermal heat pump systems at three buildings with dry fluid coolers. The major parameter measured during this project was the geothermal ground loop water temperature entering and leaving the buildings. Those water temperatures indicate the amount of heat rejection or absorption by the heat pumps in the buildings, and they also reflect the deep subsurface temperature in and around the borehole heat exchangers. The ground loop temperatures were measured for at least several months prior to the installation of each dry fluid cooler.

Once the dry fluid coolers were installed, additional monitoring included the loop water temperature entering and leaving the dry fluid coolers, and the outside air temperature. The temperature differential between the entering water and the outside air was used to control the variable rate fan speeds on the dry fluid coolers to maximize efficiency of the coolers.

### **5.2 BASELINE CHARACTERIZATION**

At the Marine Corps Air Station in Beaufort, South Carolina, most of the major buildings are heated and cooled using geothermal heat pump systems. As part of this demonstration, three of these building ground loop systems were instrumented to collect data at 15 minute intervals over the past several years. These buildings include the Base Headquarters, Building 601, the Structural Fire Station, Building 2085, and the Military Police station, Building 584. These buildings range in size from 12,500 to 24,000 sq. ft, and have geothermal ground loops that consist of 24 to 39 vertical boreholes, each about 300 ft deep.

The heating and cooling loads in these buildings can be measured by comparing the geothermal loop temperature entering and leaving the building. During heat pump air conditioning, water from the borehole heat exchangers enters the building and absorbs the heat rejected by the heat pumps inside the building. The heated water exits the building, and is routed back into the boreholes. Similarly, during building heating, heat is extracted from the loop, and the loop temperature exiting the building is lower than the entering temperature.

Multiplying the loop entering and exiting temperature difference by the loop flowrate (and correcting the units) gives the building heating or cooling load at that point in time. Those data can be integrated with respect to time to get monthly and yearly values for the building heating and cooling loads.

The 3 buildings monitored as part of this project (Buildings 601, 2085, and 584) were found to be extremely cooling dominated on an annual basis. As evidenced by the 15 minute data, these buildings are mainly heated on cold winter nights and early mornings. At other times, the buildings are undergoing cooling, even in January.

#### **5.2.1 Building 584**

Figure 5.1 shows the 12,550 sq. ft. Military Police building (Building 584). This building was converted to a geothermal heat pump system in 2004, with 24 three-hundred foot deep borehole heat exchangers located beneath the parking lot.



Building 584 is a one-story 12,550 sq. ft. building that includes the original main building, and an annex. The main part of the building (9,700 sq. ft.) was constructed in 1959 with concrete block and insulating concrete with rigid foam. An annex (2,850 sq. ft.) was added in the early 2000's. The building is at least partially occupied at all times and it has a large number of interior rooms.



***Figure 5.1. Building 584, MCAS, Beaufort, SC.***

Prior to installation of the geothermal heat pump system, the building was cooled using a 39 ton air-cooled chiller with ice storage capacity. An analysis by Trane found that that system had a cooling energy efficiency ratio of only 4.8 kBTU/kW. The building was heated using high temperature hot water from the central heat plant at the Base

The Building 584 HVAC system was converted to geothermal heat pumps in 2004, using 24 three-hundred foot deep boreholes that are located beneath the parking lot in a U shape (Figure 5.2). The average horizontal spacing between these wells is about 20 ft., but the two long rows of boreholes are separated by about 60 ft.

Water exiting the building is split into three parallel streams that each feed the inlet side of 8 borehole heat exchanger U-tubes connected in parallel. The loop water exiting the borehole U-tubes returns in three parallel lines that connect to a single line that is routed back into the building and through the heat pumps inside the building. The ground loop flow is driven by a redundant pump system using a VFD. The flow rate is allowed to drop when the HVAC demand is low, and it increases to a maximum of about 80 gpm when the building loads are high. This variable pumping rate is used to reduce pump energy costs. The initial geothermal heat pump system used a single 35 ton Florida Heat Pump water to water heat pump. That single heat pump

was replaced in 2009 with 18 smaller Trane GEH series water source heat pumps that are distributed throughout the building.

Continuous monitoring of the Building 584 ground loop temperature entering and leaving the building began in August, 2012, with readings taken every 15 minutes. These data were stored and accessed using the base-wide web control system that is in place at the MCAS Beaufort. This system allows for conditions at any of the buildings to be monitored remotely, and selected data can be archived on the web control server.

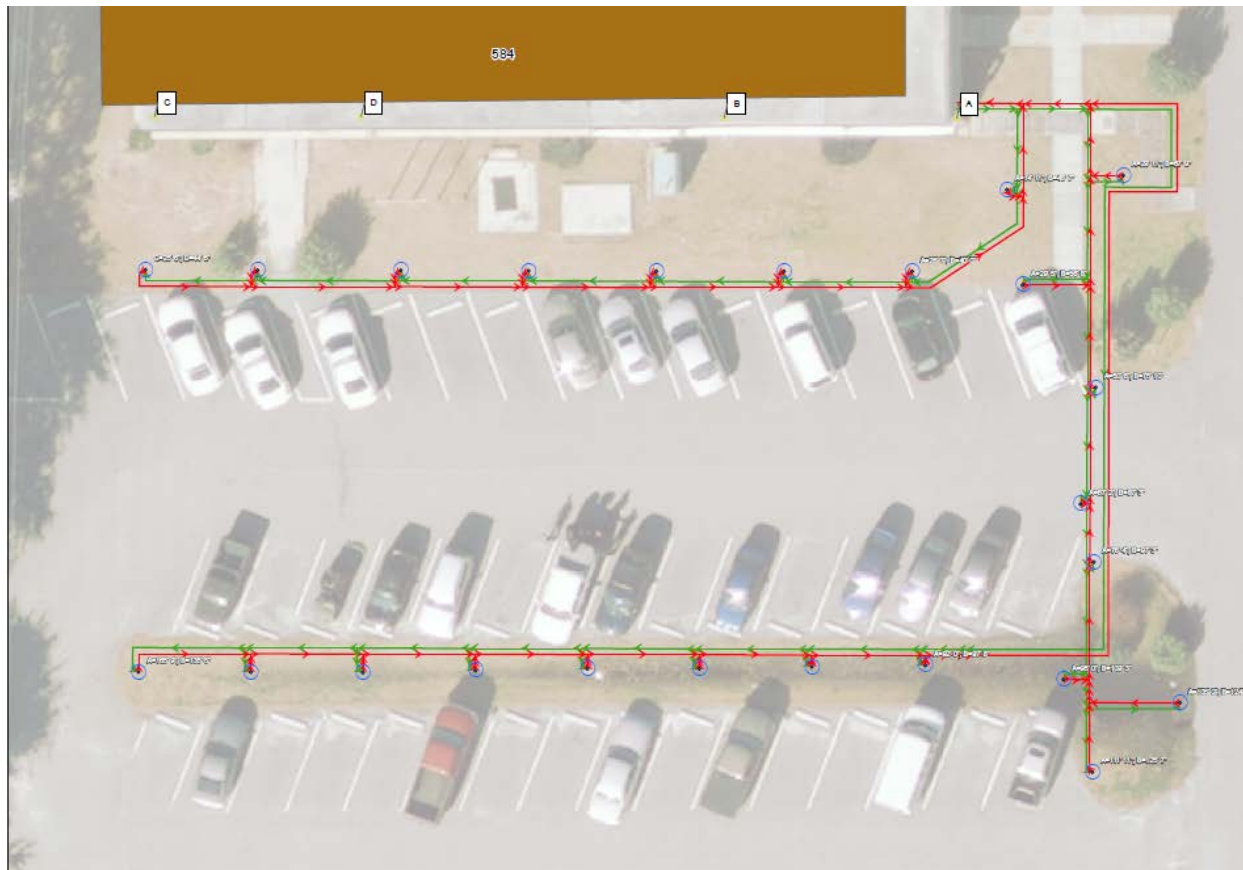


**Figure 5.2. Borehole heat exchanger locations for the Building 584 geothermal heat pump ground loop.**

The loop temperature and loop flow rate data from Building 584 were used to calculate building heating and cooling loads over the course of several years. The monthly average heating and cooling loads (kBtu per month) are listed in Table 5.1. Over the course of the year, 99.5% of the building load is for cooling. Buildings 601 and 2085 show a similar behavior, and are also extremely cooling dominated.

The continuous heat rejection from Building 584 and the other buildings at the MCAS Beaufort has led to increases in the ground loop temperatures over time. The undisturbed ground temperature below the depth of seasonal variation (a few tens of feet) is usually close to the average yearly air temperature. Using the model developed by Xing (2014) as implemented in

the GLHEPro program (IGSHPA, 2016), the ground temperature at Beaufort, SC is estimated to be 67 °F.

***Table 5.1. Average observed heating and cooling loads (kBTU) for Building 584 at the MCAS, Beaufort, SC.***

|           | heating | cooling   |
|-----------|---------|-----------|
| January   | 1844.00 | 21400.00  |
| February  | 2100.00 | 21623.00  |
| March     | 180.00  | 48880.00  |
| April     | 0.00    | 65600.00  |
| May       | 0.00    | 90241.00  |
| June      | 0.00    | 120208.00 |
| July      | 0.00    | 133906.00 |
| August    | 0.00    | 129393.00 |
| September | 0.00    | 111301.00 |
| October   | 0.00    | 80040.00  |
| November  | 256.00  | 34747.00  |
| December  | 105.00  | 32647.00  |

The August, 2012 ground loop temperatures for Building 584 are shown in Figure 5.3. The blue line shows the ground loop water temperature entering the building, and the red line shows the ground loop temperature leaving the building. The green line shows the outside air temperature. During this period, the building was continuously air conditioned, with peak cooling loads occurring in the late afternoons.

The measured ground loop temperatures from Building 584 during the latter half of January, 2013 are shown in Figure 5.4. Except for a few brief periods during cold nights, the exiting loop temperature is well above the entering loop temperature, indicating that the building is being cooled rather than heated.

The large cooling loads and small heating loads in Building 584 resulted in excessive ground loop temperatures in the summertime (Figure 5.3), with warm temperatures persisting through the year into the winter (Figure 5.4). By the summer of 2012, the ground loop temperature entering the building was consistently exceeding 95 °F, and the loop temperature leaving the building was exceeding 105 °F.

It is clear from Figures 5.3 and 5.4 that the geothermal ground loop temperatures for Building 584 were far above the background value. In particular, the late summer 2012 loop temperature entering the building was in the mid-90s, while the temperature leaving the building often exceeded 100 °F. These temperatures are far above the natural ground temperature, and are also well above the outside air temperature.

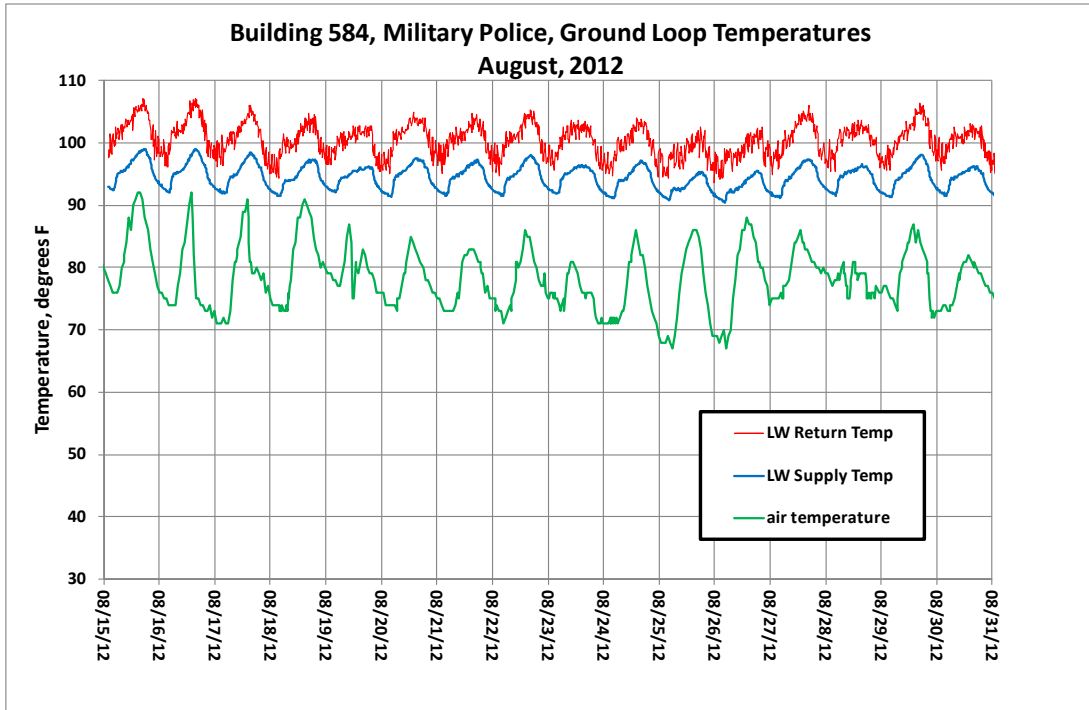


*Figure 5.3. Ground loop and outside air temperatures at Building 584 in August, 2012.*

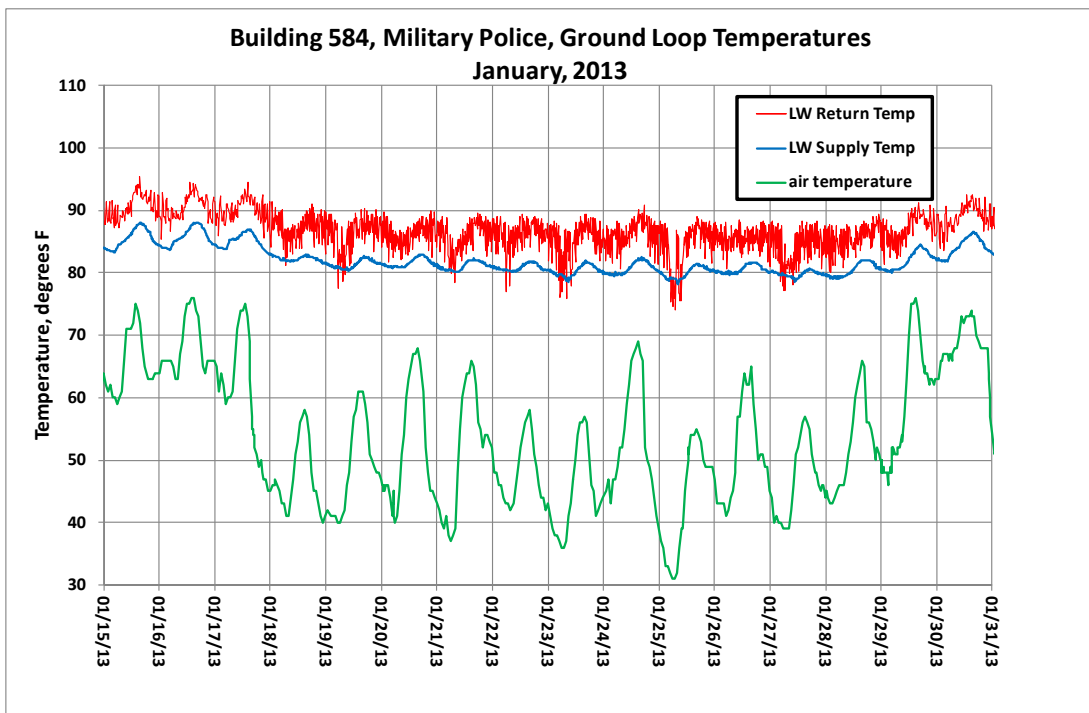


*Figure 5.4. Ground loop and outside air temperatures at Building 584 in January, 2013.*

### 5.2.2 Building 601

Building 601 (Figure 5.5) serves as the Base Headquarters/Administration Building at MCAS Beaufort. It contains the offices for the Commanding Officer and staff, and it houses a military court and a computer network room. The two-story 23,750 ft<sup>2</sup> building was originally constructed in 1958, and it has been updated several times over the years.

In 2004, heating, ventilation, and air conditioning system was converted to a ground source heat pump system (Trane, 2003). The current ground source heat pump system capacity is about 66 tons, served by a network of 39 borehole heat exchangers that are 300 feet deep (Figure 5.6). The heating and air conditioning system uses 47 console water to air geothermal heat pump units, located in the individual offices. These Trane heat pumps range in size from ½ ton (21 units) to 5 ton (3 units) capacity, depending on the size of the room served by the unit.

This building operates in a manner similar to a typical office building, and it is mainly occupied during normal working hours with very little use at night, on weekends, or during holidays.



**Figure 5.5. Building 601, MCAS Beaufort.**

An 8 fan variable rate Data Aire ® dry fluid cooler was added to Building 601 in 2010. This unit has a rated heat rejection capacity of about 60 to 80 tons at standard (summertime) operating conditions. This fluid cooler is primarily used to remove heat from building ventilation air in the summertime using a conventional hybrid type operation.



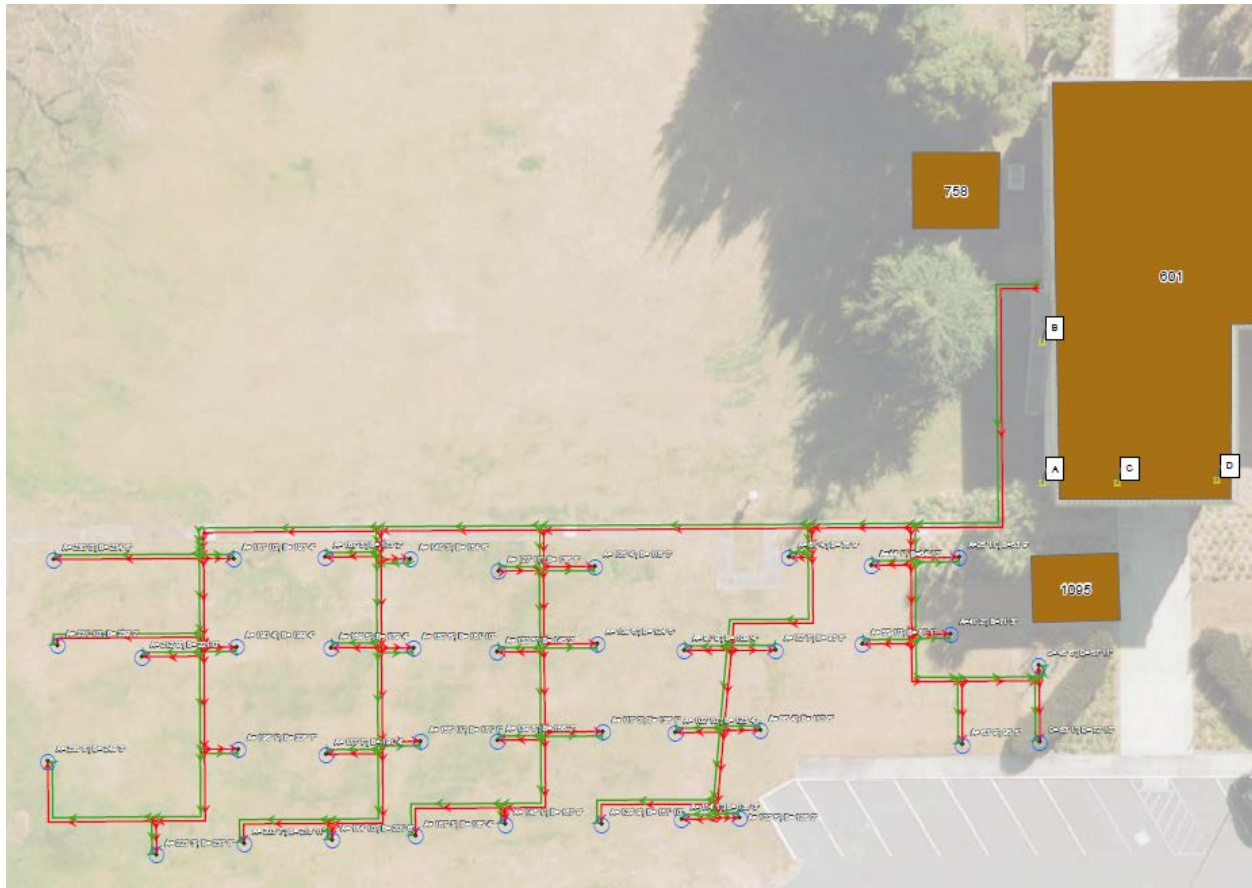


**Figure 5.6. Borehole heat exchanger locations for the Building 601 geothermal heat pump ground loop.**

The August, 2012 ground loop temperatures for Building 601 are shown in Figure 5.7. The ground loop temperatures (red and blue lines) are well above the background subsurface temperature, and are consistently higher than the outside air temperature. While these high loop temperatures reflect the unbalanced cooling load to the system, they are substantially lower than those observed at Building 584. These somewhat lower loop temperatures are likely due to the existing 8 fan dry fluid cooler. This cooler is operated using a conventional water temperature set point. During the summer, whenever the entering water temperature exceeds this set point, the cooler fans run, regardless of the outside temperature.

The Building 601 ground loop temperatures during the latter half of January, 2013 are shown in Figure 5.8. These data reflect a shutdown of the heat pump system during the Holiday weekend of January 19-21, and during the weekend of January 26-27. During those periods, the measured temperatures likely reflect the ambient temperature in the building mechanical room. These data show mixed heating and cooling (heating is observed when the loop temperature leaving the building is lower than the entering temperature). Although this ground loop was cooler than the one at Building 584, the loop temperatures were still well above the outside air temperature indicating that conditions were favorable for wintertime cooling of the loop with dry fluid coolers.

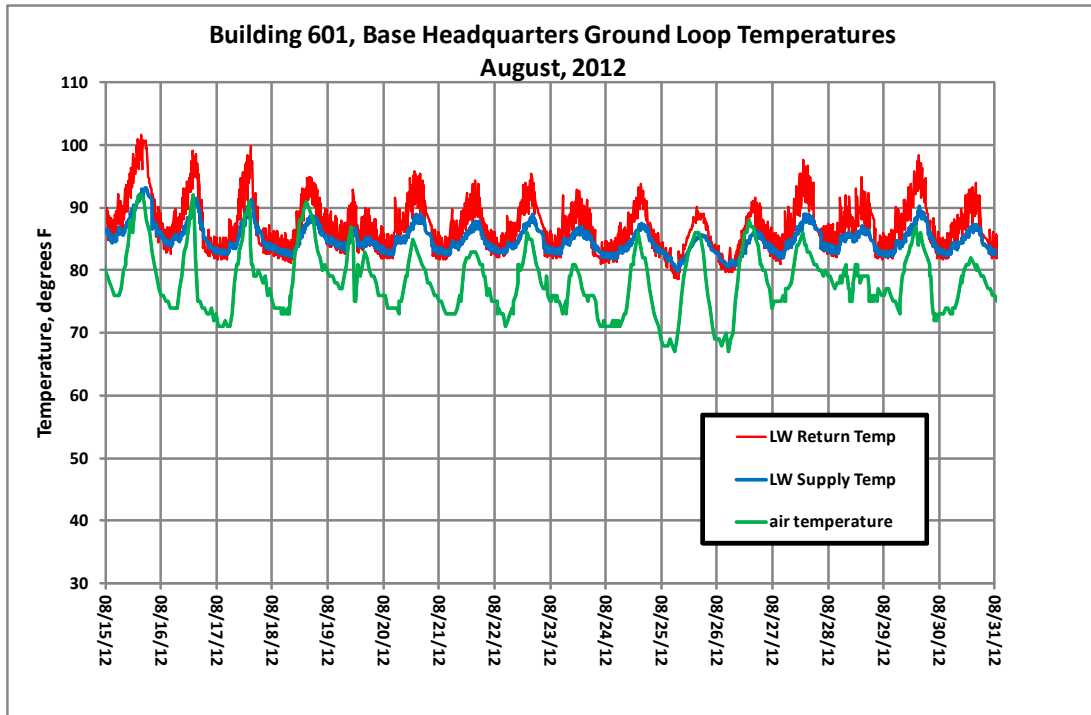


*Figure 5.7. Ground loop and outside air temperatures at Building 601 in August, 2012.*

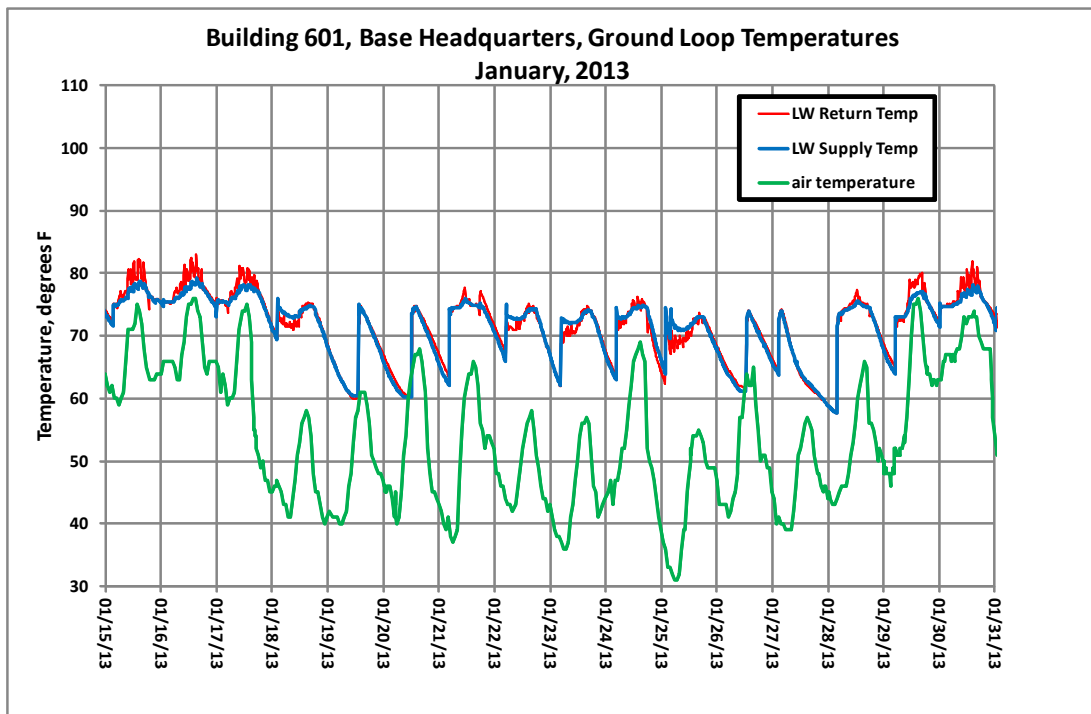


*Figure 5.8. Ground loop and outside air temperatures at Building 601 in January, 2013.*

### 5.2.3 Building 2085

Building 2085 (Figure 5.9) is the structural fire department building. It houses firefighters continuously, and contains a large high bay area. The 20,860 ft<sup>2</sup> building was constructed in 2010 with a geothermal heat pump HVAC system. This building operates continuously.



*Figure 5.9. Building 2085, MCAS Beaufort.*

The geothermal ground loop consists of 24 three-hundred foot deep borehole heat exchangers, installed in the field just to the east of the building (the lower part of the picture in Figure 5.9). The ground loop began to almost immediately heat up to temperatures well beyond the desirable range for heat pump operation.

The August, 2012 ground loop temperatures for Building 601 are shown in Figure 5.10. The ground loop temperatures (red and blue lines) at this time were well above 100 degrees, even though the building had only been in operation for 2 years. This was clearly an unsustainable condition.

The Building 601 ground loop temperatures during the latter half of January, 2013 are shown in Figure 5.11. Although the loop temperatures were cooler, the conditions are good for heat removal using a dry fluid cooler.

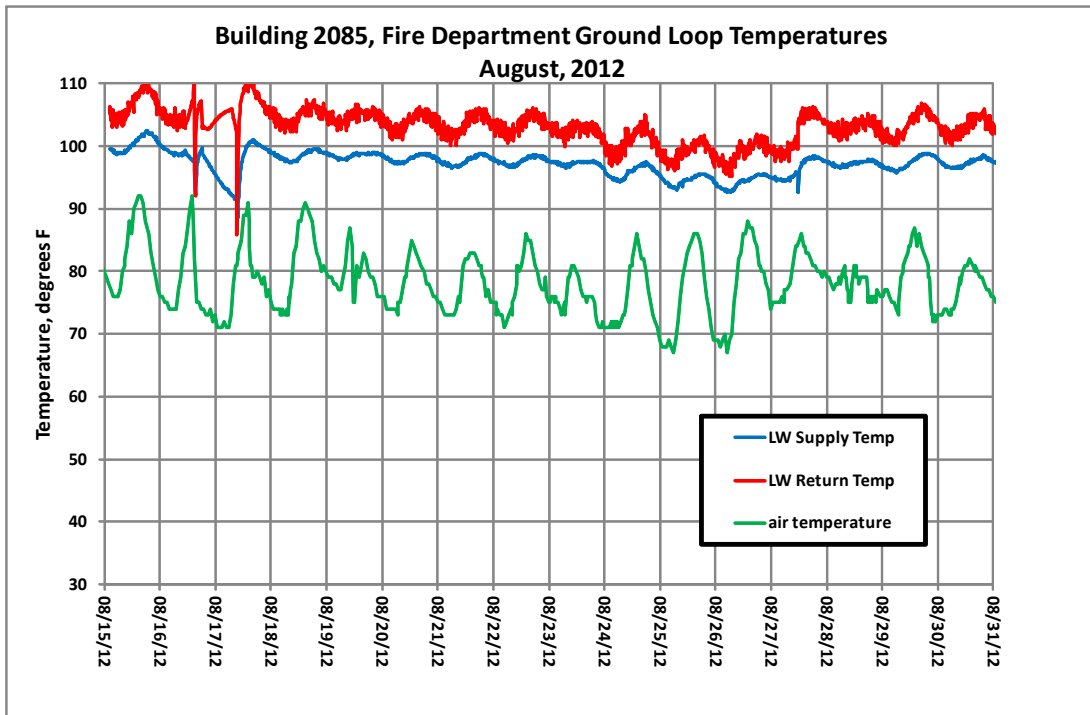


*Figure 5.10. Ground loop and outside air temperatures at Building 2085 in August, 2012.*

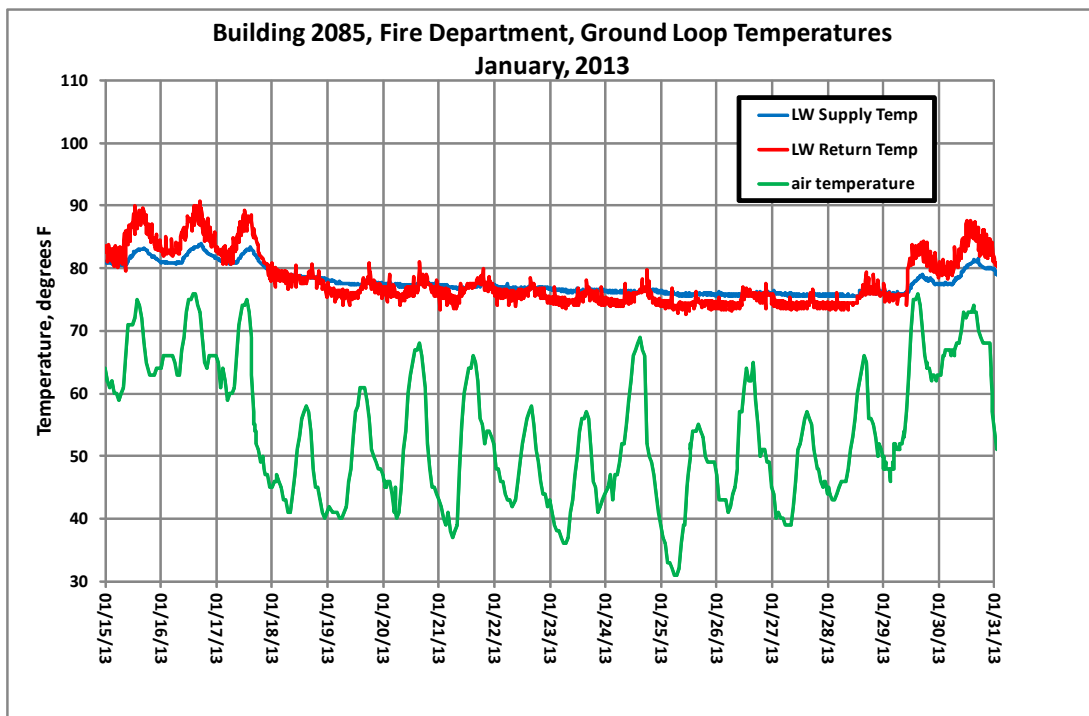


*Figure 5.11. Ground loop and outside air temperatures at Building 2085 in January, 2013.*



## 5.3 DESIGN AND LAYOUT OF TECHNOLOGY COMPONENTS

### 5.3.1 Building 584 Dry Fluid Cooler

The geothermal heat pump system at Building 584 was modified in late October, 2013 to include a 96 ton Technical Systems FC-96-1195 dry fluid cooler (Figure 5.12). This 8 fan cooler is the largest size built by the manufacturer, and it consists of two rows of 4 VFD fans with separate controls for each row. The cooler was installed adjacent to the building, close to the location where the ground loop enters and exits the building (Figure 5.12).



***Figure 5.12. Dry fluid cooler installed at Building 584.***

A small wooden shadow fence was installed around part of the cooler for aesthetic reasons. Additional system monitoring was added at this time, including the local outside air temperature, ground loop flow rate, temperatures entering and exiting the dry fluid cooler, and the dry fluid cooler fan speeds for each row of fans. All of these data are accessed and stored using the Base web control system. Continuous data have been collected from this system since December, 2013. A schematic diagram of the ground loop and dry fluid cooler configuration from the web control system is shown in Figure 5.13.

Ground loop water exiting the building enters the dry fluid cooler before continuing on to the borehole heat exchangers. The fan speeds for the two stages of fans are controlled based on the temperature difference between the outside air and the entering loop temperature. The fans begin operating when the temperature difference exceeds 5 °F, and they ramp linearly to 100% fan speed when the temperature difference reaches 20 °F. This program allows for year-round

operation, but fan speeds are higher in the wintertime, when the difference between the air temperature and the water temperature entering the cooler is larger.

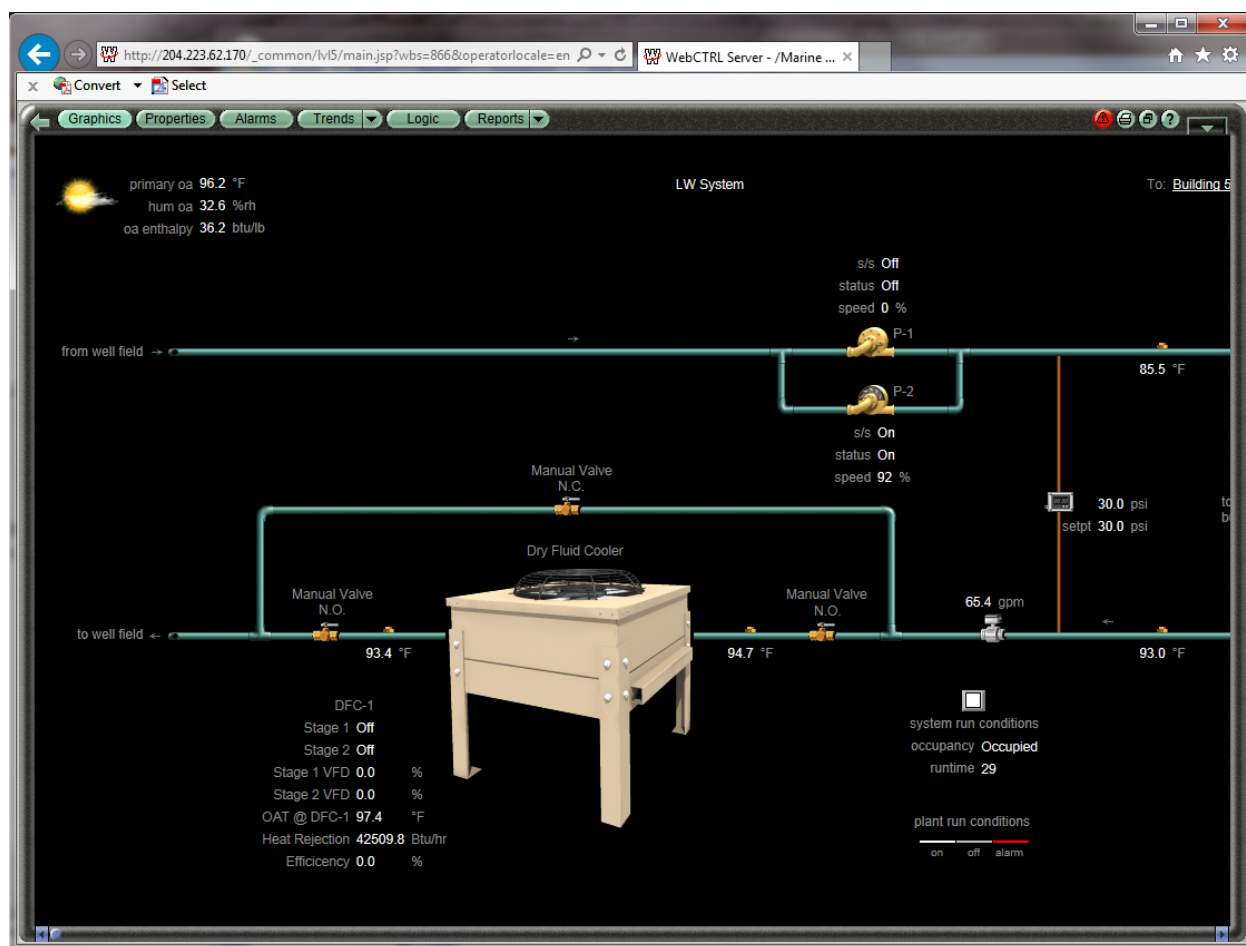


**Figure 5.13.** Layout of the Building 584 dry fluid cooler and ground loop piping.

### 5.3.2 Building 601 Dry Fluid Cooler Addition

A 96 ton Technical systems FC-96-1195 dry fluid cooler was added to the Building 601 heat pump loop in May, 2013 (Figure 5.14). This new unit was added to the existing 8 fan dry fluid cooler with a fairly complex piping and valve configuration that allows for the two coolers to be operated in series, in parallel, or for either or both coolers to be isolated from the ground loop (Figure 5.15). Under normal operation, water in the ground loop leaves the building, and flows through the new dry fluid cooler, then through the existing cooler, and on to the borehole heat exchangers. The VFD fans on the new dry fluid cooler operate on the same type of temperature ramp as those on the Building 584 cooler, where the fan speed depends on the temperature difference between the incoming water and the outside air.



**Figure 5.14. Dry fluid cooler installed in series with an existing cooler at Building 601.**

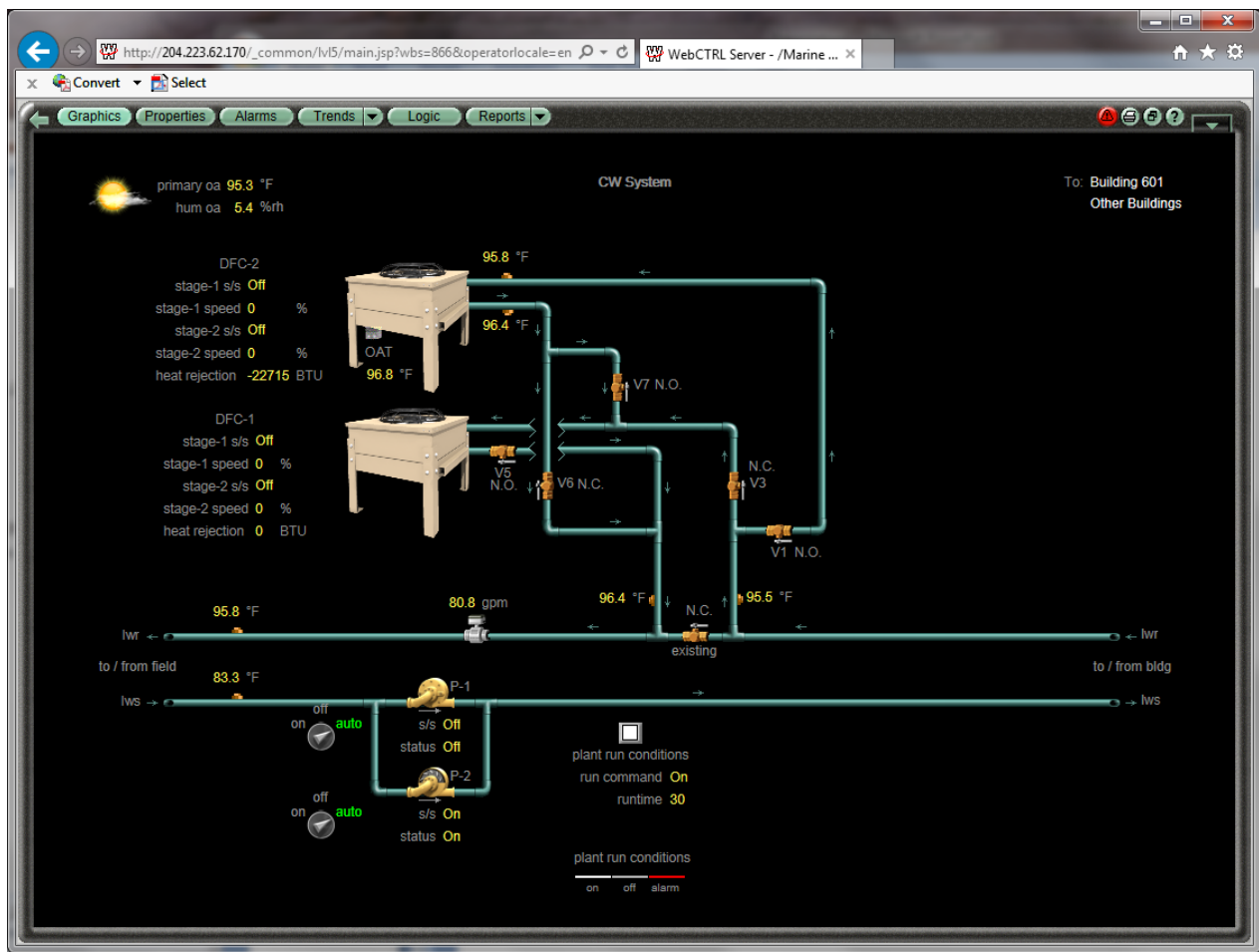


**Figure 5.15. Layout of the Building 601 dry fluid coolers and ground loop piping.**



A set of four 300 foot deep temperature monitoring wells were installed in and around the Building 601 borehole heat exchangers during the summer of 2013. One monitoring well was installed just north of the heat exchangers, one was installed about 25 feet south of the heat exchangers, and two were installed inside the field of heat exchangers (Figure 5.16). These monitoring wells are constructed in a manner very similar to the borehole heat exchangers, with HDPE U-tubes that were grouted in place (Figure 5.17).

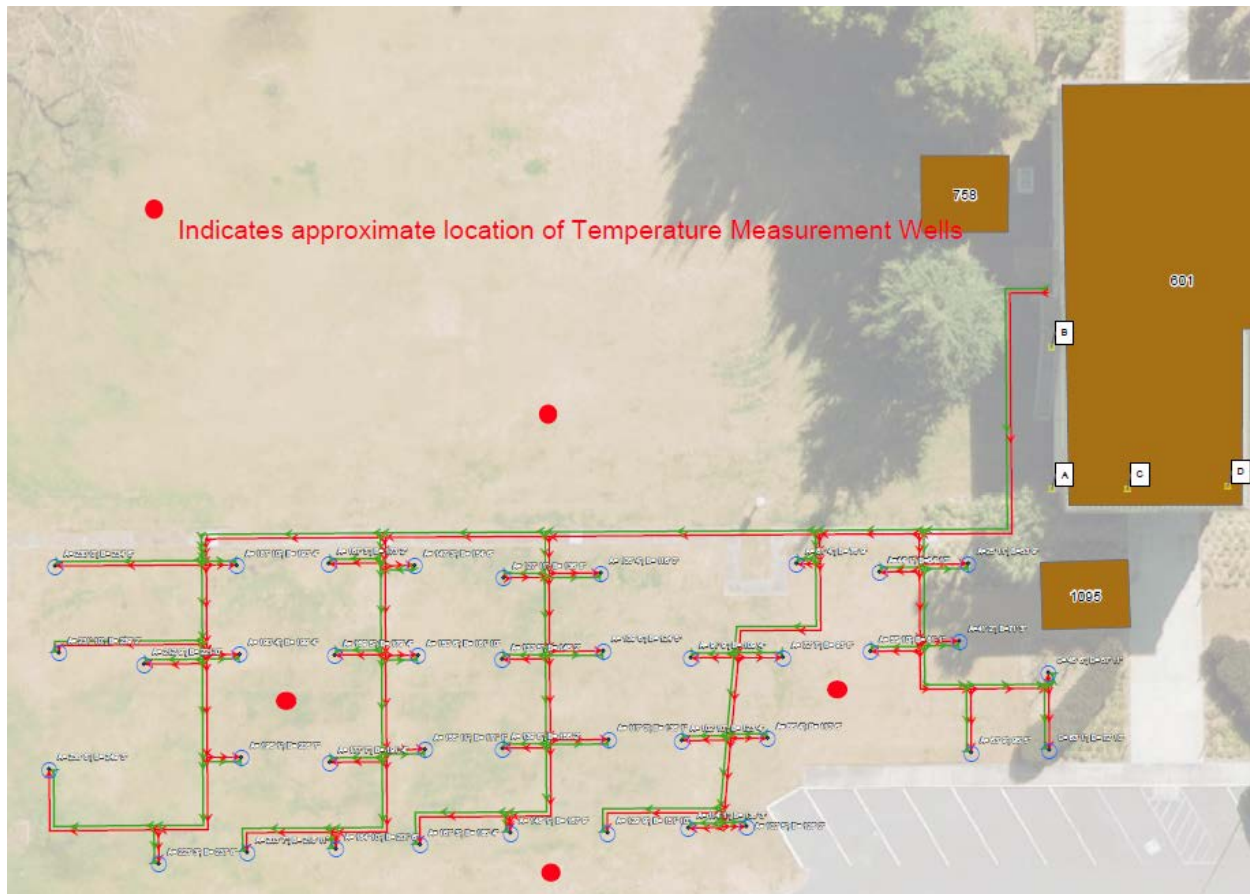


**Figure 5.16.** Location of four 300 foot deep temperature monitoring wells installed in and around the Building 601 borehole heat exchangers (the north direction is pointing down in this figure).

The vertical temperature profiles in these locations were measured periodically using a Solinst 107 TLC LM3/100m temperature probe that is attached to a 100m long marked cable. An initial test of the probe was made by recording the temperature versus depth as the probe was lowered in the U-tube in a monitoring well. This profile was compared to the temperature profile recorded as the probe was brought back up the well. This comparison showed that at any particular depth, the temperature results were repeatable to within 0.2 degrees F.



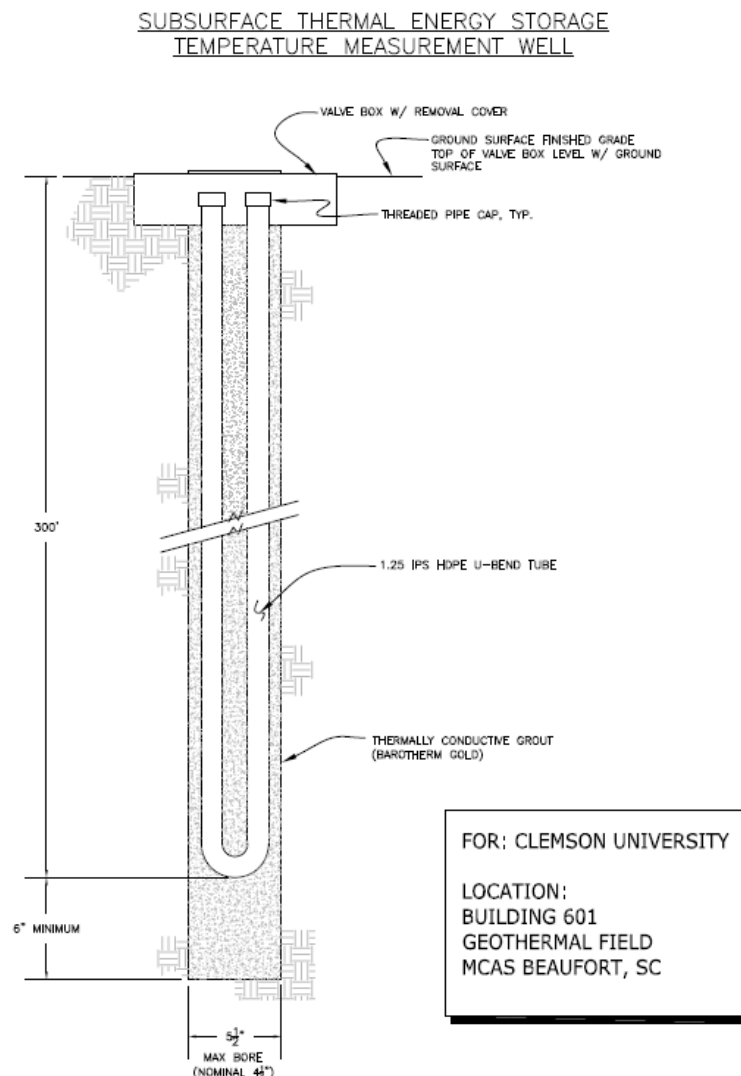


**Figure 5.17. Design of the temperature monitoring wells.**

In addition to the periodic temperature logging, a dedicated temperature probe was installed in the eastern temperature monitoring well at a depth of 190 feet at the end of October, 2013. This device, a Solinst 3001 LT Levellogger Edge M100/F300 was set to record the temperature every day, and was left in the ground through 2016.

### 5.3.3 Building 2085 Dry Fluid Cooler

A 96 ton dry fluid cooler was installed in the Building 2085 ground loop in October, 2013 (Figure 5.18). This cooler was connected to the ground loop as it leaves the building, before

entering the borehole heat exchangers. The VDF fans on the dry fluid cooler are controlled by the temperature difference between the entering water and the outside air.



*Figure 5.18. Dry fluid cooler installed at Building 2085.*

## **5.4 OPERATIONAL TESTING**

Figure 5.19 shows typical wintertime operation of the dry fluid cooler – geothermal heat pump system at Building 584. This graph shows 5 days of operation in December, 2014, with the cooler fan speed (black line), the ground loop water temperature entering the building (blue line), the ground loop water temperature leaving the building (purple line), the water temperature leaving the dry fluid cooler (dark red line), and the outside air temperature. The cooler fan speed is controlled by the difference in the outside air temperature (green line), and the loop temperature leaving the building (purple line).

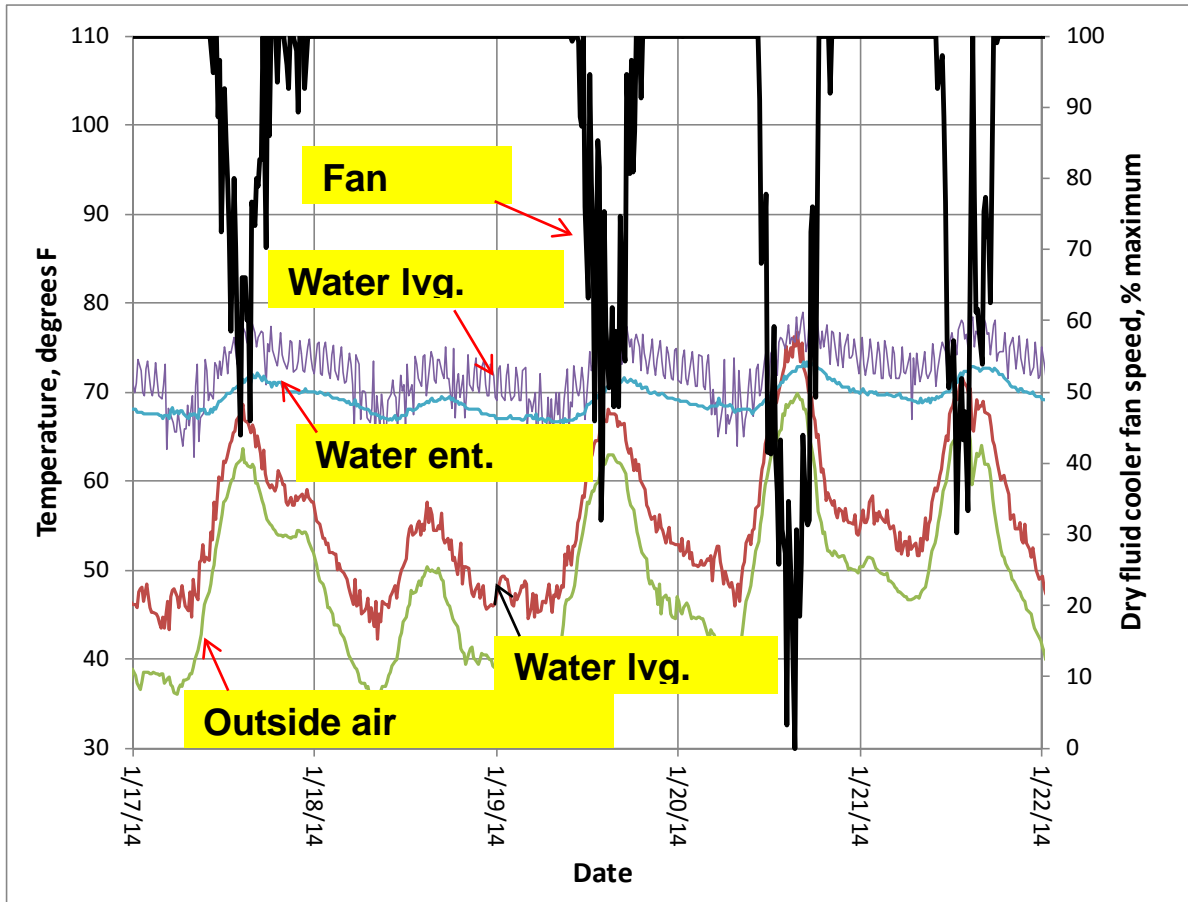


**Figure 5.19. Typical wintertime operation of the dry fluid cooler and geothermal heat pump system at Building 584.**

At night, when the air temperature is cold, the loop temperature leaving the building remains relatively warm, and the fans run at 100%. This results in a substantial amount of heat rejection by the fluid cooler, and the temperature leaving the cooler is low (dark red line), often as cool as 45 °F. That cold water flows through the borehole heat exchangers, extracting heat from the ground before re-entering the building (blue line).

On days with warm afternoons, the outside air temperature started to approach the loop temperature entering the dry fluid cooler, and the fan speed ramped down. As this happens, the rate of heat rejection from the cooler decreases, and the temperature leaving the cooler (dark red line) is closer to the temperature leaving the building.

The summertime operation of the cooler is similar, but the outside air temperature tends to be closer to (or above) the loop temperature leaving the building, so the fans are often not running, or are running at low speeds. They only very rarely reach 100% fan speed in the summer with the control program.

## **6.0 PERFORMANCE ASSESSMENT**

### **6.1 BUILDING 584**

#### **6.1.1 Ground Loop Temperature Data**

The dry fluid cooler was installed in late October, 2013, and data collection began in early December, 2013. The cooler has been in continuous operation since then. Data collection has also been continuous, but data from the cooler were lost on three occasions due to malfunctions of the data collection or web control server. As of June, 2016, there were 18 months of high quality data collected from the system.

The dry fluid cooler had a rapid effect on the ground loop temperature. The loop temperatures in January, 2014 are shown in Figure 6.1. Compared to the previous January, the ground loop temperature was about 13 degrees lower, with an average loop entering temperature of 69° F. During the first summer of operation, the ground loop temperatures were reduced by about 8 °F compared to the previous summer. The summer of 2014 was unusually warm, with record, or near record temperatures. During the latter half of August, the outside air temperature recorded at the dry fluid cooler exceed 100 °F on five days (Figure 6.2). The average ground loop entering temperature during this period was 87.1 °F, compared to 94.8 °F the previous August.

After the first year of operation, the ground loop temperatures appeared to stabilize with some additional cooling. In the second half of August, 2015 (Figure 6.3), the average ground loop supply temperature was 84.4 °F, which is more than 10 degrees cooler than the late August loop temperature prior to adding the cooler (see Figure 5.4).

The average summer loop temperature over the past several years was computed by averaging the 15 minute readings for the months of June, July, August, and September. In 2013, before adding the dry fluid cooler, the entering loop temperature averaged 94.1 °F. In 2014, after one season of cooler operation, the entering loop temperature averaged 85.6 °F, and in 2015 it averaged 84.8 °F.

As will be discussed later, it should be possible to reduce the ground loop temperatures further with some adjustment to the ground loop pumping system and dry fluid cooler control.

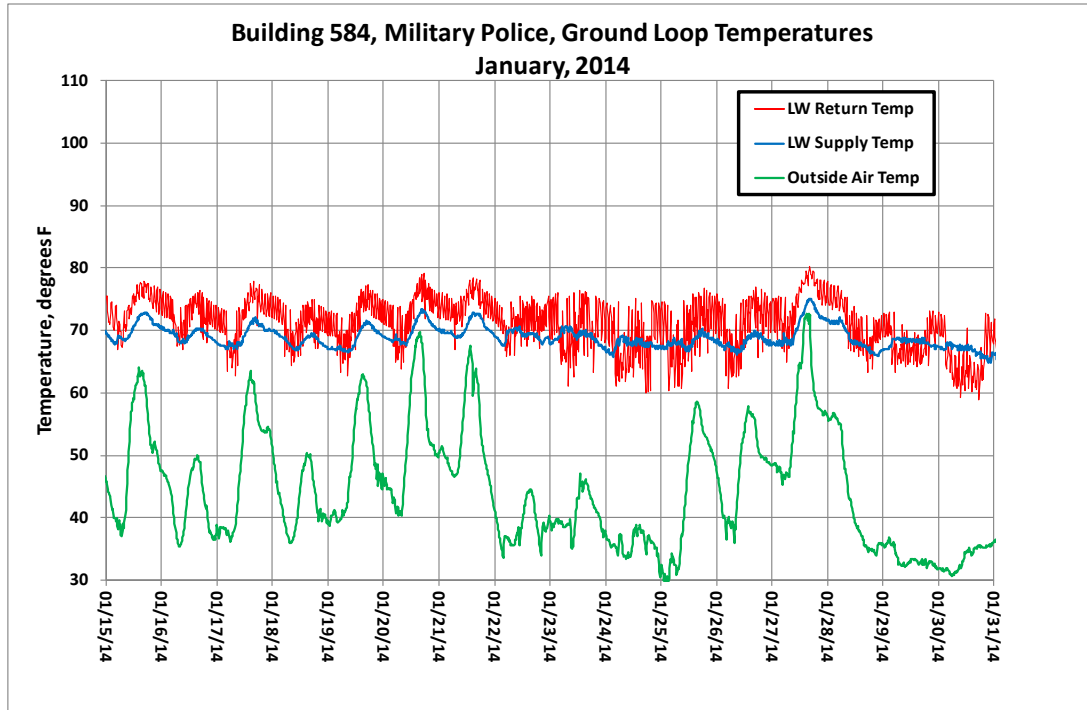


*Figure 6.1. Ground loop temperatures at Building 584 in January 2014.*

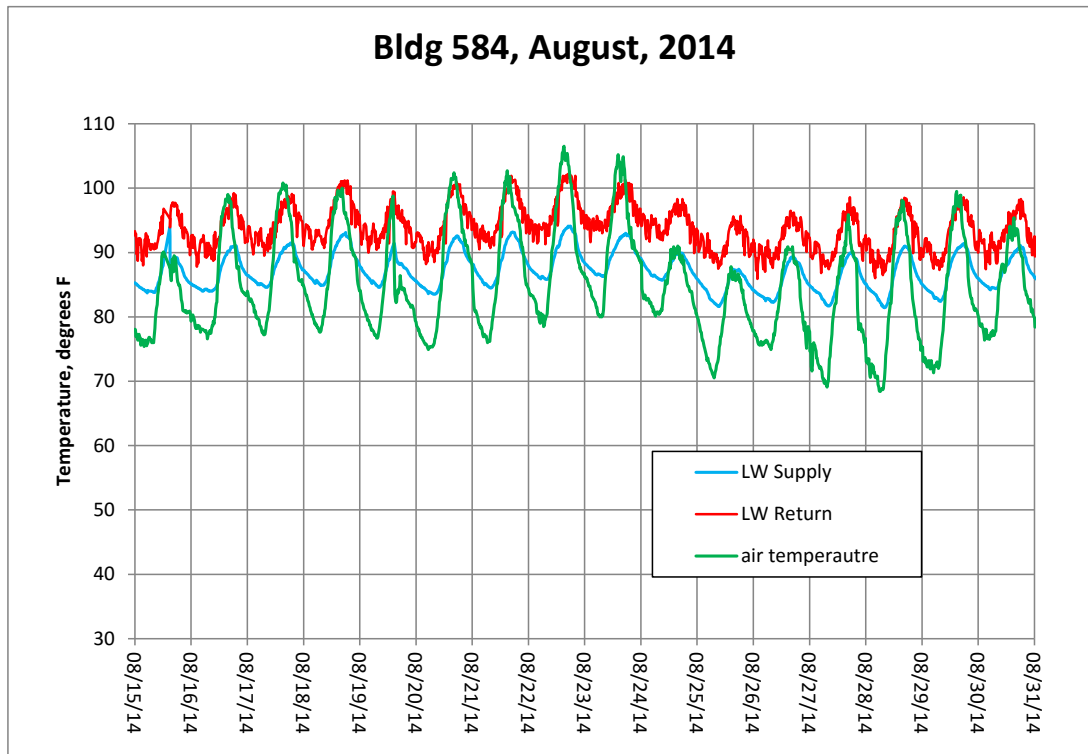


*Figure 6.2. Ground loop temperatures in Building 584 in August, 2014.*

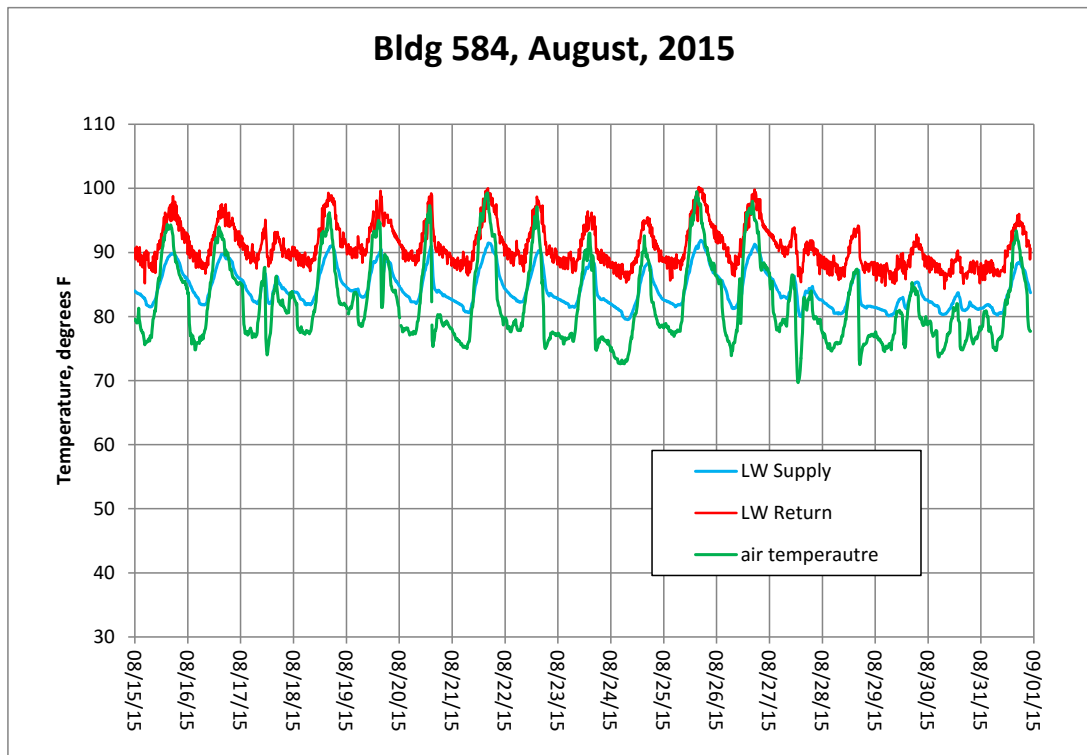


**Figure 6.3. Ground loop temperatures in Building 584 in August, 2015.**

The dry fluid cooler heat rejection at Building 584 was calculated for each 15 minute measurement interval using the loop flow rate, and the temperature difference between the water entering and leaving the cooler. These data were integrated to get monthly heat rejection values over the 3 year measuring period (Table 6.1). These results show that the dry fluid cooler heat rejection was relatively uniform during the year (the result for November is probably not reliable due to problems with the data collection system during that month).

Over the course of a year, the dry fluid cooler has been rejecting about 1.09 million kBTUs from the ground loop. The amount of heat rejected from the building into the ground loop includes the normal building cooling load and the waste heat from the heat pumps, minus the building heating load. These data were shown previously in Table 5.1 for Building 584. Over a year, about 886,000 kBTUs were rejected into the ground loop. Prior to the installation of the dry fluid cooler, this load imbalance had resulted in dramatic heating of the borehole heat exchangers. However, this trend has been reversed following installation of the dry fluid cooler, because now there is a net heat removal from the ground loop of about 204,000 kBTUs per year. This heat removal has allowed the ground loop to cool by about 10 degrees over the last couple of years. In other words, the ground loop/borehole heat exchanger system at Building 584 is currently being rehabilitated following years of excessive heat rejection.

**Table 6.1. Average monthly heat rejection by the Building 584 dry fluid cooler, kBTU.**

| Month     | heat rejection |
|-----------|----------------|
| January   | 97058.62       |
| February  | 100276.00      |
| March     | 79951.79       |
| April     | 80517.20       |
| May       | 75150.23       |
| June      | 82211.34       |
| July      | 92744.25       |
| August    | 98950.29       |
| September | 103201.42      |
| October   | 103448.14      |
| November  | 75978.03       |
| December  | 98823.06       |

It would be expected that the rate of heat rejection by the cooler should have been substantially larger in the wintertime due to the larger average temperature difference between the entering water temperature and the outside air temperature. This was not the case, however, due to the variable flow rate ground loop water pumps. When operated at 100%, the loop pumping rate is about 80 gpm, but this rate was reduced to levels as low as 10 gpm during periods when the building load was small. These low-load periods mainly occur in the wintertime, and the resulting low flowrate greatly reduces the efficiency of the dry fluid cooler.

During the initial operation of the dry fluid cooler, before the control system was fully implemented, there were periods where the fan ran at 100% regardless of the water/air temperature difference. These data were normalized by computing the heat rejection rate (from the loop flowrate and the temperature drop entering and exiting the cooler), and dividing it by the temperature difference between the incoming water and the outside air. This ratio, in units of kBTU/hr/ $\Delta T$ , gives the relative cooler performance. The observed dry fluid cooler performance is plotted as a function of the loop flowrate in Figure 6.4. The cooler performance is essentially a linear function of the loop flowrate over the range of observed values.

At low loop flowrates, the rate of heat rejection per degree of temperature difference is very low, only a few kBTU/hr/ $\Delta T$ . This rate increases to a maximum of about 22 kBTU/hr/ $\Delta T$  at the maximum flowrate of about 80 gpm. Manufacturers data for the FC-96 cooler are consistent with our measurements, and show approximately linear performance up to a flow rate of about 120 gpm. From 120 gpm to about 250 gpm, the cooler performance becomes only a weak function of temperature, with heat rejection rates varying from about 31 to 38 kBTU/hr/ $\Delta T$ .

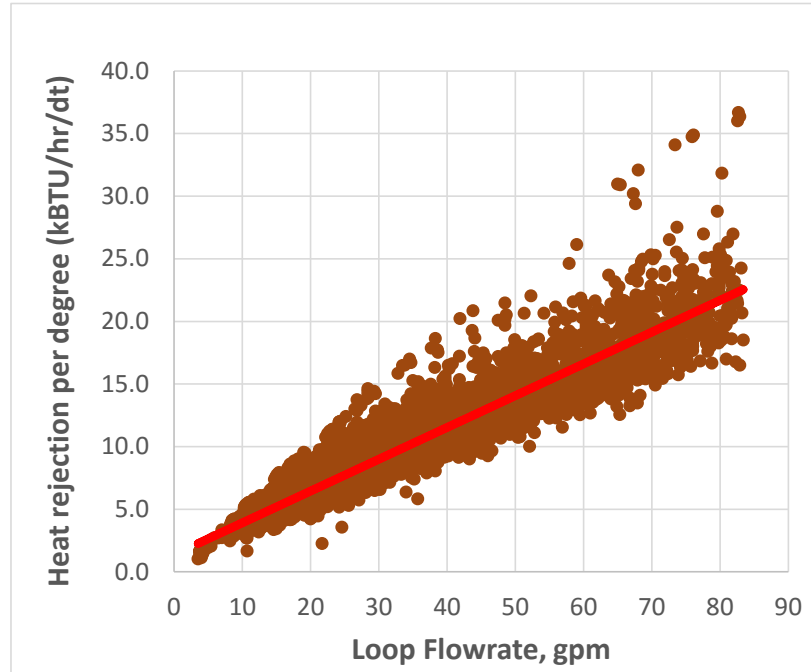


**Figure 6.4. Observed dry fluid cooler normalized heat rejection (kBTU/hr/ΔT) as a function of the ground loop flowrate with cooler fans operating at 100%.**

While the VFD controlled loop water pump at Building 584 reduces water pumping costs, it has a negative effect on the performance of the dry fluid cooler, which would operate much more efficiently at a constant flowrate of 80 gpm or more. It is also apparent that similar heat rejection rates could be achieved using a smaller dry fluid cooler (such as a 4 fan FC-48) that is designed for lower flowrates than the FC-96. From the manufacturers data, an FC-48-597A, operating at 80 gpm and 100% fan speed has a heat rejection rating of about 20.4 kBTU/hr/ΔT, which is similar to the performance observed with the larger fluid cooler (Figure 2.6).

The electrical energy used by the dry fluid cooler was calculated using the fan speed data that were collected every 15 minutes. The dry fluid cooler at Building 584 has 8 one-horsepower electric fans. When these fans operate at 100% fan speed, the electrical power is 6 kW. As the fan speed is reduced, the power drops by the cube of the fan speed, so at 50% fan speed, the electrical power use is only 0.75 kW. The fan electrical energy use was integrated over time to get monthly values. An additional power cost for using the dry fluid cooler is due to pumping costs to overcome the water pressure drop in the cooler. At the low flowrates used in this application these pumping costs are very small, but they become significant as the flowrate increases relative to the size of the cooler.

The average monthly dry fluid cooler heat rejection, electrical energy use, energy efficiency ratio, loop flowrate, fan speed, and temperature difference between the entering water and outside air are shown in Table 6.2 (as in Table 6.1, the November results for heat rejection and EER are probably not reliable).



**Table 6.2. Monthly average dry fluid cooler data from Building 584.**

|           | heat reject. | electricity | EER        | flowrate | fan speed | delta T  |
|-----------|--------------|-------------|------------|----------|-----------|----------|
| Month     | kBTU         | kWhr        | kBTU/hr/kW | gpm      | % max     | degree F |
| January   | 97058.62     | 3053.74     | 31.78      | 17.49    | 74.52     | 26.19    |
| February  | 100276.00    | 2473.01     | 40.55      | 32.78    | 70.56     | 18.53    |
| March     | 79951.79     | 1460.04     | 54.76      | 43.54    | 49.53     | 12.88    |
| April     | 80517.20     | 1626.77     | 49.50      | 40.91    | 53.58     | 12.81    |
| May       | 75150.23     | 1945.50     | 38.63      | 49.10    | 56.46     | 10.43    |
| June      | 82211.34     | 555.52      | 147.99     | 52.21    | 32.01     | 9.52     |
| July      | 92744.25     | 601.59      | 154.16     | 53.34    | 32.81     | 9.96     |
| August    | 98950.29     | 618.03      | 160.11     | 51.88    | 35.17     | 10.26    |
| September | 103201.42    | 1033.49     | 99.86      | 50.79    | 48.90     | 12.32    |
| October   | 103448.14    | 2028.20     | 51.00      | 42.10    | 63.64     | 15.33    |
| November  | 75978.03     | 3231.51     | 23.51      | 25.60    | 83.53     | 23.28    |
| December  | 98823.06     | 2820.87     | 35.03      | 26.90    | 81.23     | 21.58    |

The thermal energy efficiency ratio (EER) shown in the fourth column is calculated by dividing the heat rejection by the electrical energy use. Surprisingly, the summer months of June, July, and August have consistently shown the most efficient heat rejection from the dry fluid cooler. This counter intuitive result is due to two factors: the low loop flowrates in the winter, and the higher fan speeds in the winter. The average loop flowrates in the winter months (column 5) were only about half of the average rate in the summer. As was discussed earlier, the low flowrates severely reduce the amount of heat rejection.

The higher average winter fan speeds result from the fan control schedule, which increases the fan speeds as the water/air temperature difference increases over the range of 5 to 20 degrees. Because the temperature difference was greater in the wintertime, the fan speeds were higher then, increasing the electricity consumption. The higher fan speeds would normally have increased heat rejection, but the low loop flowrates prevented this.

The yearly average heat rejection EER of the dry fluid cooler was 50.7 kBTU/hr/kW. Using the same equipment, this performance could likely be improved to an EER of between 200 and 300 kBTU/hr/kW by operating the ground loop at a constant flowrate of 80 gpm, and by adjusting the dry fluid cooler fan control so that the maximum fan speed is reached when the temperature difference is 30 degrees or more. These adjustments would be expected to produce efficiency results similar to those shown in Table 2.3 and Figure 2.6.

### 6.1.2 Numerical Simulations.

A commercial geothermal heat pump simulation model (GLHEPro) was used along with spreadsheet models of dry fluid cooler performance to simulate the Building 584 system, and to explore alternative strategies for controlling the ground loop temperature. These simulations lead to a system optimization and economic analysis for the combined geothermal heat pump/dry fluid cooler combination using wintertime heating.

The GLHEPro ground source heat pump simulation program was used to simulate the building ground loop performance prior to the addition of the dry fluid cooler. GLHEPro (IGSHPA, 2016) is a commercial program used for the design and analysis of geothermal heat pump ground loops. The code uses semi-analytical and numerical solutions for three-dimensional heat conduction from various geometry ground loop configurations. For the analysis described here, only vertical closed-loop boreholes with single U-tubes were considered, but the model can simulate other vertical borehole designs and as well as horizontal trenches.

The basic inputs to GLHEPro are the monthly building heating and cooling loads on the heat pumps, the local ground temperature, the borehole heat exchanger system geometry (number, location, and depth), construction details of the heat exchangers, subsurface thermal properties, loop flowrate, and the heat pump properties. The model output consists primarily of the predicted monthly ground loop entering and exiting temperatures and the electrical energy consumed by the heat pumps. The simulation period is controlled by the user, and may extend for decades.

Normally the building heating and cooling loads would be simulated using a building simulation program such as eQUEST. For the simulation of Building 584, the building loads are known from the ground loop data (Table 5.1). The ground loop load data shown in Table 5.1 include the waste heat from the heat pumps. Because GLHEPro uses the building load on the heat pumps, it was necessary to remove the waste heat component from the cooling loads in Table 5.1. The heat pump waste heat was estimated from heat pump performance data included in the GLHEPro heat pump library. The building cooling loads in Table 5.1 were multiplied by 0.8 to correct for the waste heat. The simulation was started in January, 2005, and run for a period of 30 years. The simulated ground loop temperature entering the building is compared to the observed monthly temperatures in 2012 and 2013 prior to the installation of the dry fluid cooler in Figure 6.5. The GLHEPro simulation tool appears to do a very good job of reproducing the observed temperatures after 8-9 years of operation, showing the same level of upward yearly temperature drift in the ground loop.

This comparison is shown again in Figure 6.6, with the full 30 year GLHEPro prediction. The model predicts that in the absence of supplemental cooling or other adjustments, the loop temperature will continue to increase over time, with average monthly inlet temperatures exceeding 100 °F. The simulation shows that the ground loop heating occurs rapidly, and substantial heating of the loop (~11 degrees) occurs in the first year. After 10 years, the loop yearly average temperature is about 21 degrees warmer than background, and by 30 years, it is 27 degrees warmer.

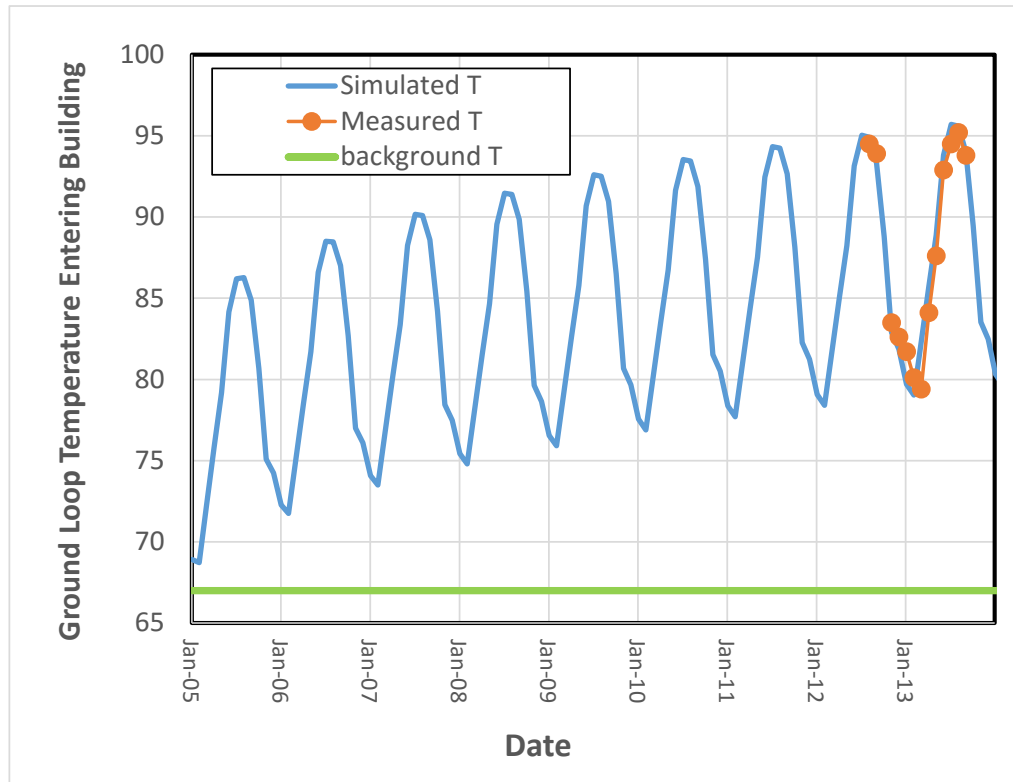


**Figure 6.5.** Results of GLHEPro simulation of Building 584 ground loop prior to the installation of the dry fluid cooler.

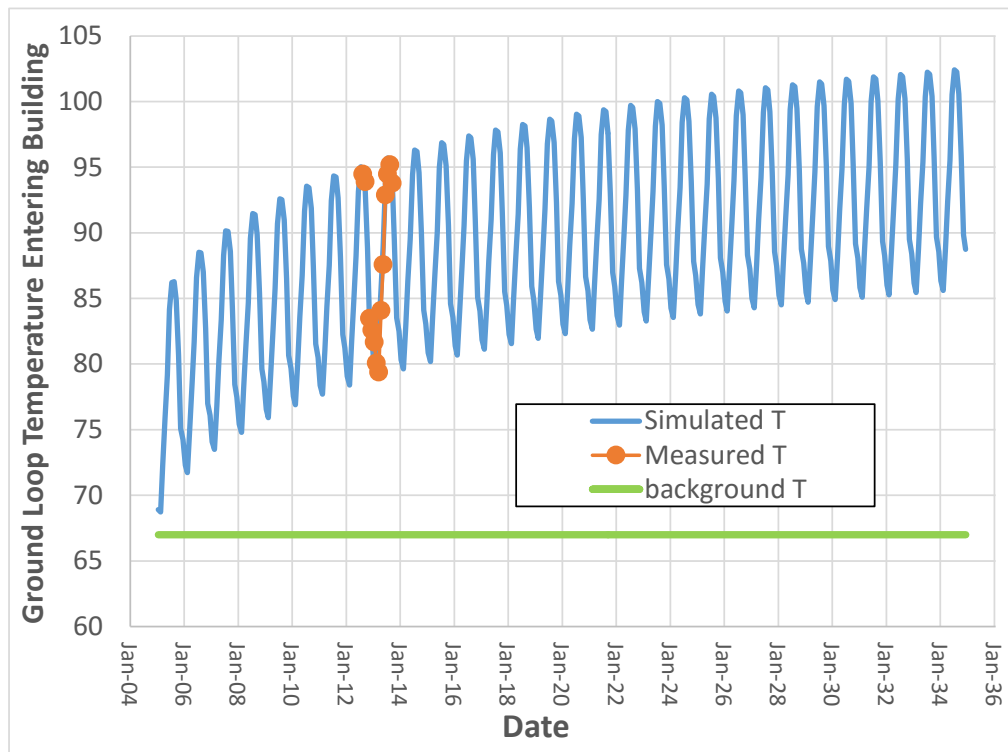


**Figure 6.6.** GLHEPro simulation showing predicted temperatures for 30 years of operation.

Figure 6.7 shows the simulation results along with ground loop temperature data collected after the installation of the dry fluid cooler (which is not accounted for in this simulation). It is apparent that use of the cooler has stopped the trend of increasing ground loop temperature

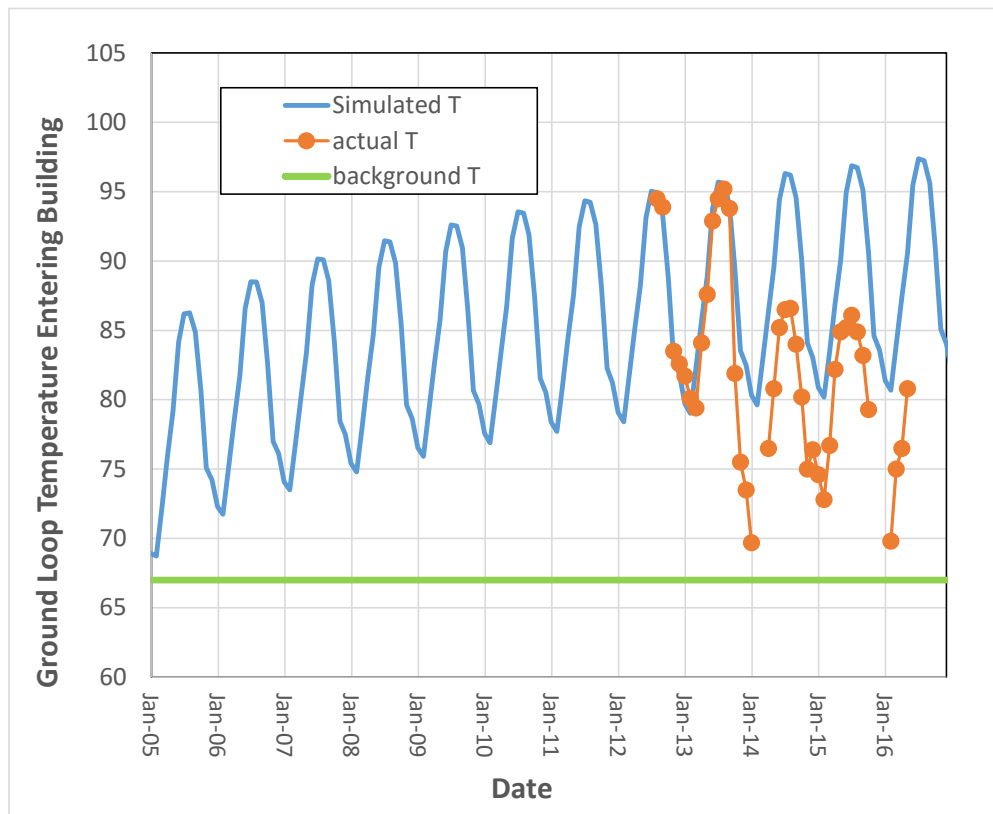


**Figure 6.7 Simulated and observed ground loop temperatures. The dry fluid cooler began operation in November, 2013.**

### 6.1.3 Calculation of Ground Loop Size Necessary to Stabilize Loop Temperature

A series of GLHEPro simulations were performed to determine the number of borehole heat exchangers that would have been needed to avoid an excessive temperature build up in the ground loop. These simulations assumed that the larger well field was installed back in 2004, at the time of the initial geothermal heat pump installation.

The borehole depth (300 ft), construction characteristics, and spacing (20 ft) were held constant, while the number of boreholes was increased. It was found that as the size of the ground loop was increased, that the magnitude of the yearly temperature fluctuations decreased, but the overall average temperature still drifted upward. In other words, the heat loss in the subsurface from flowing groundwater and conduction out the sides and top is too small to prevent the long-term heating in the ground loop. The ground loop temperature is predicted to increase with time even when the number of borehole heat exchangers is tripled. Figure 6.8 shows the GLHEPro simulation results using a borehole array with 3 rows of 25 boreholes each (75 total). This

configuration gives a maximum monthly average summer temperature of 81.4 °F, at year 30 of the simulation, with a yearly average temperature of 79.6 °F. That still represents a 12.6 degree temperature increase over the natural background temperature. With the cost for installing borehole heat exchangers at the MCAS Beaufort of about \$17/ft., these additional boreholes would add about \$260,000 to the system capital cost.

This large capital expenditure would be difficult to justify for a building of this size, and it would likely be difficult to find the room to install the additional boreholes. For these reasons, enlarging the ground loop does not seem like it would be a practical solution for dealing with highly unbalanced systems.

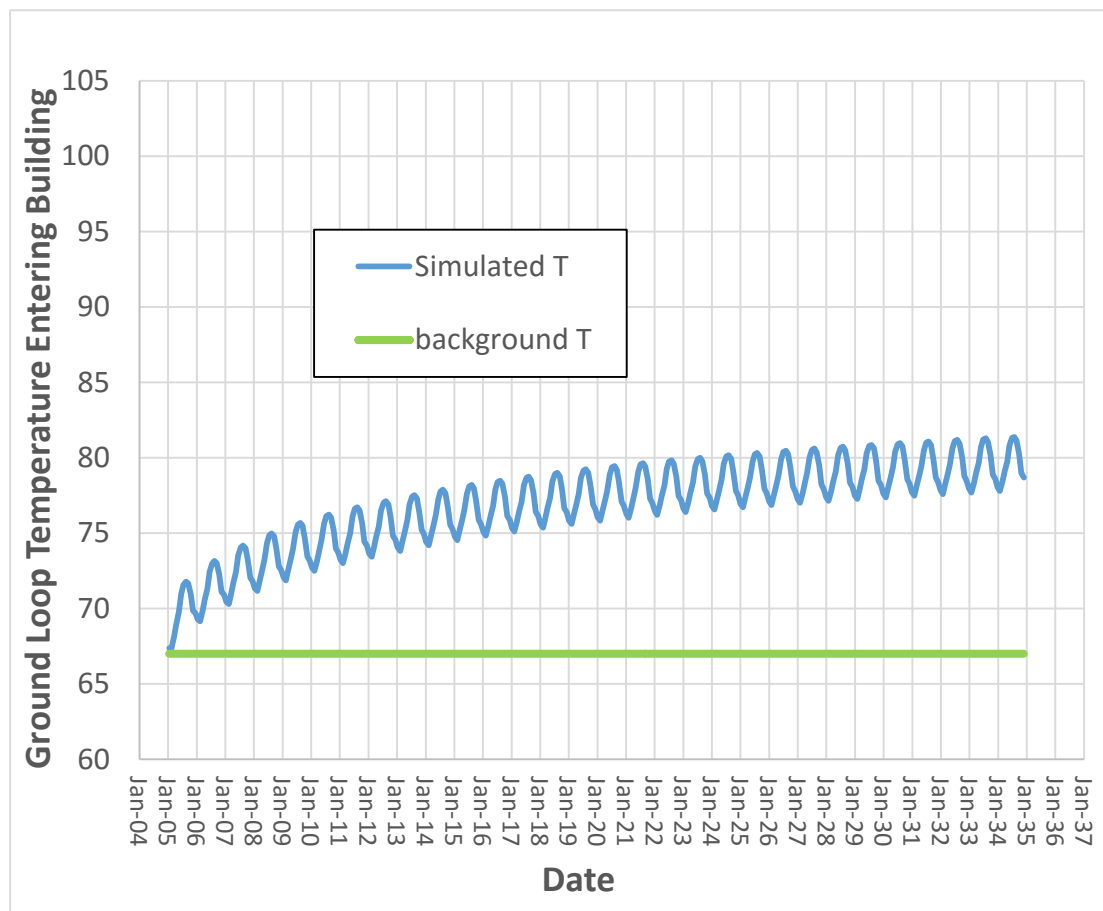


**Figure 6.8.** *GLHEPro simulation of Building 584 using 75 three-hundred foot deep borehole heat exchangers.*

#### 6.1.4 Optimal Sizing and Operation of Dry Fluid Cooler with Existing Ground Loop

A second series of GLHEPro simulations of Building 584 were performed to explore optimized operation of a smaller dry fluid cooler. As was discussed earlier, the existing 96 ton dry fluid

cooler is oversized for the Building 584 ground loop maximum flowrate of 80 gpm. In retrospect, similar cooling performance could be achieved using a cooler that is half the size of the installed unit.

The objective of these simulations is to identify a design and operation scheme that can economically stabilize the ground loop temperatures over time using the existing array of 24 borehole heat exchangers. The simulation assumes that the dry fluid cooler was added at the same time that the system began operation, at the start of 2005.

The dry fluid cooler heat rejection is included in the GLHEPro simulation by adding in an equivalent monthly heating load to the ground loop. The removal of heat from the ground loop by the cooler drops the temperature in the loop, which has the effect of reducing the efficiency of the fluid cooler due to the lower temperature difference. This negative feedback between the ground loop temperature and the dry fluid cooler efficiency is not accounted for in GLHEPro, which uses constant monthly values for the building loads and dry fluid cooler heat rejection. Therefore, it was necessary to iterate between a separate model of the dry fluid cooler performance and GLHEPro until the loop temperature stabilized for a particular design.

The monthly dry fluid cooler performance was calculated using a spreadsheet-based model that contains measured hourly temperatures from the MCAS Beaufort over a one-year period in 2010-2011. Those temperature data were compiled by month, and then sorted into 5 degree temperature “bins”. This allows for calculation of the number of hours in each temperature range, during each month (Table 6.3).

**Table 6.3. Sorted hourly temperatures from 2010-2011 at the MCAS Beaufort, SC.**

| temperature bins |       |           |           |           |           |           |            |            |           |            |           |           |           |
|------------------|-------|-----------|-----------|-----------|-----------|-----------|------------|------------|-----------|------------|-----------|-----------|-----------|
| T range          | ave T | Jan hours | Feb hours | Mar hours | Apr hours | May hours | June hours | July hours | Aug hours | Sept hours | Oct hours | Nov hours | Dec hours |
| 21-25            | 23    | 12        | 0         | 0         | 0         | 0         | 0          | 0          | 0         | 0          | 0         | 0         | 12        |
| 26-30            | 28    | 44        | 0         | 0         | 0         | 0         | 0          | 0          | 0         | 0          | 0         | 0         | 60        |
| 31-35            | 33    | 83        | 8         | 1         | 0         | 0         | 0          | 0          | 0         | 0          | 0         | 0         | 120       |
| 36-40            | 38    | 117       | 49        | 7         | 0         | 0         | 0          | 0          | 0         | 0          | 0         | 0         | 134       |
| 41-45            | 43    | 101       | 82        | 32        | 0         | 0         | 0          | 0          | 0         | 0          | 0         | 0         | 113       |
| 46-50            | 48    | 160       | 119       | 96        | 12        | 0         | 0          | 0          | 0         | 0          | 9         | 89        | 96        |
| 51-55            | 53    | 129       | 116       | 85        | 72        | 1         | 0          | 0          | 0         | 0          | 46        | 79        | 110       |
| 56-60            | 58    | 58        | 92        | 160       | 93        | 7         | 0          | 0          | 0         | 0          | 93        | 131       | 52        |
| 61-65            | 63    | 33        | 95        | 154       | 135       | 26        | 0          | 2          | 0         | 13         | 143       | 109       | 29        |
| 66-70            | 68    | 11        | 49        | 103       | 173       | 119       | 8          | 17         | 5         | 128        | 121       | 134       | 13        |
| 71-75            | 73    | 5         | 36        | 55        | 122       | 239       | 66         | 53         | 26        | 188        | 140       | 53        | 0         |
| 76-80            | 78    | 0         | 23        | 25        | 91        | 173       | 227        | 212        | 251       | 151        | 122       | 17        | 0         |
| 81-85            | 83    | 0         | 2         | 20        | 18        | 132       | 184        | 203        | 251       | 111        | 69        | 0         | 0         |
| 86-90            | 88    | 0         | 0         | 5         | 1         | 42        | 139        | 143        | 150       | 113        | 1         | 0         | 0         |
| 91-95            | 93    | 0         | 0         | 0         | 0         | 4         | 76         | 75         | 92        | 16         | 0         | 0         | 0         |
| 96-100           | 98    | 0         | 0         | 0         | 0         | 0         | 17         | 20         | 2         | 0          | 0         | 0         | 0         |
| 101-105          | 103   | 0         | 0         | 0         | 0         | 0         | 1          | 2          | 0         | 0          | 0         | 0         | 0         |

Given the ground loop temperature exiting the building, the dry fluid cooler performance rating (kBTU/hr/ΔT), and the fan speed, it is possible to calculate the heat rejection and energy consumption for each of these temperature ranges. The monthly total heat rejection and energy cost is then found using the number of hours associated with each temperature range for the month. At each temperature range, the fan speed is calculated based on the temperature

difference with the loop water, using a linear variation over a specified temperature range (as in Table 2.3).

The simulation process started with an initial estimate of dry fluid cooler performance, using an assumed yearly ground loop temperature profile. The cooler fan speed was set so that the fan speed starts at 40% when the temperature difference is 5 degrees, and then increase to 100% when the difference reaches 25 degrees. The dry fluid cooler selected for this design is a Technical Systems FC-48-597a, operated with a constant flowrate of 80 gpm. This 4 fan unit is exactly one-half the size of the installed cooler at Building 584, but it has a similar heat rejection rating at the design flowrate of 80 gpm. At 100% fan speed this unit is rated at 20.4 kBTU/hr/ $\Delta T$ .

The calculated monthly heat rejection results from the spreadsheet model are used as inputs in the initial GLHEPro simulation. The predicted GLHEPro monthly loop temperatures resulting from the building loads and the dry fluid cooler operation were then used to refine the cooler spreadsheet model calculations. By iterating between the spreadsheet cooler performance model and GLHEPro, a workable design was obtained where the ground loop temperature is nearly stable over time. The monthly dry fluid cooler heat rejection, power consumption (including loop pumping costs), and ground loop temperature is shown in Table 6.4

**Table 6.4. Simulated dry fluid cooler performance for optimized design.**

| <b>Month</b> | <b>Heat Rejection, kBTU</b> | <b>Energy Use, kW-hr</b> | <b>Ground Loop Temp.</b> |
|--------------|-----------------------------|--------------------------|--------------------------|
| January      | 101490                      | 636                      | 53                       |
| February     | 63848                       | 431                      | 59                       |
| March        | 58767                       | 403                      | 64                       |
| April        | 40889                       | 309                      | 69                       |
| May          | 19036                       | 202                      | 77                       |
| June         | 19561                       | 204                      | 83                       |
| July         | 27138                       | 239                      | 85                       |
| August       | 21688                       | 212                      | 85                       |
| September    | 38796                       | 292                      | 81                       |
| October      | 50343                       | 359                      | 72                       |
| November     | 76582                       | 511                      | 63                       |
| December     | 124858                      | 764                      | 53                       |
| <b>Total</b> | <b>642994</b>               | <b>4562</b>              | <b>average = 70</b>      |

The yearly heat rejection by the cooler of 643,000 kBTU is about 72% of the cooling load delivered from the building and heat pumps to the loop (see Table 5.1; it is about 90% of the building load). This heat is removed using 4600 kW-hr of electricity, of which about ¼ is used to pump the water through the cooler. The average energy efficiency ratio (EER) of this operation would be about 141 kBTU/hr/kW.

The simulated ground loop temperature entering the building is shown in Figure 6.9. The loop temperature has been nearly stabilized by the dry fluid cooler operation, using a cooler that is ½

the size of the one currently installed at Building 584. The yearly loop average temperatures now fall well within the range needed for efficient heat pump operation.

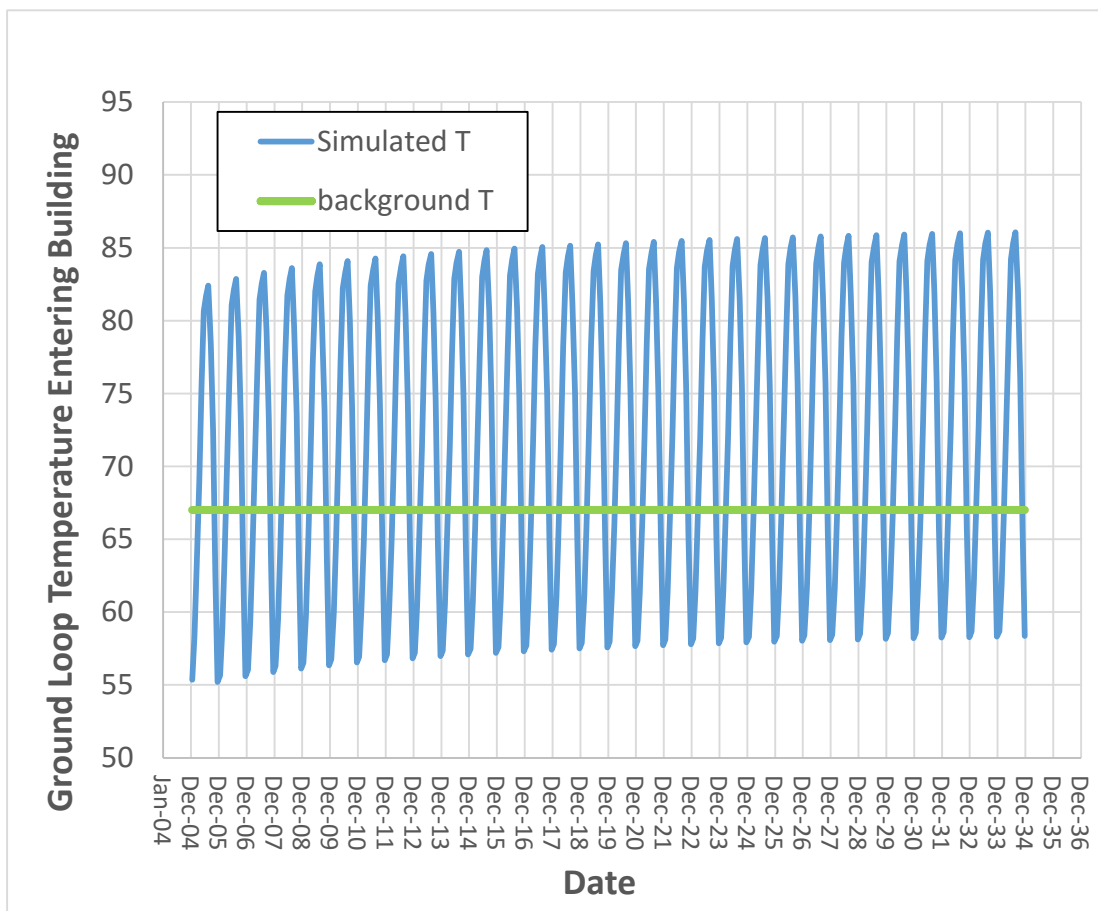


**Figure 6.9. Simulated Building 584 ground loop temperatures with optimized dry fluid cooler heat rejection (blue fluctuating lines). The dry fluid cooler begins operation immediately after the system is installed. The background temperature is the straight line in green.**

The purchase cost of the 96 ton 8-fan dry fluid cooler installed at Building 584 was about \$29,000 delivered to the site. We would expect a smaller 48 ton 4-fan unit to be about half the cost, or about \$15,000. A reasonable estimate for the installation cost would be \$5,000 for a total cost of about \$20,000. This is far lower than the capital cost for increasing the size of the wellfield, but the dry fluid cooler uses additional electrical energy to power the fans and pump.



## 6.2 BUILDING 601

### 6.2.1 Ground Loop Temperature Data

The additional dry fluid cooler was installed at Building 601 in May, 2013. By January, 2014, this cooler had a significant effect on the ground loop temperatures, lowering them by about 10 degrees or more compared to the previous January (Figure 6.10; compare with Figure 5.8).

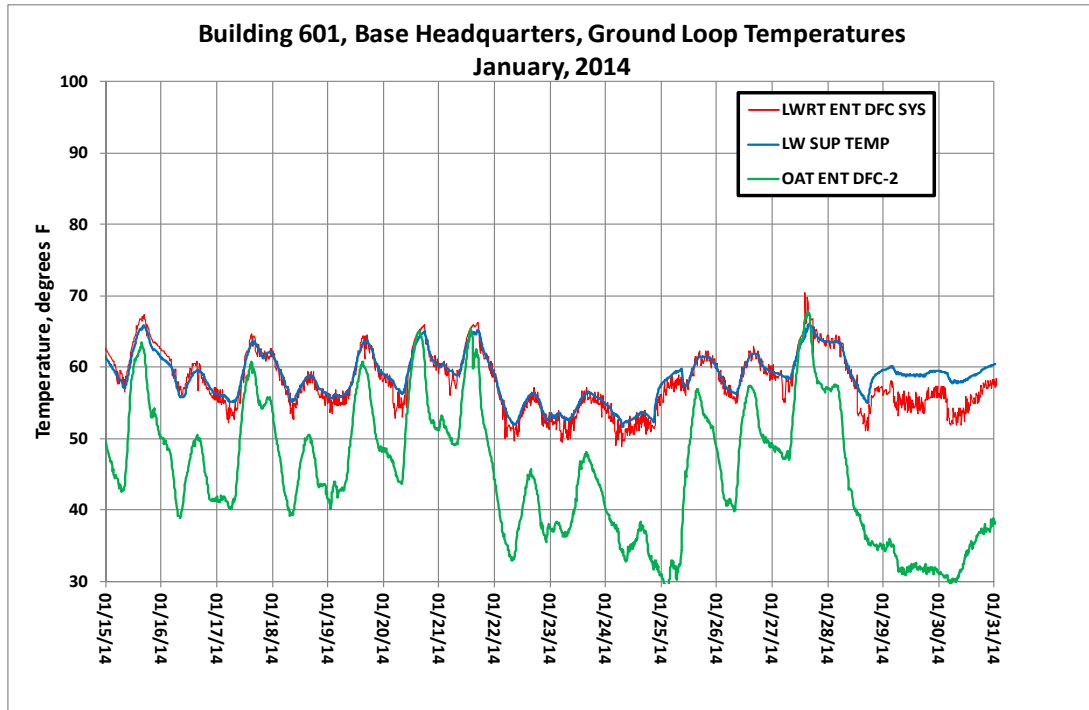


**Figure 6.10.** Ground loop temperatures at Building 601 in January, 2014.

The ground loop temperatures the following August (Figure 6.11) were similarly lowered by several degrees compared to data collected in August 2012 before the cooler was added (Figure 5.7). Despite the record or near record air temperature during this period, the ground loop water temperature entering the building (blue line) was substantially lower than the outside air temperature.

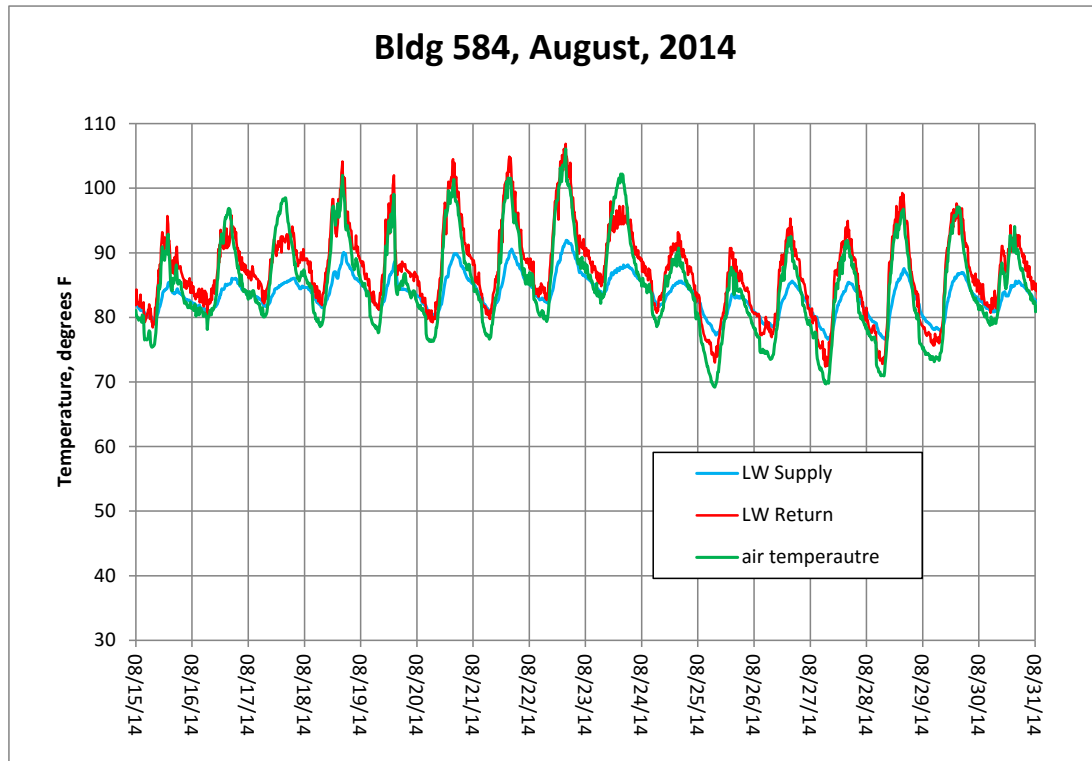


**Figure 6.11. Ground loop temperatures in Building 601 in August, 2014.**

### 6.2.2 Freeze Damage

The geothermal heat pump systems at the MCAS Beaufort have historically been operated using water without any antifreeze. Although hard freezes are rare at Beaufort, SC, they do occur every few years. The freeze protection program in place at Beaufort forces the ground loop water pumps to circulate water through the ground loops when temperatures are low. The fans to dry fluid coolers are also set to stop when loop temperatures drop below a set temperature (usually 40 to 45 °F). In the past, these precautions had been sufficient to prevent freeze damage to the ground loops and dry fluid coolers in the winter time.

However, in the winter of 2014, and again in 2015, there were severe cold periods with nighttime temperatures in the mid 20s. Damage occurred to dry fluid coolers during both of these periods. The February, 2015 cold temperatures were forecast several days in advance. In an effort to prevent freeze damage to the Building 601 dry fluid coolers, local building maintenance workers isolated the dry fluid cooler with valves, and attempted to drain the cooler. Apparently they were not aware of the fact that this cooler cannot be fully drained by gravity, and their attempt left water in the lower coils. Since the dry fluid cooler was now isolated from the flowing ground loop, when the temperatures dropped on the night of February 19, 2015, the water in the lower coils froze and burst the coil pipes (Figure 6.12).

This type of damage to a dry fluid cooler is difficult to repair, and it was necessary to replace the entire coil system for the dry fluid cooler. This repair was not completed until April, 2016. Since that time, a propylene glycol antifreeze has been added to the ground loops in buildings that have dry fluid coolers. Unlike ethylene glycol, which is toxic, propylene glycol is a food additive that is used in many consumer products.



**Figure 6.12.** Freeze damage to coils in the Building 601 dry fluid cooler.

### 6.2.3 Temperature Monitoring Well Data

Subsurface temperatures have been periodically logged in four temperature monitoring wells located in and around the Building 601 borehole heat exchangers (Figures 5.16 and 5.17). The temperature at a depth 190 feet in eastern temperature monitoring well was recorded continuously since November, 2013, shortly after the dry fluid cooler was added. This monitoring well is located inside the heat exchanger pattern, about 20 feet from adjacent active heat exchangers. The initial temperature at this depth in November, 2013 was about 80 °F, which is about 13 degrees above the natural ground temperature in this region. During the first year of wintertime cooling, the subsurface temperature dropped by about 4 degrees at this location (Figure 6.13). During the summer and early fall of 2014, the temperature rose slightly (by less than a degree) before resuming its decline during the winter of 2015. The freeze damage to the dry fluid cooler in late February, 2015 reduced the cooling during this second winter, but overall the subsurface temperature at this location was reduced by more than 5 degrees.

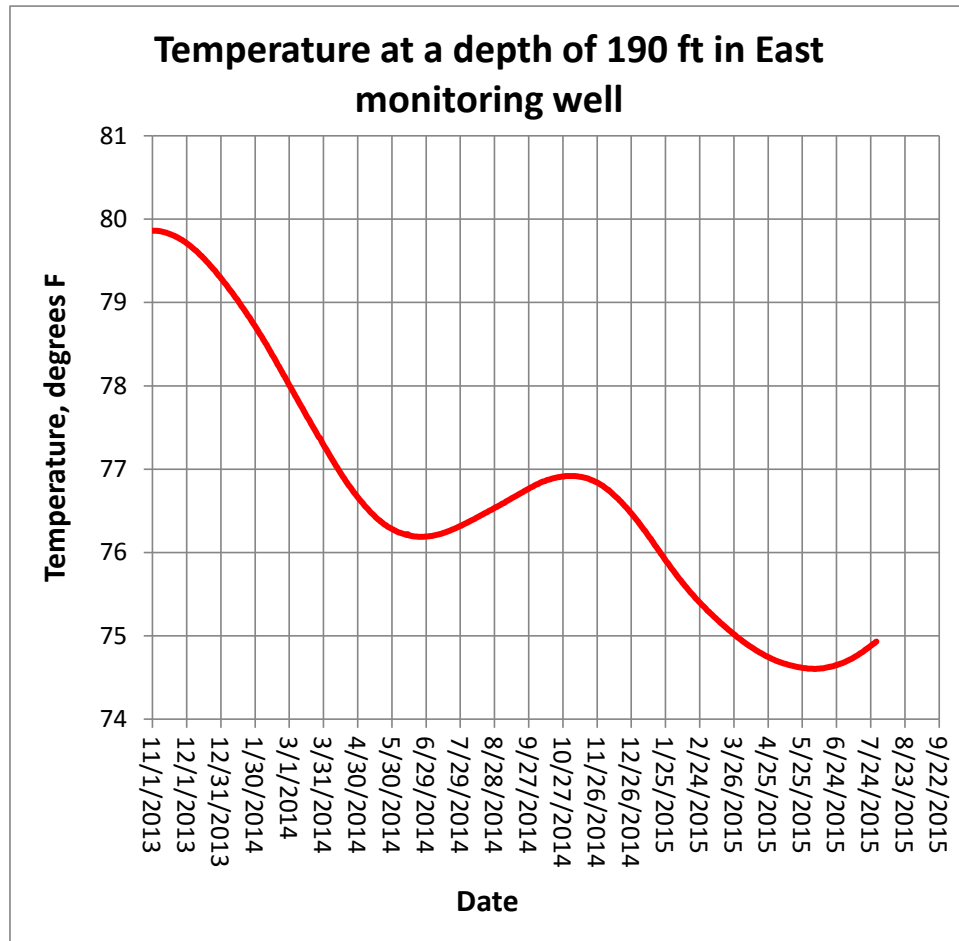


**Figure 6.13.** *Subsurface temperature measured at a depth of 190 feet in a temperature monitoring well located in the Building 601 borehole heat exchanger field.*

The vertical temperature profiles in the east, west, north, and south temperature monitoring wells are shown in Figures 6.14-6.17, respectively. A strong seasonal temperature variation is seen in these profiles at the shallowest depths, but this seasonal effect only penetrates about 20-30 feet into the ground. The eastern monitoring well (Figure 6.14) showed the largest temperature decline between September, 2013 and January, 2015, with an average drop of 4 degrees at all depths except for the bottom of the well. This monitoring well is surrounded by borehole heat exchangers, and it had the highest initial temperatures. The remaining three monitoring wells showed lower levels of subsurface cooling, likely due to their larger distance from the active borehole heat exchangers. The southern monitoring well (Figure 6.17) showed very little change in temperature below a depth of 150 ft. This monitoring well is located outside of the heat exchanger array, and it is further from the array than the northern well (Figure 6.16) which is also outside of the array. An interesting pattern is seen in the eastern, northern, and western observation wells, where the temperatures between depths of about 60 and 150 feet are lower than the temperatures above or below that depth. This may be due to cooling from groundwater flow, although this effect is not seen in the southern well.

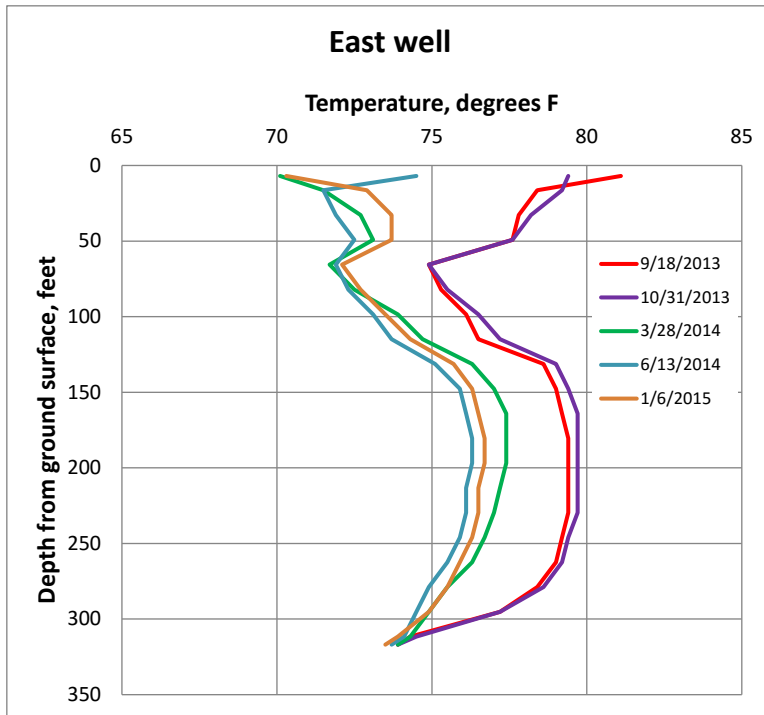


**Figure 6.14.** Vertical temperature profiles measured in the eastern temperature monitoring well at Building 601.

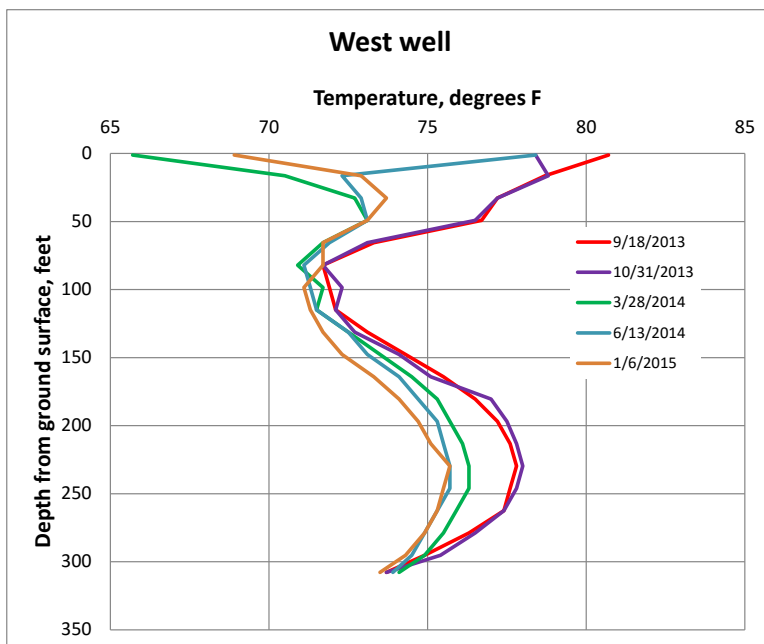


**Figure 6.15.** Vertical temperature profiles measured in the western temperature monitoring well at Building 601.

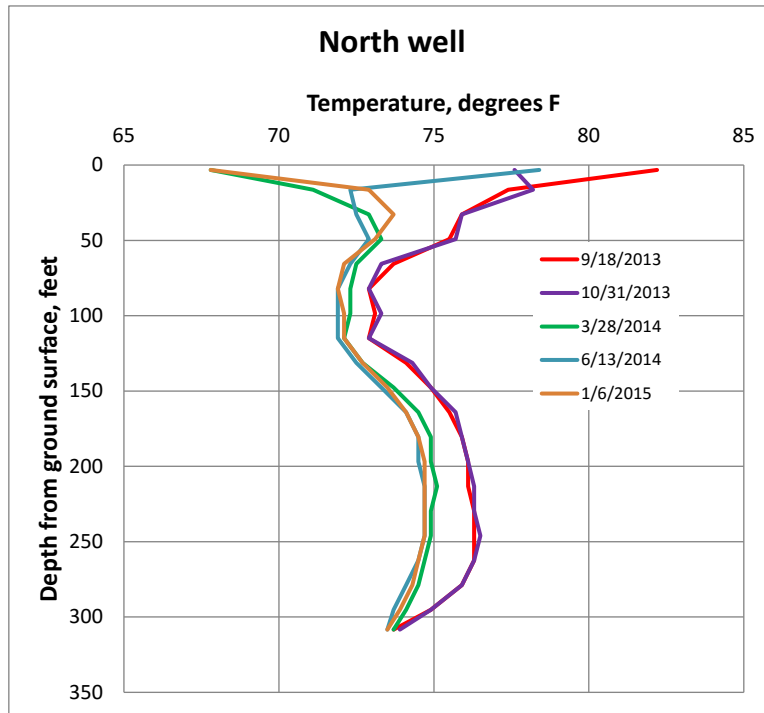


**Figure 6.16.** Vertical temperature profiles measured in the northern temperature monitoring well at Building 601.

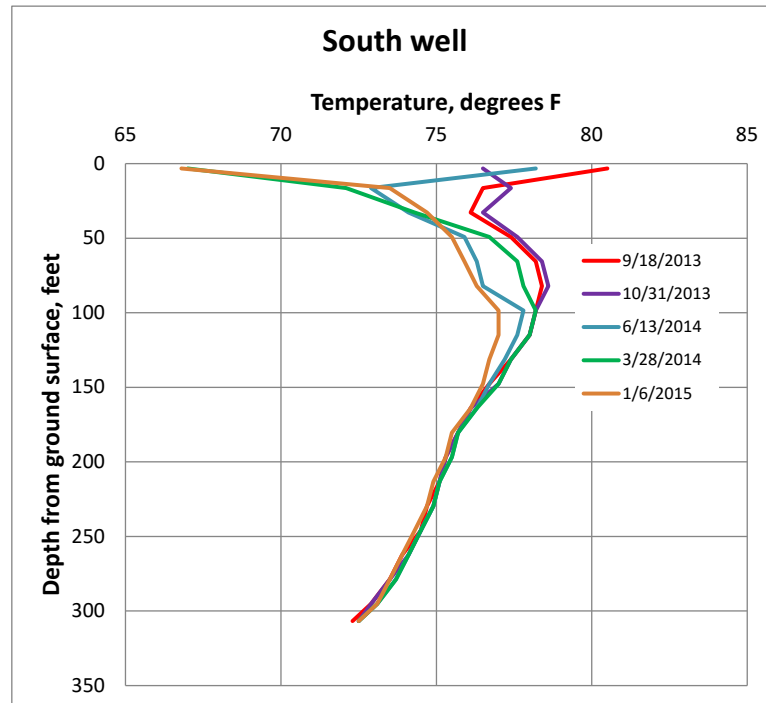


**Figure 6.17.** Vertical temperature profiles measured in the southern temperature monitoring well at Building 601.

It is also interesting that the temperature at the bottom of these wells was nearly constant with time, but still several degrees above the expected natural background temperature.

## **6.3 BUILDING 2085**

### **6.3.1 Freeze Damage**

Unfortunately, the Building 2085 dry fluid cooler was severely damaged shortly after it was put in service. There were exceptionally cold temperatures that occurred on the night of January 6-7, 2014. As the temperature approached 20 °F, power outages and power surges occurred across the base. These power spikes apparently caused a fault in the Building 2085 control system that caused the ground loop water pumps to shut down. This allowed the stagnant water in the dry fluid cooler to freeze, and burst the coils (Figure 6.18).



***Figure 6.18. Freeze damage to the Building 2085 dry fluid cooler that occurred on January 6-7, 2014.***

Although the dry fluid cooler coil was replaced in June, 2014, the temperature data collected from this building since then appear to be unreliable due to apparent short circuiting in the ground loop. This is evidenced by the fact that the loop temperature measured leaving the dry fluid cooler is practically identical to the loop temperature entering the building from the borehole heat exchangers. This means that the geothermal heat pump system is not in contact with most of the borehole heat exchangers, and little or no cooling of the ground is occurring.

## **6.4 ANALYSES FOR OTHER LOCATIONS IN THE UNITED STATES**

A series of GLHEPro simulations including dry fluid coolers were performed for conditions in six cities around the US: Minneapolis, MN, Chicago, IL, Philadelphia, PA, Oklahoma City, OK, Jacksonville, FL, and Phoenix, AZ. These cities have a range of climate conditions, with average ground temperatures ranging from a low of 48.4 °F in Minneapolis, to a high of 78.2 °F in Phoenix. As a result of the different climates, these locations have much different building load profiles.

### **6.4.1 Methodology**

The GLHEPro simulations are based on heating and cooling loads for a hypothetical 25,000 sq. ft. two-story office building. The building loads were calculated for each city using the eQUEST building simulation tool, and are shown in Figure 2.4. The hourly building loads calculated in eQUEST were converted to monthly loads for use in GLHEPro using the Peak Load Analysis Tool. This tool is distributed with the GLHEPro program. The average ground temperature for each city was calculated in GLHEPro using the internal database. The building loads for these locations range from nearly balanced (Minneapolis), to extremely cooling dominated (Oklahoma City, Jacksonville, and Phoenix).

Two simulations were performed for each location: a base case simulation with no dry fluid cooler, and a simulation using the same ground loop with a supplemental dry fluid cooler. Different ground loop configurations were used for the different cities due to the large variation in building loads. A ground loop consisting of 30 three-hundred foot deep boreholes with 20 ft spacing arranged in a 3x10 rectangle with a flow rate of 90 gpm was used for the cities of Minneapolis, Chicago, Philadelphia, and Oklahoma City. A larger loop with 42 boreholes in a 3x14 rectangle with a flow rate of 120 gpm was used for Jacksonville, while a loop with 60 boreholes (3x20) and a flow rate of 160 gpm was used for Phoenix. The larger ground loops were needed in Jacksonville and Phoenix to avoid excessively high temperatures.

The simulations with a dry fluid cooler assume cooler operation similar to what was described in Section 6.1.4. The cooler was assumed to operate year-round, but at only a fraction of its rated capacity, typically about 10-15%. It is assumed that the dry fluid cooler uses a variable speed fan drive with a control system that increases fan speed as the temperature difference between the entering water and the air increases. This results in more cooling in the winter months, and the distribution of heat rejection was assumed to be the same as it was for the Beaufort MCAS example (Table 6.5).



**Table 6.5. Monthly distribution of dry fluid cooler heat rejection assumed in the GLHEPro simulations.**

| Month     | Fraction of Yearly Heat Rejection by Dry Fluid Cooler |
|-----------|---|
| January   | 16%   |
| February  | 10%   |
| March     | 9%  |
| April     | 6%  |
| May       | 3%  |
| June      | 3%  |
| July      | 4%  |
| August    | 3%  |
| September | 6%  |
| October   | 8%  |
| November  | 12%   |
| December  | 19%   |

The dry fluid cooler was sized according to the building load and the loop flowrate. No cooler was required for the Minneapolis and Chicago buildings, which had more balanced cooling loads and low background temperatures. For the Philadelphia building, a 36 ton, 3 fan unit would be appropriate. The Oklahoma City example would likely require a 48 ton 4 fan unit, while the Jacksonville and Phoenix cases use a 72 ton 6 fan and a 96 ton 8 fan unit, respectively due to their higher cooling loads.

The dry fluid cooler simulations used the cooler to reject either 90% (Philadelphia and Oklahoma City) or 100% (Jacksonville, Phoenix) of the building net cooling load. It should be remembered that the building cooling load only represents about 80% of the load received by the ground loop due to the waste heat produced by the heat pumps, so the systems are still not completely balanced.

#### **6.4.2 Balanced Heating/Cooling Load Base Case**

The eQUEST simulated building loads for a two-story office building in Minneapolis are shown in Table 6.6. The heating and cooling loads are nearly balanced (not including the heat pump waste heat). This balance, combined with the low ground temperature of 48.4 degrees results in almost ideal conditions for operation of a conventional ground source geothermal heat pump system.

**Table 6.6. Simulated building heating and cooling loads for Minneapolis, MN example.**

| <b>Month</b> | <b>Heating Loads, kBTU</b> | <b>Cooling Loads, kBTU</b> |
|--------------|----------------------------|----------------------------|
| January      | 104,532                    | 0                          |
| February     | 74,250                     | 235                        |
| March        | 42,283                     | 992                        |
| April        | 4,112                      | 9,900                      |
| May          | 3                          | 43,043                     |
| June         | 0                          | 88,714                     |
| July         | 1                          | 100,308                    |
| August       | 1                          | 98,967                     |
| September    | 0                          | 56,680                     |
| October      | 2,547                      | 12,508                     |
| November     | 38,002                     | 1,696                      |
| December     | 86,070                     | 6                          |
| <b>Total</b> | <b>351,802</b>             | <b>413,049</b>             |

The GLHEPro simulation results for this case are shown in Figure 6.19. Over the 30 year simulation period, the ground loop temperature increases slightly, but not enough to significantly decrease the air conditioning efficiency. In fact, the heat pump system becomes slightly more efficient over time due to improved heating efficiency with the higher loop temperatures. It appears that no supplemental cooling would be needed for this building.

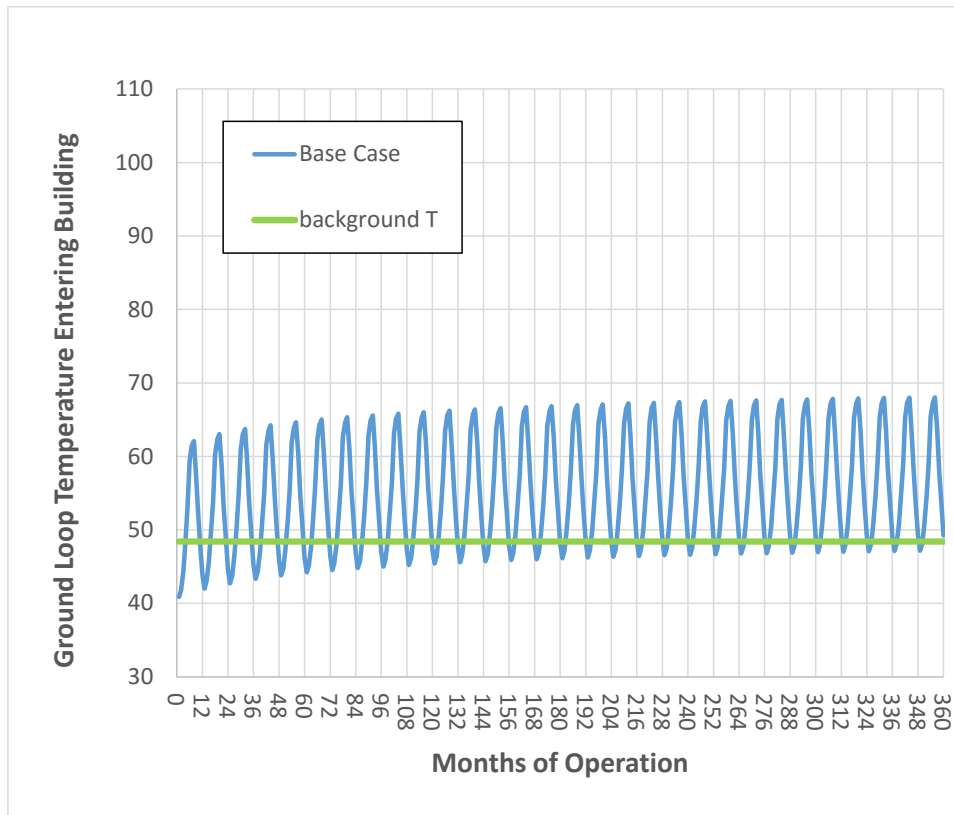


**Figure 6.19.** *Simulated ground loop temperatures for a two-story office building in Minneapolis, MN.*

### 6.4.3 Cooling Dominated Examples

**Chicago.** The simulated loads for an office building in Chicago are shown in Table 6.7. The heating and cooling loads are somewhat unbalanced, but not strongly so (not including the heat pump waste heat). The local ground temperature of 51.9 degrees combined with the relatively weak load imbalance results in a ground loop system that does not undergo an excessive temperature increase over time.

The GLHEPro simulation results for Chicago are shown in Figure 6.20. Over the 30 year simulation period, the ground loop temperature increases slightly, but not enough to substantially decrease the air conditioning efficiency, and this loss is mostly offset by the increase in heating efficiency. Over the course of the 30 year simulation, the system efficiency is nearly constant. It appears that no supplemental cooling would be needed for this building.

**Table 6.7. Simulated building heating and cooling loads for Chicago, IL example.**

| Month        | Heating Loads, kBTU | Cooling Loads, kBTU |
|--------------|---------------------|---------------------|
| January      | 71,139              | 41                  |
| February     | 53,902              | 164                 |
| March        | 36,867              | 771                 |
| April        | 4,326               | 8,455               |
| May          | 0                   | 43,546              |
| June         | 1                   | 91,747              |
| July         | 0                   | 108,460             |
| August       | 2                   | 100,789             |
| September    | 0                   | 66,050              |
| October      | 1,029               | 16,721              |
| November     | 20,329              | 3,776               |
| December     | 58,584              | 29                  |
| <b>Total</b> | <b>246,180</b>      | <b>440,550</b>      |

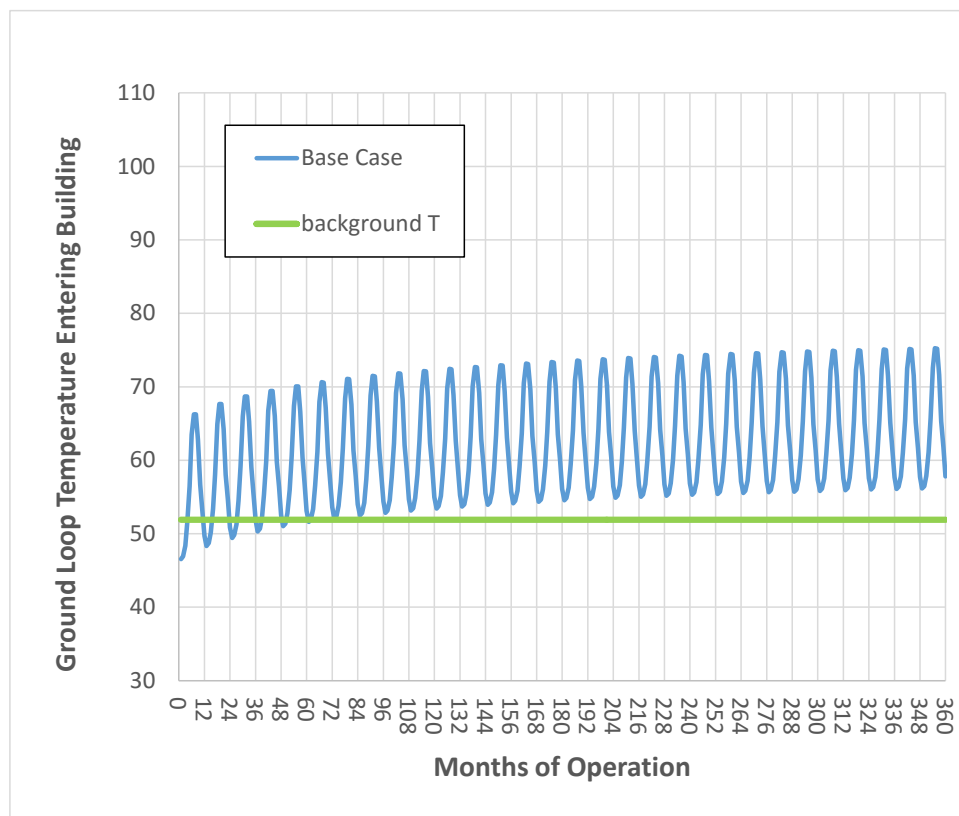


**Figure 6.20. Simulated ground loop temperatures for a two-story office building in Chicago, IL.**

**Philadelphia.** The simulated loads for an office building in Philadelphia are shown in Table 6.8. The heating and cooling loads are more strongly imbalanced, although there are relatively large heating loads in the winter. The local ground temperature is about 57.1 degrees.

**Table 6.8. Simulated building heating and cooling loads for Philadelphia, PA example.**

| Month        | Heating Loads, kBTU | Cooling Loads, kBTU |
|--------------|---------------------|---------------------|
| January      | 52,833              | 337                 |
| February     | 39,656              | 323                 |
| March        | 15,480              | 3,132               |
| April        | 1,586               | 16,089              |
| May          | 0                   | 48,735              |
| June         | 2                   | 93,182              |
| July         | 0                   | 113,367             |
| August       | 0                   | 107,768             |
| September    | 0                   | 81,508              |
| October      | 557                 | 33,880              |
| November     | 8,645               | 9,191               |
| December     | 36,969              | 408                 |
| <b>Total</b> | <b>155,727</b>      | <b>507,920</b>      |

The GLHEPro simulation results for Philadelphia are shown in Figure 6.21. Over the 30 year simulation period, without a dry fluid cooler, the ground loop temperature increases by almost 20 degrees. While these loop temperatures are not excessively high compared to the more southern examples, the increased temperature reduces the air conditioning efficiency. This reduction of cooling efficiency is not offset by the increase in heating efficiency due to the lower heating loads. Over the 30 year simulation period, the heat pump system would become about 12% less efficient.

The dry fluid cooler simulation removes 90% of the cooling load imbalance (317,000 kBTU) over the course of a year, with most of the cooling occurring in the wintertime (Table 6.5). This amount of heat rejection does not completely balance the load to the ground loop, but it is enough to stabilize the temperature over time, with only a few degree rise in temperature (Figure 6.21). This system would have a nearly constant efficiency over time. A 36 ton, 3 fan dry fluid cooler would be an appropriate size for this building.

Given the fact that the degree of ground loop heating in this case is not severe, the argument for adding a dry fluid cooler would not be as strong as it would be for a building with a larger cooling load (or a smaller ground loop).

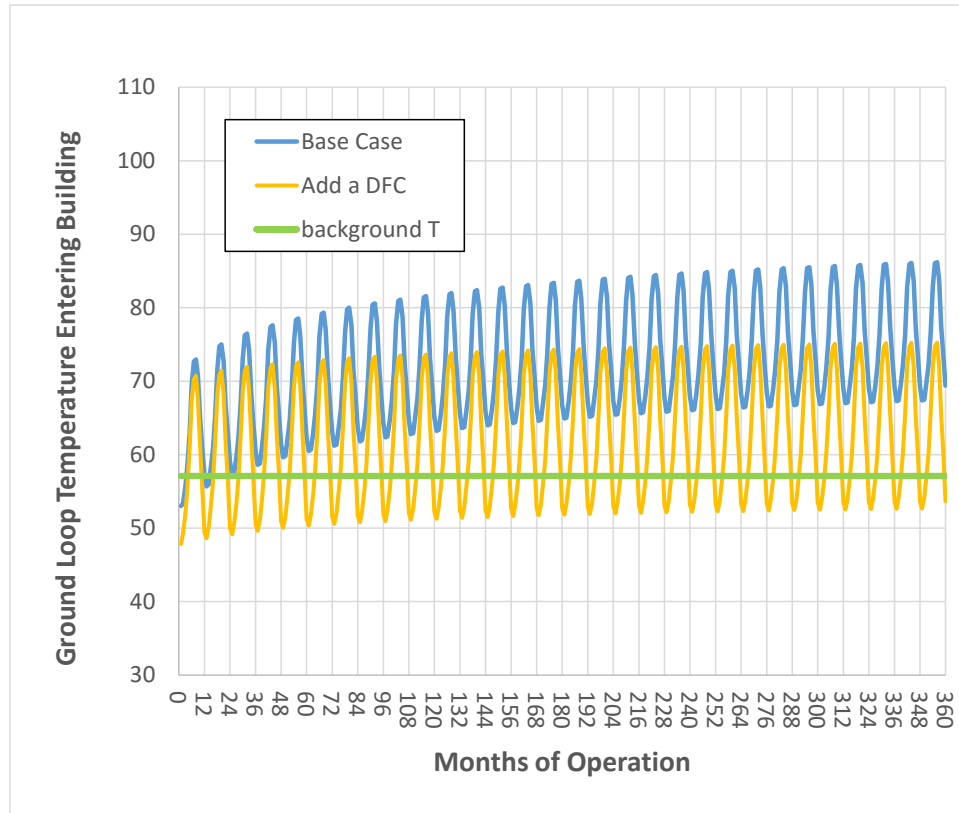


**Figure 6.21. Simulated ground loop temperatures for a two-story office building in Philadelphia, PA.**

**Oklahoma City.** The simulated loads for an office building in Oklahoma City are shown in Table 6.9. The heating and cooling loads are strongly imbalanced, and there are very high cooling loads in the summer months. The local ground temperature is about 62.4 degrees. This building would be a good candidate for the addition of a dry fluid cooler. As in the previous 3 simulations, a 30 borehole heat exchanger system is used for the simulations, with a flowrate of 90 gpm.

The GLHEPro simulation results for Oklahoma City are shown in Figure 6.22. Over the 30 year simulation period, without a dry fluid cooler, the ground loop temperature increases by more than 30 degrees, reaching a level that would likely start to be beyond the heat pump operating range. A large degree of heating is seen in the first year, and by the end of the simulation, the heat pump efficiency has dropped by about 30% compared to first year operation.

**Table 6.9. Simulated building heating and cooling loads for Oklahoma City, OK example.**

| Month        | Heating Loads, kBTU | Cooling Loads, kBTU |
|--------------|---------------------|---------------------|
| January      | 42,813              | 1,479               |
| February     | 16,090              | 3,007               |
| March        | 3,330               | 14,909              |
| April        | 188                 | 41,951              |
| May          | 3                   | 70,891              |
| June         | 1                   | 114,429             |
| July         | 2                   | 127,299             |
| August       | 0                   | 142,298             |
| September    | 2                   | 93,904              |
| October      | 0                   | 52,583              |
| November     | 911                 | 15,970              |
| December     | 14,087              | 6,822               |
| <b>Total</b> | <b>77,428</b>       | <b>685,541</b>      |

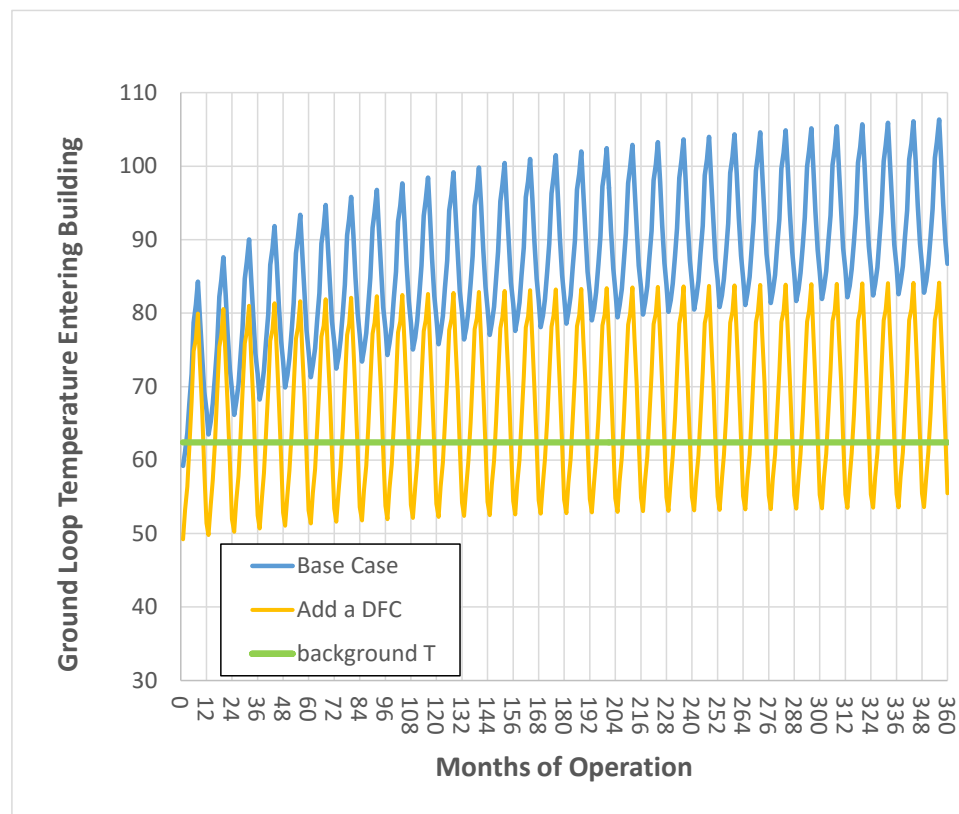


**Figure 6.22. Simulated ground loop temperatures for a two-story office building in Oklahoma City, OK.**

The dry fluid cooler simulation removes 90% of the cooling load imbalance (609,300 kBTU) over the course of a year, with most of the cooling occurring in the wintertime (Table 6.5). This amount of heat rejection does not completely balance the load to the ground loop, but it is enough to stabilize the temperature over time, with only a few degree rise in temperature (Figure 6.22). This system would have a nearly constant efficiency over time. A 48 ton, 4 fan dry fluid cooler would be an appropriate size for this building.

**Jacksonville.** The simulated loads for an office building in Jacksonville are shown in Table 6.10. The building load is virtually all cooling, with high loads in the summer, and significant loads year-round. The local ground temperature is about 69.3 degrees. It was found necessary to increase the size of the ground loop for this example to prevent excessively high loop temperatures. These simulations increase the ground loop by 12 boreholes, to a total of 42, with a loop flowrate of 120 gpm. With its very high cooling load, this building is an excellent candidate for the addition of a dry fluid cooler.

The GLHEPro simulation results for Jacksonville are shown in Figure 6.23. Over the 30 year simulation period, without a dry fluid cooler, the ground loop temperature increases by more than 30 degrees, reaching a level that would likely start to be beyond the heat pump operating range. A large degree of heating is seen in the first year, and by the end of the simulation, the heat pump efficiency has dropped by nearly 50% compared to first year operation.

The dry fluid cooler simulation removes 100% of the cooling load imbalance (971,000 kBTU) over the course of a year, with most of the cooling occurring in the wintertime (Table 6.5). This amount of heat rejection does not completely balance the load to the ground loop (due to the additional waste heat from the heat pumps), but it is enough to stabilize the temperature over time, with only a few degree rise in temperature (Figure 6.23). This system would have a nearly constant efficiency over time. A 72 ton, 6 fan dry fluid cooler would be an appropriate size for this building.

**Table 6.10. Simulated building heating and cooling loads for Jacksonville, FL example.**

| Month        | Heating Loads, kBTU | Cooling Loads, kBTU |
|--------------|---------------------|---------------------|
| January      | 1,705               | 13,989              |
| February     | 222                 | 22,896              |
| March        | 62                  | 55,816              |
| April        | 4                   | 86,323              |
| May          | 3                   | 98,058              |
| June         | 0                   | 129,072             |
| July         | 0                   | 134,101             |
| August       | 0                   | 139,598             |
| September    | 1                   | 125,691             |
| October      | 0                   | 87,551              |
| November     | 1                   | 53,894              |
| December     | 147                 | 26,061              |
| <b>Total</b> | <b>2,145</b>        | <b>973,050</b>      |



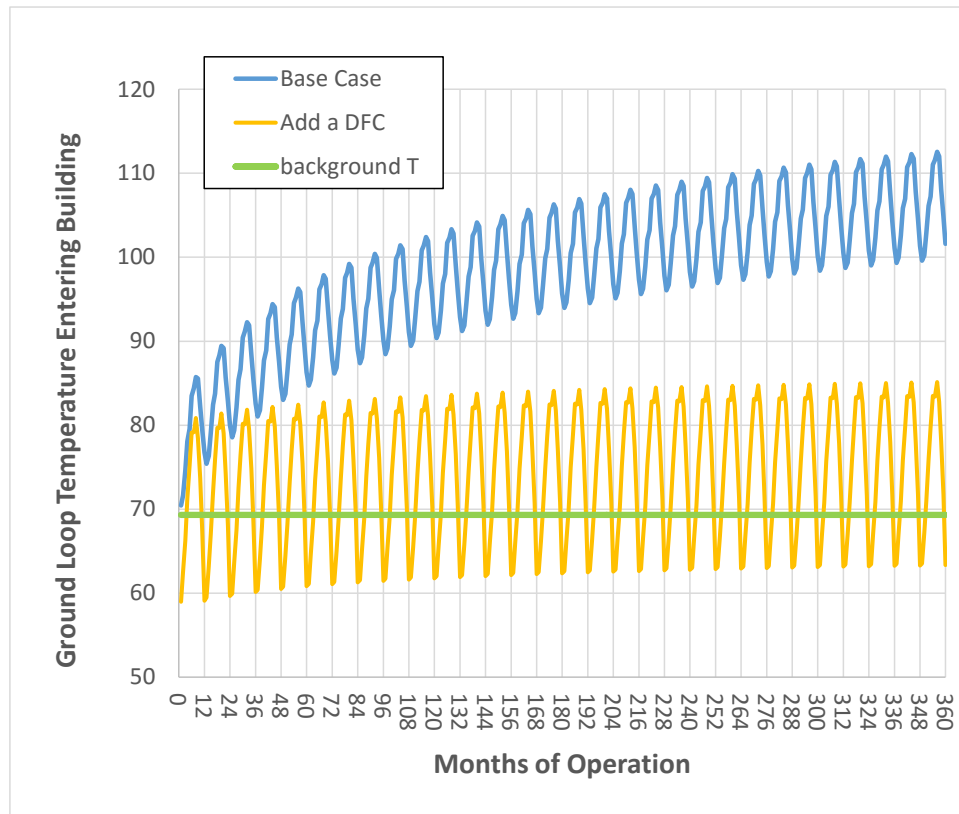


**Figure 6.23.** Simulated ground loop temperatures for a two-story office building in Jacksonville, FL.

**Phoenix.** The simulated loads for an office building in Phoenix are shown in Table 6.11. The building load is virtually all cooling, with extremely high loads in the summer, and significant loads year-round. The local ground temperature is about 78.2 degrees, which is far warmer than the previous examples. It was found necessary to again increase the size of the ground loop for this example to prevent excessively high loop temperatures. These simulations increase the original ground loop by 30 boreholes, to a total of 60, with a loop flowrate of 160 gpm. With its extremely high cooling load, this building is an excellent candidate for the addition of a dry fluid cooler.

The GLHEPro simulation results for Phoenix are shown in Figure 6.24. Over the 30 year simulation period, without a dry fluid cooler, the ground loop temperature increases by about 30 degrees, reaching a level that would likely start to be beyond the heat pump operating range. A large degree of heating is seen in the first year, and by the end of the simulation, the heat pump efficiency has dropped by nearly 40% compared to first year operation.

**Table 6.11. Simulated building heating and cooling loads for Phoenix, AZ example.**

| Month        | Heating Loads, kBTU | Cooling Loads, kBTU |
|--------------|---------------------|---------------------|
| January      | 457                 | 24,775              |
| February     | 29                  | 30,333              |
| March        | 4                   | 69,503              |
| April        | 3                   | 87,853              |
| May          | 3                   | 100,331             |
| June         | 0                   | 149,613             |
| July         | 0                   | 159,107             |
| August       | 0                   | 160,018             |
| September    | 0                   | 141,656             |
| October      | 10                  | 94,121              |
| November     | 7                   | 62,093              |
| December     | 916                 | 27,814              |
| <b>Total</b> | <b>1,429</b>        | <b>1,107,216</b>    |

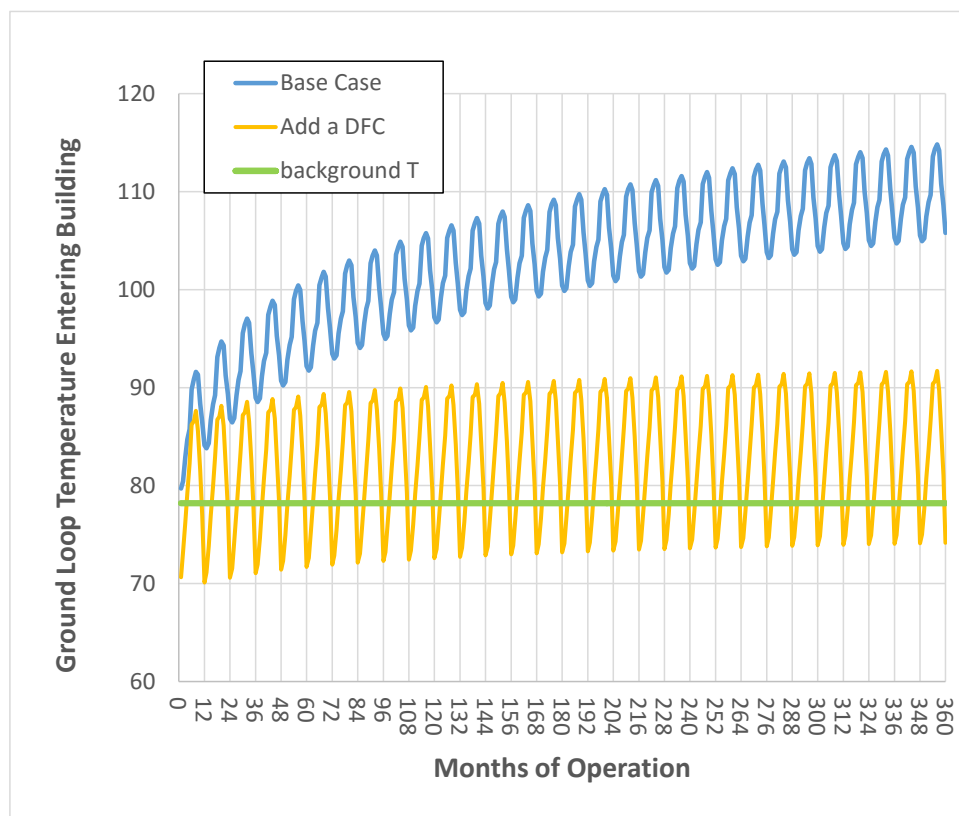


**Figure 6.24. Simulated ground loop temperatures for a two-story office building in Phoenix, AZ.**

The dry fluid cooler simulation removes 100% of the cooling load imbalance (1,106,000 kBTU) over the course of a year, with most of the cooling occurring in the wintertime (Table 6.5). This amount of heat rejection is enough to stabilize the temperature over time, with only a few degree rise in temperature (Figure 6.24). This system would have a nearly constant efficiency over time. A 96 ton, 8 fan dry fluid cooler would be an appropriate size for this building.

It was possible to stabilize the ground loop temperature using moderately sized loops in each of these examples by using a dry fluid cooler to reject an amount of heat approximately equal to the building cooling load imbalance. Most of this heat can be rejected in the winter time, when it is most efficient to do so. This lowering of the ground loop temperature each winter pays dividends the following summer as loop temperatures remain lower.

## 7.0 COST ASSESSMENT

### 7.1 COST MODEL

Estimating the costs for adding a dry fluid cooler during the installation of a geothermal heat pump system are relatively straightforward, although we experienced unexpectedly high installation costs for our building retrofits. The cost model for adding a dry fluid cooler to the system is summarized in Table 7.1

**Table 7.1. Cost Model for Including a Dry Fluid Cooler in a Geothermal Heat Pump System**

| Cost Element                      | Data Tracked During the Demonstration   | Estimated Costs   |
|-----------------------------------|---|---|
| <b>Hardware capital costs</b>     | Cost of 96 ton dry fluid cooler   | \$28,733 delivered. Cost is proportional to size of cooler  |
| <b>Installation costs</b>         | Labor and material required to install dry fluid cooler   | \$27,000 for 96 ton cooler retrofit to existing ground loops. Cost are expected to be much lower for a typical installation |
| <b>Consumables</b>                | Estimates based on rate of consumable use during the field demonstration  | None.   |
| <b>Facility operational costs</b> | Reduction in energy required vs. baseline data  | Energy use decreases with time, up to 20% lower than conventional system  |
| <b>Maintenance</b>                | <ul style="list-style-type: none"><li>• Frequency of required maintenance</li><li>• Labor and material per maintenance action</li></ul> | Periodic servicing of fans, cost not established  |
| <b>Hardware lifetime</b>          | Estimate based on components degradation during demonstration   | Unknown but likely 30 years   |
| <b>Operator training</b>          | Estimate of training costs  | Essentially none.   |

#### Hardware capital costs

The hardware for this technology consists of an appropriately sized dry fluid cooler. The dry fluid cooler should be sized to match the ground loop flowrate; the flowrate should fall within the cooler design range. The dry fluid cooler should be sized and operated so that it can reject an amount of heat equal to the yearly cooling load minus the yearly heating load. Using variable frequency drive fan motors, the fan speeds should be controlled by the temperature difference between the water entering the cooler and the outside air, reaching maximum fan speeds when the temperature difference is large (~20 degrees or more). Most of the loop heat will be rejected in the winter using this type of operation, and the heat rejection energy efficiency can be very high.

On a yearly average basis, the dry fluid cooler should be sized so that the heat rejection is on the order of 10-20% of the cooler rated capacity. For example, if the desired yearly cooler heat rejection is 600,000 kBTU, this is equivalent to an average rate of about 5.7 tons. This would be

about 12% of the rated capacity of a 4-fan, 48 ton dry fluid cooler. During the peak cooling months of December and January, the cooler is likely to be operating at 25-35% of the rated capacity (averaged over the month).

Our cost for a 96 ton dry fluid cooler was \$28,733, delivered. We received a quote of \$16,833 for a 48 ton dry fluid cooler. It is expected that the cost of the dry fluid cooler is proportional to the rated capacity of the cooler.

### **Installation costs**

Our costs for installing the dry fluid coolers were about \$27,000 per cooler. This cost seemed very high to us, and we would expect the installation cost for a typical application to be about 1/3 of this amount. Possible reasons for our high installation costs were: 1) these were building retrofits, which required excavating and rerouting the ground loop piping; 2) there were large mobilization charges for heavy equipment involved, and 3) there was limited competition for the contract due to the small number of companies that were able to bid on the project.

### **Consumables**

The dry fluid cooler does not consume anything other than electricity

### **Facility operational costs**

The system with a dry fluid cooler is expected to reduce heat pump electricity consumption over the life of the system. The reduction is minimal in early years, but it can increase to as much as 20% or more after 30 years

### **Maintenance**

The only moving parts on the dry fluid coolers are the fans. These probably require periodic maintenance or replacement, but none was required during the project.

### **Hardware lifetime**

The fans have a limited life, but they are the only moving parts. As long as the system is protected from freeze damage (by using antifreeze), the cooler lifetime should be 30 years or more.

### **Operator training**

Once the system is installed, and the control system is in place, no direct operator interaction is required.

## **7.2 COST DRIVERS**

Supplemental wintertime cooling using a dry fluid cooler is appropriate for building geothermal heat pump systems that have unbalanced cooling dominated loads. For locations that have highly cooling dominated loads, the size and cost of the dry fluid cooler is proportional to the amount of heat that needs to be rejected in order to approximately balance the loads on a yearly basis. The examples in Section 6.4 show the need for, and the size of a dry fluid cooler will vary with location. When the loads are nearly balanced, and the natural ground temperature is low, there is no need for a dry fluid cooler. As the load imbalance increases, and the natural ground temperature increases, the optimal size of a dry fluid cooler also increases. These more extreme conditions also show a larger benefit from the supplemental cooling.

### 7.3 COST ANALYSIS AND COMPARISON

#### **Comparison of Heat Pump System With and Without Dry Fluid Cooler at Building 584.**

Based on the observed loop temperatures and the GLHEPro simulation results, it does not appear that continued operation of the heat pump system without supplemental cooling would be desirable. After only about 8 years of operation, the late summer loop temperatures entering the building were in the mid- to upper 90s (Figure 5.4). The GLHEPro simulation of the heat pump system predicts that the ground loop temperature would have continued to increase over the next 20 years, with average loop temperatures entering the building well over 100 °F (Figure 6.6). The simulation also shows that peak loop temperatures on hot summer afternoons could reach almost 120 °F in the later years of the system operation. Loop temperatures that high would probably be beyond the safe operating range for the heat pumps, and might result in temporary system shutdowns, or damage to the system.

The heating of the ground that would occur with the conventional system, while not permanent, would take a long time to reverse, and would likely discourage continued use of geothermal heat pumps at the site in the future.

The unbalanced geothermal system without supplemental cooling becomes significantly less efficient with time as the loop temperature increases. This is in contrast to a system in which much of the excess cooling load is rejected using a dry flood cooler. Table 7.2 compares the simulated monthly electrical energy use for the geothermal heat pump system with and without the addition of the dry fluid cooler. The base case referred to here is continued Building 584 operation without supplemental cooling, as described in Section 6.1.2, while dry fluid cooler case uses the optimized design described in Section 6.1.4, and it includes the electrical energy used by the cooler.

***Table 7.2. Simulated Building 584 electrical energy use (kW-hr) for the geothermal heat pump system with and without a dry fluid cooler.***

| <b>Month</b> | <b>Year 10 Base Case</b> | <b>Year 10 Dry Fluid Cooler</b> | <b>Year 30 Base Case</b> | <b>Year 30 Dry Fluid Cooler</b> |
|--------------|--------------------------|---------------------------------|--------------------------|---------------------------------|
| January      | 1108                     | 1499                            | 1195                     | 1509                            |
| February     | 951                      | 1224                            | 1019                     | 1232                            |
| March        | 2201                     | 2094                            | 2404                     | 2129                            |
| April        | 3610                     | 3180                            | 3943                     | 3240                            |
| May          | 5203                     | 4568                            | 5679                     | 4659                            |
| June         | 7446                     | 6484                            | 8119                     | 6614                            |
| July         | 8522                     | 7352                            | 9286                     | 7498                            |
| August       | 8221                     | 7162                            | 8954                     | 7304                            |
| September    | 6910                     | 5916                            | 7524                     | 6031                            |
| October      | 4651                     | 4047                            | 5065                     | 4122                            |
| November     | 1865                     | 1899                            | 2029                     | 1927                            |
| December     | 1625                     | 1853                            | 1768                     | 1875                            |
| <b>Total</b> | <b>52311</b>             | <b>47277</b>                    | <b>56984</b>             | <b>48139</b>                    |

Comparing the yearly totals, during the tenth year of operation, the system with the dry fluid cooler is about 10% more efficient than the base case. In the 30<sup>th</sup> year of operation, the system with the dry fluid cooler is about 16% more efficient than the base case.

The monthly electricity use during year 30 is plotted in Figure 7.1. The energy savings occur mainly during the summer months of June, July, August, and September, when building cooling loads are at their highest. Energy use in the cooler months of November, December, January, February, and March are similar for the two systems. The energy savings during these months that result from the cooler ground loop temperatures are offset by the cost to operate the dry fluid cooler.

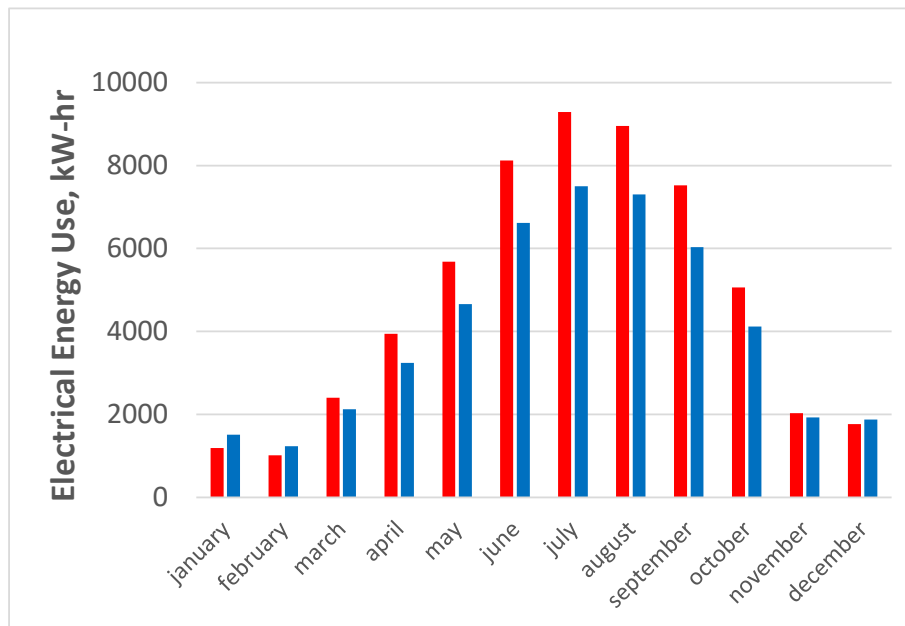


**Figure 7.1. Simulated monthly energy use for Building 584 in year 30. The red bars represent the base case and the blue bars include the dry fluid cooler.**

An economic comparison of these systems requires assumptions about the costs of electricity over time relative to the general inflation rate. An analysis of the system economics was performed using the National Institute of Standards and Technology (NIST) building life cycle cost (BLCC) program for MILCON analysis (NIST, 2016). This program uses the current Department of Energy forecasts for electricity price escalation relative to general inflation. The currently predicted electricity escalation rates are in the range of a few percent over the next several years, decreasing to near zero in future decades. The NIST-BLCC program requires input of the annual electricity savings from the alternative being considered. This is somewhat problematic in the current analysis because the energy savings are low or nonexistent in the first few years before increasing in later years. For the purpose of this life-cycle analysis, the cumulative electricity savings after 30 years were averaged over the 30 year period. This gives an average annual electricity savings of 5,863 kW-hr. The complete cost of the dry fluid cooler was estimated to be \$19,480 including design, construction, supervision, and inspection. The initial (current) cost of electricity was entered as \$0.115/kW-hr, which is the average of an assumed non-peak cost of \$0.08 /kW-hr and a peak cost of \$0.15/kW-hr.

The NIST-BLCC program predicts a total discounted operational savings of \$14,963 over a 30 year operational period, with a simple payback period of 28.9 years, and an adjusted internal rate of return of 2.10%.

An alternative analysis considers an initial non-peak energy cost (\$/kW-hr), a peak energy cost (\$/kW-hr) that would apply to summertime weekday afternoons and evenings, an annual energy cost inflation rate, and a general inflation rate. With this model, the energy costs would be escalated at the energy cost inflation rate. Over time, the calculated monthly energy costs can be converted to present dollars using the general inflation rate. Table 7.3 shows the projected energy costs assuming that ½ of the June, July, August, and September cooling costs occur during peak hours. The initial non-peak energy cost was \$0.08/kW-hr; the initial peak energy cost was \$0.15/kW-hr; the energy inflation rate was 5%, and the overall inflation rate was 2% in this example.

The energy costs (in current dollars) in this model increase substantially over time, due to the differential between the assumed energy cost inflation rate and the overall inflation rate, and due to the declining efficiency of the heat pumps. We acknowledge that if electrical energy prices remain low over the next 30 years, that this projection would overestimate the future energy costs. However, it seems likely that electrical energy costs will increase substantially in the future, and these increases amplify the costs of heating and cooling system inefficiencies.

**Table 7.3. Comparison of monthly electricity costs (in current dollars) after 10 and 30 years of system operation.**

| <b>Month</b> | <b>Year 10 Base Case</b> | <b>Year 10 Dry Fluid Cooler</b> | <b>Year 30 Base Case</b> | <b>Year 30 Dry Fluid Cooler</b> |
|--------------|--------------------------|---------------------------------|--------------------------|---------------------------------|
| January      | \$115                    | \$156                           | \$222                    | \$281                           |
| February     | \$99                     | \$128                           | \$190                    | \$230                           |
| March        | \$230                    | \$219                           | \$449                    | \$398                           |
| April        | \$378                    | \$333                           | \$738                    | \$607                           |
| May          | \$547                    | \$480                           | \$1,066                  | \$874                           |
| June         | \$1,128                  | \$982                           | \$2,196                  | \$1,789                         |
| July         | \$1,294                  | \$1,116                         | \$2,517                  | \$2,033                         |
| August       | \$1,251                  | \$1,090                         | \$2,433                  | \$1,985                         |
| September    | \$1,054                  | \$903                           | \$2,050                  | \$1,643                         |
| October      | \$495                    | \$431                           | \$962                    | \$783                           |
| November     | \$199                    | \$202                           | \$386                    | \$367                           |
| December     | \$174                    | \$198                           | \$337                    | \$358                           |
| <b>Total</b> | <b>\$6,964</b>           | <b>\$6,238</b>                  | <b>\$13,547</b>          | <b>\$11,346</b>                 |

The cost savings from the system with the dry fluid cooler increase over time due to the fact that the system does not lose efficiency compared to the base system, and also due to the assumption that energy costs rise faster than the general rate of inflation. The cumulative energy costs for the two systems over a 30 year period is shown in Figure 7.2. In the early years, before the base case system ground loop has heated up, the two systems have similar efficiencies, and therefore, similar costs. However, as the base case system loses efficiency, and as the relative cost of



electrical energy rises, the cumulative costs for the base system begins to rise more rapidly. The difference in the two curves at any time is the net energy cost savings, in current dollars. Therefore, given the capital costs for adding the dry fluid cooler, the payback period can be calculated. The 48 ton unit that we added to the existing system in this example costs about \$20,000. From the figure, it can be seen that the payback period would be about 23 years for this case. This time would be reduced if the cost of energy was higher than assumed in the calculations, or if the cooling unit could be acquired at a lower cost.

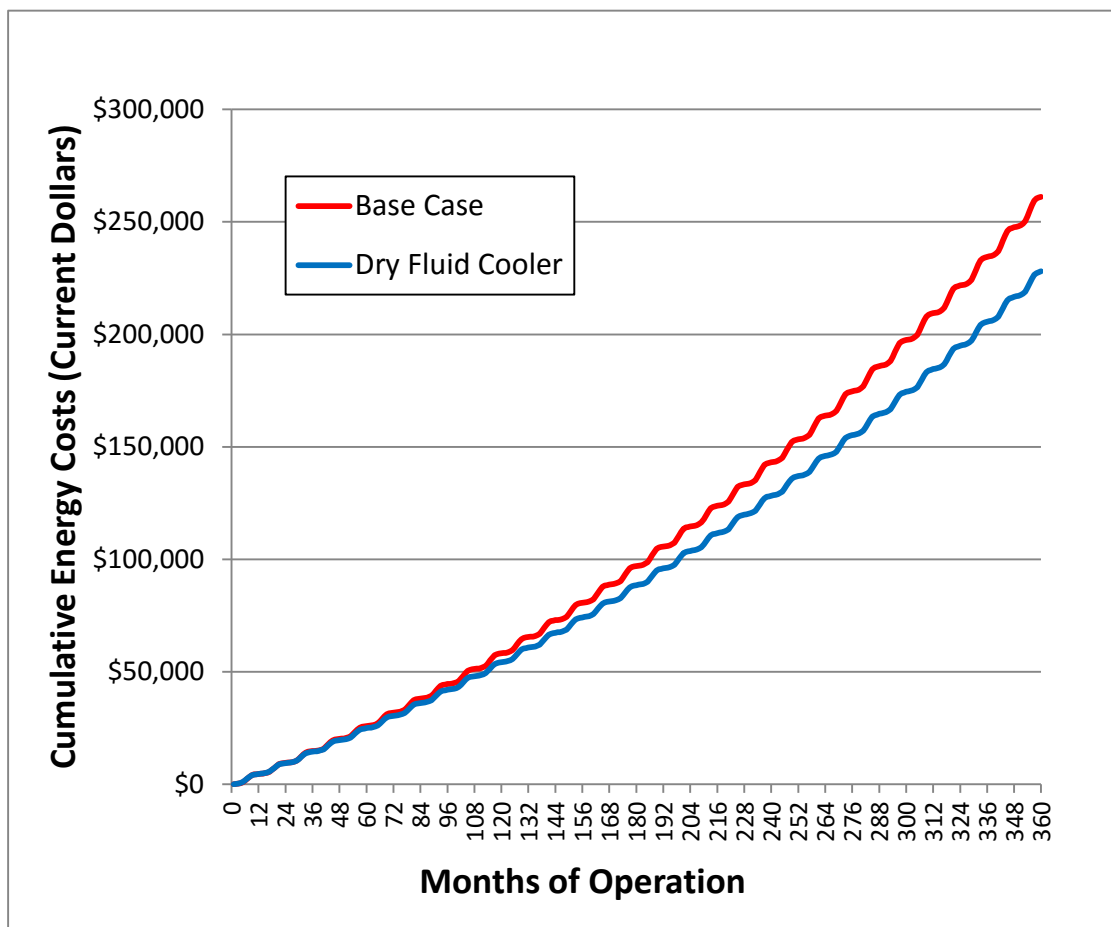


**Figure 7.2. Cumulative electrical energy costs for the base case and the case with a dry fluid cooler.**

The economic analysis is sensitive to the assumed rate of energy inflation relative to the general inflation rate. A comparison of the projected cumulative energy cost savings using different energy inflation rates is shown in Figure 7.3. With a low energy inflation rate of 2% that is equal to the general inflation rate, the cost savings accumulate approximately linearly with time, and the payback period is about 30 years or more. This result is similar to the NIST-BLCC MILCON analysis, which assumed a low energy inflation rate. With a high energy inflation rate of 8% and a general inflation rate of 2%, the cost savings accumulate more quickly, and the payback period is around 20 years.

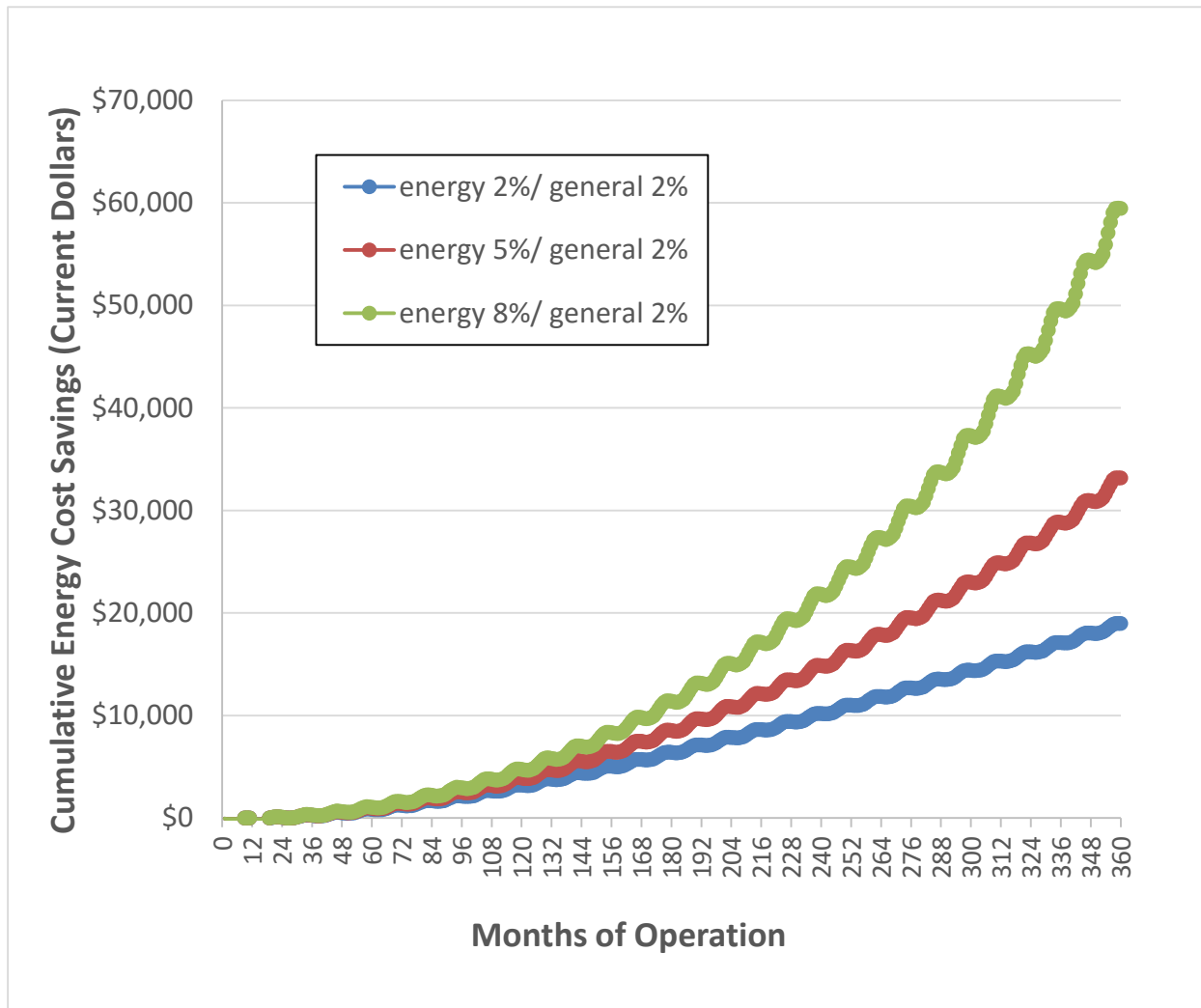


**Figure 7.3. Cumulative electrical energy cost savings with energy inflation rates of 2%, 5%, and 8% with a general inflation rate of 2%.**

The energy cost savings curves presented in Figure 7.3 represent likely upper and lower bounds for potential savings in this example.

It should be noted that there are often substantial electrical energy demand costs that are charged on the basis of the maximum peak and non-peak energy usage rates (recorded over the past month); these electrical energy demand costs can be as large as the real energy costs. The dry fluid cooler system has the advantage of reducing electrical energy consumption during periods when the energy usage is likely to reach a maximum value, especially during the summertime peak hours. Therefore, the dry fluid cooler system can likely reduce the energy demand costs, improving the economics of the system.

It was stated earlier that this system would likely not be able to continue operation without some form of supplemental cooling. An alternative to adding a dry fluid cooler (or cooling tower) would be to increase the size of the geothermal ground loop. However, the analysis of this

option presented in Section 6.1.3 showed that the number of borehole heat exchangers would need to be tripled in order to maintain reasonably cool ground loop temperatures. The estimated capital cost for this increase was about \$260,000, which is far above the \$20,000 capital cost of adding a dry fluid cooler to the system.

## 8.0 IMPLEMENTATION ISSUES

The following guidelines are provided for application of wintertime cooling using dry fluid coolers to new systems. **The first three steps are recommended for every geothermal system installed in cooling dominated areas** (climatically hot areas such as the ones shown in Figure 2.4 where the blue bars significant larger than the red bars).

- 1) Calculate building heating and cooling loads using a building simulation tool such as eQUEST (Hirsch & Associates, 2016).
  - 2) Simulate a conventional geothermal heat pump system using a ground loop simulation tool such as GLHEPro (IGSHPA, 2016). There is a trade-off between increased ground loop size, and loop temperature. With the addition of a dry fluid cooler, a smaller ground loop can be used, but it must still be large enough to accommodate a reasonable flow rate for the building load.
  - 3) Using reasonable ground loop sizes, assess the degree to which the ground loop temperature will increase over the expected life of the system. **If the average loop temperature increases by more than about 15 degrees F, a dry fluid cooler would be beneficial.**
  - 4) The dry fluid cooler should be sized to match the ground loop flowrate; the flowrate should fall within the cooler design range.
  - 5) The dry fluid cooler should be sized and operated so that it can reject an amount of heat equal to the yearly cooling load minus the yearly heating load. Using variable frequency drive fan motors, the fan speeds should be controlled by the temperature difference between the water entering the cooler and the outside air, reaching maximum fan speeds when the temperature difference is large (~20 degrees or more). Most of the loop heat will be rejected in the winter using this type of operation, and the heat rejection energy efficiency can be very high.
- On a yearly average basis, the dry fluid cooler should be sized so that the heat rejection is on the order of 10-20% of the cooler rated capacity. For example, if the desired yearly cooler heat rejection is 600,000 kBTU, this is equivalent to an average rate of about 5.7 tons. This would be about 12% of the rated capacity of a 4-fan, 48 ton dry fluid cooler. During the peak cooling months of December and January, the cooler is likely to be operating at 25-35% of the rated capacity (averaged over the month).
- 6) The ground loop system should include antifreeze to prevent damage to the dry fluid cooler during freezing temperatures.

For existing systems that are suffering from high ground loop temperatures, a retrofit following steps 4) through 6) can be used to stabilize and reduce the temperatures. In this case, the dry fluid cooler heat rejection during the first year or two of operation will higher due to the higher ground loop temperatures.

## 9.0 REFERENCES

- Agency for Toxic Substances and Disease Registry, 2007. Ethylene Glycol and Propylene Glycol Toxicity What Are the U.S. Standards for Ethylene Glycol Exposure Levels? > <https://www.atsdr.cdc.gov/csem/csem.asp?csem=12&po=7> accessed Oct. 16, 2016.
- Chiasson, A.D., and C. Yavuzturk, 2009, A design tool for hybrid geothermal heat pump systems in cooling-dominated buildings, ASHRAE Transactions 115(2), 74-87.
- Cullin, 2008, Improvements in Design Procedures for Ground Source and Hybrid Ground Source Heat Pump Systems, MS Thesis, Oklahoma State University.
- Cullin, J.R., and J.D. Spitler, 2010, Comparison of simulation-based design procedures for hybrid ground source heat pump systems, Proceedings of the 8<sup>th</sup> International Conference on System Simulation in Buildings, Liege, Belgium, December 13-15, 2010.
- Hackel, S., G. Nellis, and S. Klein, 2009, Optimizations of cooling-dominated hybrid ground-coupled heat pump systems, ASHRAE Transactions 115(1), 565-580.
- Hirsch & Associates, 2016, eQUEST Quick Energy Simulation Tool, <http://www.doe2.com/equest/>, accessed 9/12/16.
- IGSHPA, 2016, GLHEPro 5.0 For Windows User's Guide, Oklahoma State University, distributed by the International Ground Source Heat Pump Association, 150 p.
- Kavanaugh, S.P., 1998, A design method for hybrid ground-source heat pumps, ASHRAE Transactions, 104(2): 691-698.
- Klotzbücher, T. A.s Kappler, K. L. Straub, S. B. Haderlein, 2007. Biodegradability and groundwater pollutant potential of organic anti-freeze liquids used in borehole heat exchangers, Geothermics, Volume 36, Issue 4, August 2007, Pages 348-361, ISSN 0375-6505, <http://dx.doi.org/10.1016/j.geothermics.2007.03.005>.
- National Institute of Standards and Technology (NIST), 2016, Building Life Cycle Cost Programs, <http://energy.gov/eere/femp/building-life-cycle-cost-programs>, accessed 11/15/16.
- Technical Systems, 2016, FC Series Fluid Coolers, <http://www.raecorp.com/Upload/TSI/Series%20FC%20Fluid%20Coolers.pdf> accessed 9/12/16.
- Trane, 2003, Operations & Maintenance Manual for Bldg 601, Headquarters Building, Marine Corps Air Station, Beaufort, SC
- Xing, L., 2014, Estimations of Undisturbed Ground Temperatures Using Numerical and Analytical Modeling. PhD Thesis, Oklahoma State University, Stillwater, OK.
- Xu, X., 2007, Simulation and Optimal Control of Hybrid Ground Source Heat Pump Systems, PhD Thesis, Oklahoma State University.

## APPENDICES

### Appendix A: Points of Contact

| <b>POINT OF CONTACT<br/>Name</b> | <b>ORGANIZATION<br/>Name<br/>Address</b>   | <b>Phone<br/>Fax<br/>E-mail</b>   | <b>Role in Project</b>                     |
|----------------------------------|--|---|--|
| Ronald W. Falta                  | Clemson University<br>340 C Brackett Hall<br>Clemson, SC 29634-0919              | (864) 656-0125<br>(864) 656-1041 fax<br>(864) 710-3448 cell<br>faltar@clemson.edu | Principal Investigator                     |
| Fred J. Molz                     | Clemson University<br>156 Rich Lab<br>342 Computer Ct<br>Anderson, SC 29625-6510 | (864) 656-1003<br>(864) 656-0672<br>fredi@clemson.edu                             | Co-Investigator                            |
| Charles Newell                   | GSI Environmental Inc.<br>2211 Norfolk Suite 1000<br>Houston, TX 77098           | (713) 522-6300<br>cjnewell@gsi-net.com  | Co-Investigator                            |
| Neil Tisdale                     | MCAS Beaufort<br>Bldg 616 Public Works<br>MCAS<br>Beaufort, SC 29904-5001        | (843) 228-6317<br>(843) 321-6702 cell<br>belton.tisdale@usmc.mil                  | Base Utilities Director/<br>Energy Manager |